

博士論文 (要約)

Isolation and characterization of iron-reducing bacteria, potential drivers of reductive nitrogen transformation in paddy soils

(水田土壌の還元的窒素変換を担う鉄還元細菌の分離と性状解析)

許 振興

Doctorate Thesis (Abridged)

Isolation and characterization of iron-reducing bacteria, potential drivers of reductive nitrogen transformation in paddy soils

By

Zhenxing Xu

Department of Applied Biological Chemistry
Graduate School of Agricultural and Life Science
The University of Tokyo

Table of contents

Chapter 1: General introduction	1
1.1 Introduction of paddy soils	1
1.2 Carbon cycles in paddy soils.....	4
1.2.1 Carbon source utilization	4
1.2.2 Methane production and impact factors.....	5
1.3 Nitrogen metabolism in paddy soils	7
1.3.1 Major nitrogen metabolic pathways.....	7
1.3.2 Nitrification process.....	7
1.3.3 Denitrification process	9
1.3.4 Dissimilatory nitrate reduction to ammonium (DNRA) process	10
1.3.5 Nitrogen fixation process	11
1.3.6 N ₂ O production and reduction	13
1.4 Iron reduction in paddy soils.....	15
1.4.1 Natural features of iron	15
1.4.2 Microbial interaction with iron redox cycle.....	16
1.4.3 Microbial iron reduction coupled with nitrogen cycles	17
1.4.4 Iron reducing microbes in paddy soils	18
1.5 Research objective	19
Chapter 2: Isolation and identification of <i>Geobacter</i>-like and <i>Anaeromyxobacter</i>-like strains and reclassification of the family <i>Geobacteraceae</i>	22
2.1 Introduction.....	22
2.2 Materials and Methods.....	25
2.2.1 Sampling sites, enrichment and isolation.....	25
2.2.2 16S rRNA gene amplification and analysis	26
2.2.3 Genomic fingerprints	27

2.2.4 Genome sequencing and comparison.....	28
2.2.5 Phylogenetic analysis.....	30
2.2.6 Phenotypic characterization.....	31
2.2.7 Chemotaxonomic characterization.....	31
2.2.8 Reclassification of the family <i>Geobacteraceae</i>	32
2.3 Results and discussion	33
2.3.1 Isolation of different <i>Geobacter</i> -like and <i>Anaeromyxobacter</i> -like strains	33
2.3.2 Polyphasic taxonomy of <i>Geobacter</i> -like and <i>Anaeromyxobacter</i> -like strains	34
2.3.3 Taxonomic conclusion	43
2.3.4 Description of novel genera and novel species.....	45
2.4 Chapter Conclusion.....	55
Chapter 3: Habitat preferences and biogeochemical roles of <i>Geomonas</i> and <i>Oryzomonas</i> strains	86
3.1 Introduction.....	86
3.2 Materials and methods	88
3.2.1 Meta-analysis for distribution and relative abundance of <i>Geomonas</i> and <i>Oryzomonas</i> species.....	88
3.2.2 Ferric irons reduction.....	89
3.2.3 Carbon source utilization	90
3.2.4 Determination of nitrogen-fixing ability.....	91
3.3 Results and discussion	92
3.3.1 Distribution of <i>Geobacteraceae</i> strains in various environments.....	92
3.3.2 Ferric irons reduction.....	95
3.3.3 Carbon source utilization	97
3.3.4 Determination of nitrogen fixing ability.....	98
3.4 Chapter conclusion.....	100
Chapter 4: Conclusion and prospect.....	114
References.....	117

Supplementary materials	137
Abstract.....	139
Acknowledgements	144

Chapter 1: General introduction

1.1 Introduction of paddy soils

Rice, as one of the important cereal grains, feeds more than half of the world's population and provides for more than one-fifth of the energy consumed worldwide (Tilman and Clark, 2014). Rice is the seed of paddy (*Oryza glaberrima* or *Oryza sativa*) and planted in the paddy field with the third-highest worldwide production just after sugarcane and maize (From Wikipedia: <https://www.wikiwand.com/en/Rice>). As reported in FAO of 2017, the total rice cultivation area was estimated at 167.2 million ha, corresponding to 6.0% of the agricultural land worldwide. Global rice production is 770 million tons, of which more than 90% is produced in Asia, followed by Latin America, and Caribbean. Among them, the five Asia counties, that is China, India, Indonesia, Bangladesh, and Vietnam, as the first top five rice producer, have been playing a dominating role in total rice production, due to the befitting weather conditions (Ali et al., 2019). The first two counties, China and India, also the most densely populated countries in the world, account for 20.0% and 28.5% of the global rice area, respectively. In China, approximately 90% of the rice fields are reported to be irrigated, while in India, more than 46% of the rice fields are irrigated. Besides, irrigated rice fields, as an integral part of the rice production system, were reported to contribute about 75% to global rice production in Asian countries, indicating irrigation is the major type for paddy soil managements in Asian counties (Ali et al., 2019).

Although partial of the paddy (ca. 25%) is planted with less water and named as “upland rice” or “mountain rice” based on its planting pattern, they are not widely cultivated owing to their less production (Roger et al., 1993). In view of the planting features in Japan, we, herein, just focus on paddy fields with cyclic

irrigations. Japan is not a major country as the rice producer, but the paddy field area accounts for more than half of all arable soils, which indicates the paddy field is the major land utilization type in Japan and makes the researches focusing on the paddy field in Japan are of great potentials (Terasawa, 1975). Paddy soil, the substrate of paddy field, is the largest anthropogenic wetlands on Earth and represent a unique ecosystem that cycles between waterlogged and drained states during long-term paddy cultivation. Detailly, the paddy fields are initially under completely drained condition before rice cultivation, in which fertilization is carried out. After that, paddy fields are waterlogged during the cultivation process. Under this condition, soil redox potential (Eh) or electron activity in soil decreases gradually, and an anoxic environment develops within the plowed layer of soil. When the time goes to harvest approaches, the paddy fields are drained again and hold in the same condition till the next cultivation season (Itoh et al., 2013). These seasonal cycles between waterlogged and drained conditions of paddy soils also cause the aerobic and anaerobic conditions revolved, which great effects the soil properties and sets in motion a series of unique physical, chemical, and biological processes not found in dryland soils (Kimura, 2000; Liesack et al., 2000; Roger et al., 1993).

Structurally, paddy soils mostly belong to alluvial soils and low humic gley soils (or Entisols and Inceptisols) and occur in landscapes where both surface and internal drainage are poor, indicating most paddy soils are existed in deltas and adjacent flood plains, in valleys, and coastal plains (Ponnamperuma, 1981). These special geographical locations in the lowlands help paddy soils receive new sediments deposited from run-off that carries eroded topsoil down from the uplands, thus sustaining soil fertility and productivity (Ali et al., 2019). Owing to the effect of long-term afloat and the grayzation process caused by the irrigation water, paddy soils usually form a grey layer near the soil surface, where iron, manganese, silica, and phosphate become more soluble and diffuse to the surface and move by diffusion and mass flow to the roots and to the subsoil, providing

more nutrition for microbial metabolisms (Ponnamperuma, 1972). This special layer also distinct paddy-type soils from other upland soils, which are formed by weathering and leaching processes rather than impacted by water logging (Terasawa, 1975).

Moreover, the paddy soils are also reported as the model systems involved in structure-function relationships between microbial groups and interactions of microorganisms with rice plants owing to three special physiochemical conditions: oxic surface soil, anoxic bulk soil, and rhizosphere soil plus rhizoplane, corresponding the chemical and microbial gradients across different layer of soils (Liesack et al., 2000). For example, oxygen has only been detected both in the field and in the laboratory at the surficial 1-3 mm from the floodwater-soil boundary layer, which usually treated as oxic surface soil (Revsbech et al., 1999). The presence of oxygen further induced an O_2 -dependent reaction, nitrification, transforming ammonium, the major composition of fertilizer, to nitrite and nitrate, providing reaction substrates to microbial denitrification (Ishii et al., 2011a). Then, the generated nitrate and nitrite were sink downward to deeper layer of soil in absence of oxygen, also treated as anoxic bulk soil, and stimulate microbial activities related to denitrification and dissimilarity nitrate reduction to ammonium (DNRA), causing nitrogen loss with N_2 production or return to ammonium forming a nitrogen transformation cycle (Ishii et al., 2011a; Kuypers et al., 2018). This is just a small case simply showing the relationship between microbial activities and soil properties at different soil layers, more biotic and abiotic factors, such as metals, pH, water, microfauna and so on, make multiple reactions coupled together, causing much conflict reaction pathways in the real condition of paddy soils (Kim and Liesack, 2015; Li et al., 2020b, 2020a; Tipayno et al., 2018).

1.2 Carbon cycles in paddy soils

1.2.1 Carbon source utilization

Biogeochemical process in ecology and Earth science, also namely substance turnover or cycling of substances, is a pathway by which a chemical substance moves through biotic (biosphere) and abiotic (lithosphere, atmosphere, and hydrosphere) compartments of Earth. Therein, carbon cycle and nitrogen cycle, as two key processes, coupled many other reactions together and then formed a conflict metabolic network in real environments. The carbon cycle is usually reported to be started in paddy soils from rice straw, the most abundant plant residues left in paddy field after rice harvested. The major compositions of rice straw were reported on average 30.3 – 38.2% cellulose, 19.8 – 31.6% hemicellulose, 7.2 – 12.8% lignin, as well as a number of minor organic compounds (Jin and Chen, 2007), providing large molecular carbon source to target microbes, which can secrete special enzymes to degrade these large molecules to small ones and further feeding various microbes. During this decomposition process, Devêvre and Horwáth (2000) noted that rice straw was decomposed mainly under flooded conditions, because substrate use efficiency was higher than aerobic conditions, but less straw-C was mineralized in contrast to aerobic conditions. Then, Nakamura et al. (2003) showed that Gram-negative bacteria and fungi under upland conditions and Gram-positive bacteria and anaerobic Gram-negative bacteria under flooded conditions were major players in rice straw decomposition based on a field experiments using phospholipid fatty acid (PLFA) analysis. Using metatranscriptomic rRNA, it was further reported that *Clostridiaceae*, *Lachnospiraceae*, *Ruminococcaceae*, *Veillonellaceae* and *Pseudomonadaceae* were identified to be the most abundant and the most dynamic bacterial groups related to rice straw decomposition at a paddy soil slurry test (Wegner and Liesack, 2016). Thus, the decomposition of rice straw

was tightly coupled with the microbial activities and started the carbon cycle in the paddy soils.

1.2.2 Methane production and impact factors

Paddy soils were also reported to be the major source for generation of methane (CH_4), an important greenhouse gas with a global warming potential of 25 compared to same molecules of CO_2 (averaged over 100 years), resulting from the decomposition of organic materials and high activity of methanogens (CH_4 production microbes) under anaerobic conditions (Kimura et al., 2004). Generally, about 80% of methane on Earth is biologically produced by methanogenesis, a form of anaerobic respiration only known to be conducted by partial members of the domain archaea, which can convert CO_2 with H_2 , methanol, methylamines, methylsulfides, or acetate into CH_4 , constructing one of the core networks of the carbon cycle (Dean et al., 2018; Thauer et al., 2008). Methanogens were reported to be metabolic actively and distributed widely in anoxic environments, such as landfills and other soils, ruminants, the guts of termites, and the anaerobic sediments below the seafloor and the bottom of lakes (Serrano-silva et al., 2014; Sirohi et al., 2010). This explained the fact that rice fields, as the largest anthropogenic wetlands on Earth, generate large amounts of methane (5-19% of the global anthropogenic CH_4 budget) during plant growth.

Although the huge contribution of paddy soil to CH_4 emission is inalienably true, many literatures also point out that the gas emission is obviously affected by different biotic and abiotic factors. Sander et al. (2014) has noted that CH_4 emissions significantly increased when crop residues were incorporated prior to planting due to higher amounts of readily available carbon stimulating soil microbial activity. But it was also reported that incorporation of rice residues immediately after harvest and subsequent aerobic decomposition of the residues

before soil flooding for the next crop reduced CH₄ emissions by 2.5–5 times and also improved nutrient cycling in paddy field, implying that field management of crop residues is a vital factor affecting CH₄ emission in the tested paddy field. Furthermore, based on a field experiment, Sass et al., (1991) found CH₄ production was significantly affected by temperature with the emission peak present around 37 °C, and little CH₄ produced at lower (< 10 °C) or higher (> 55 °C) temperatures, which was consistent with the microbial activities at different degrees of temperature. Although many reports also indicated that biochar application in paddy soils had obvious influence on CH₄ emission, those conclusions were divergent. For example, Karhu et al. (2011) reported a 96 % increase in the average cumulative CH₄ uptake with biochar addition to an agricultural soil, probably owing to the improved soil aeration and CH₄ diffusion through soil, whereas Liu et al. (2011) demonstrated that biochar reduced CH₄ emission from a waterlogged paddy soil due to inhibition of methanogenic activity, stimulation of methanotrophic activity, and enhancement of CH₄ adsorption in soil. Knoblauch et al. (2011) noted that applying biochar increased the total amount of CH₄ emission by 1.6 times during a 96-day rice growing season due to the labile components of biochar that were the predominant source of methanogenic substrates. But, Spokas and Reicosky (2009) evaluated the impacts of 16 different biochar on CH₄ production in three soils and showed decreased or unaltered rates of CH₄ oxidation. However, a recent report showed that the biochar obtained from different temperature resulted in a different effect on CH₄ production in paddy soils that low-temperature (300 °C) biochar increased methane yields, whereas higher-temperature (700 °C) decreased methane production (Ji et al., 2020). Thus, the influence of biochar on CH₄ emission are multiple and different sources or conditions for biochar preparation may cause reverse impact effect on CH₄ production.

1.3 Nitrogen metabolism in paddy soils

1.3.1 Major nitrogen metabolic pathways

Apart from the carbon cycle as described above, nitrogen cycle is the other key process within the biogeochemical processes connecting other redox reactions of different elements in environments. In paddy soils, the waterlogged and drained states during long-term paddy cultivation are circularly occurred. Besides of the common aerobic reaction, nitrification ($\text{NH}_4^+ \rightarrow \text{NH}_2\text{OH} \rightarrow \text{NO}_2^- \rightarrow \text{NO}_3^-$), the temporal waterlogged conditions also cause many anaerobic biogeochemical processes actively occurred, particularly the biological reductive nitrogen transformation (RNT), including denitrification ($\text{NO}_3^- \rightarrow \text{NO}_2^- \rightarrow \text{NO} \rightarrow \text{N}_2\text{O} \rightarrow \text{N}_2$), dissimilatory nitrate reduction to ammonium (DNRA, $\text{NO}_3^- \rightarrow \text{NO}_2^- \rightarrow \text{NH}_4^+$), and nitrogen fixation ($\text{N}_2 \rightarrow \text{NH}_4^+$), which contribute to reduced leaching of nitrogen pollutants (NO_3^- , NO_2^- , and N_2O) and increased retention of nitrogen-based nutrients (NH_4^+) for rice plants in paddy soils relative to upland soils (Ishii et al., 2011a; Itoh et al., 2013). (Fig. 1.1). Generally, paddy fields were fertilized at drying condition prior to paddy planting. Because rice seedlings uptake ammonium better than nitrate, ammonium-based fertilizers, including ammonium sulfate and urea, have been frequently applied in rice cultivation practices, resulting in more synthetic ammonium applied to paddy soils (Sasakawa and Yamamoto, 1978). Besides, organic fertilizers, containing much more organic N, are also commonly used in paddy fields. Organic N is transferred to ammonium at first by a biological process namely ammonification, also inputting more ammoniacal nitrogen in paddy soils.

1.3.2 Nitrification process

Although most of the applied ammoniacal nitrogen is sink to the deeper layer of soils after water-flooded to support microbes and plants growth, there is still

less ammonium converted to nitrite or nitrate by nitrification process at surface oxidized layer in rice paddy soils. This process was a biological oxygen-dependent pathway and mainly driven by ammonia-oxidizing bacteria (AOB), ammonia-oxidizing archaea (AOA), nitrite-oxidizing bacteria (NOB) and complete ammonia oxidizers (comammox). AOB and AOA are two microbial groups with wide distribution on Earth and oxidize ammonium to nitrite as the first step of nitrification process (Könneke et al., 2005), while NOB oxidizes nitrite to nitrate as the second step of nitrification process (Mancinelli, 1996). Comammox is a recently discovered bacterial group belonging to the bacterial genus *Nitrospira* with the special ability that oxidizing ammonium to nitrate on their own (Daims et al., 2015; van Kessel et al., 2015). Moreover, Francis et al. (2007) reported that AOA was more abundant than AOB in the ocean, but in the semi-arid soils, Banning et al. (2015) noted that AOB was the dominant group of ammonium oxidation. In rice paddy soil, Li et al. (2007) found a positive correlation between nitrification activity and the abundance of AOB; thus, AOB seems more responsible than AOA for nitrification in rice paddy soil, however, in the paddy rhizosphere, the abundance of AOA and AOB both increased after urea fertilizer applications (Hussain et al., 2011), indicating more studies are required to clarify the relative contributions of AOA and AOB to ammonium oxidation in paddy soils. The strains of NOB and comammox belong to same bacteria genus, *Nitrospira*, but to date, no *Nitrospira* species isolated from paddy soil has been described, thus, the population structure of NOB and comammox in paddy soils is still unclear. However, recent study based on environmental DNA analysis with 16S rRNA gene amplicon sequences found the presence of *Nitrospira*-like 16S rRNA sequences in rice paddy soil (Ishii et al., 2009), implying the potential role of NOB and comammox in paddy soils.

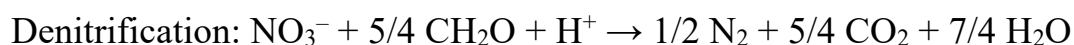
1.3.3 Denitrification process

The nitrate from nitrification process or applied fertilizer was settled into deeper layer of paddy soils with the paddy water sinking, inducing a microbial respiratory process, denitrification, occurred. Different with the target several genera of nitrification microbes, denitrification strains are sporadically distributed among different taxonomical groups of bacteria as well as some fungi and archaea (Hayatsu et al., 2008; Philippot et al., 2007), indicating the species diversity of denitrification drivers. The process of denitrification is started with nitrate and ended with N_2 gas, along with the regular intermediates, nitrite, NO and N_2O , making this process to be the only step in the N cycle where fixed N re-enters the atmosphere as N_2 ; thus it serves to close the global N cycle (Ranatunga et al., 2018). In the paddy soil, denitrification microbes are very active during rice planting, owing to the anaerobic condition of waterflooded soils. Based on a survey using culture-based investigations, approximately 10^5 – 10^6 g^{-1} soil of denitrifying bacteria is present in paddy soils, higher abundance than those in upland soils (Gamble et al., 1977), suggesting their crucial functional role in N cycle in paddy soils. Moreover, recent studies have clarified the functional microbes responsible for denitrification in rice paddy soils with multiphasic methods, such as stable isotope probing (SIP), denitrification functional gene analysis, comparative 16S rRNA gene analysis, and the functional single-cell (FSC) isolation method. Therein, using the SIP approach of labeled ^{13}C -succinate, Saito et al. (2008) found that bacteria belonging to orders *Burkholderiales* and *Rhodocyclales* were dominant members for succinate-assimilating population under denitrifying conditions in paddy soils. Besides, based on comparative 16S rRNA gene analysis, Ishii et al. (2009) reported that the bacteria belonging to the order *Burkholderiales*, especially those belonging to the genus *Herbaspirillum*, and *Rhodocyclales*, were more frequently detected in rice paddy soils under denitrification-inducing conditions than under no denitrifying conditions.

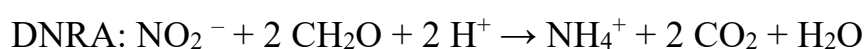
Furthermore, Scheid et al. (2004) observed that the abundance of the bacteria genus *Dechloromonas* belonging to the order *Rhodocyclales* obviously increased when nitrate was added to Italian paddy soil. These consistent results demonstrated that the denitrifiers are distributed in wide-scaled taxonomical positions, but their communities in paddy soils are conserved, indicating the environmental type seems the key factor determining the distribution of different denitrifiers.

1.3.4 Dissimilatory nitrate reduction to ammonium (DNRA) process

In addition to the denitrification under anaerobic condition in paddy soils, nitrate can also be dissimilatory reduced to ammonium, namely DNRA process, with the intermediate nitrite, which supplies ammonium to rice roots in paddy soils. Distinct from denitrification process with N loss, DNRA is a N retention process by preventing N loss via denitrification and reducing water-leachable nitrate to ammonium, which is more likely to be adsorbed by negatively charged soil particles (Rütting et al., 2011). Due to the limited amount of nitrate under reductive conditions in paddy soils, DNRA and denitrification processes compete each other for nitrate, causing different balance points at distinct conditions. Theoretically, DNRA process yields more free energy per molecule of NO_3^- reduction than complete denitrification process, whereas the complete denitrification reaction yields more free energy for every electron or carbon oxidation, which were shown by the equations below (Strohm et al., 2007; van den Berg et al., 2015).



($\Delta G^\circ = -445 \text{ kJ per mol carbon, } -556 \text{ kJ per mol NO}_3^-$)



($\Delta G^\circ = -311 \text{ kJ per mol carbon, } -623 \text{ kJ per mol NO}_3^-$)

Thus, DNRA seems more favorable than denitrification in NO_3^- -depleted environments. Practically, Tiedje et al. (1983) reported that nitrate was used by DNRA or denitrification can be explained by the ratio of available carbon to electron acceptor. Under a carbon-rich and NO_3^- -poor environment, such as the rumen, almost all nitrate was converted to ammonium via DNRA, however, under a condition with low supply of carbon substrates but more NO_3^- , such as the agricultural soils, most nitrate was converted to N_2 gas by denitrification. Similar results were also from the isolated bacteria experiment with strain *Shewanella loihica* PV-4 that high carbon-to-nitrate ratios improved DNRA process with more ammonium production, while low carbon-to-nitrate ratios favored denitrification process with more N_2O generation (Yoon et al., 2015). These consistent results highlighted the key factor of carbon/nitrite ratio in determining the type of nitrate reduction. In paddy soils, the amount of carbon substrate is relatively low and there are various alternative electron acceptors under waterlogged conditions, which suggested that DNRA should not be very active in rice paddy fields under regular conditions (Ishii et al., 2011a). However, recent study noted that DNRA occurred to a similar extent to denitrification and appeared to be enhanced by a nitrate limitation relative to organic carbon based on a paddy soil microcosm experiment using ^{15}N tracer analyses (Nojiri et al., 2020), implying more studies are needed to understand well of the role of DNRA in paddy soils.

1.3.5 Nitrogen fixation process

Although N_2 is emitted from rice paddy soil to the atmosphere during the denitrification process with N loss, atmospheric N_2 can also be absorbed into soil and rhizosphere under paddy field conditions by biological nitrogen fixation. Nitrogen fixation is also a key process, drove by nitrogenase, within nitrogen cycle and the only reaction to fix atmospheric nitrogen gas to ammonium, further

supplying nutrients to soils. Nitrogenases are complex metalloenzymes and mostly consisted by two conserved structural domains, iron (Fe) protein and molybdenum–iron (MoFe) protein, with functions as the ATP-dependent electron donor and enzyme catalytic domain, respectively (Dixon and Kahn, 2004). Both of the two domains of the nitrogenase are extremely oxygen sensitive, suggesting the waterflooded paddy soils are favored conditions for nitrogen fixation. Moreover, similar with denitrification microbes, nitrogen fixing organisms also did not show conserved phylogenetic groups but widely distributed among different taxonomical groups of bacteria as well as some archaea. By now, no eukaryote has been found containing nitrogen fixing ability (Dixon and Kahn, 2004). In paddy soils, the nitrogen fixing microbes showed high activity due to the oxygen-depleted conditions, but these activities have been reported to be obviously affected by various environmental factors. Kondo (1993) noted that nitrogen fixing activity in bulk soil of paddy fields without N fertilization was greater than those with conventional fertilization. Hirano et al. (2001) also reported that nitrogen-fixing activity under natural farming without tilling, fertilizers, and pesticides was greater than under conventional farming. Besides, Ohta et al. (1986) reported an obvious difference in nitrogen fixation activities among rice genotypes. An Indica type rice strain, under low nitrogen fertilization conditions, showed high nitrogen fixing activity in the rhizosphere with no reduction of grain yield in contrast to conventional fertilization, indicating the potential application of nitrogen fixation microbes in combination with certain rice genotypes for constructing a sustainable agricultural system. Thus, for a rigorous nitrogen fixation experiment, field conditions should also be taken into consideration.

1.3.6 N₂O production and reduction

N₂O is a potent greenhouse gas that is considered the major factor causing ozone layer destruction (Montzka et al., 2011). Over the last 100 years, atmospheric N₂O concentrations have been steadily increased by 18%, from 270 ppbv during the preindustrial era to 319 ppbv in 2005 (IPCC, 2007). The present global human driven emission of N₂O was estimated to be approximately 6.7 Tg N yr⁻¹, among which agricultural emission is the biggest contributor, accounting for 42% of the human-driven emission (IPCC, 2007). Thomson et al. (2012) reported that denitrification and nitrification processes are two major sources of N₂O production and account for more than two-thirds of all emission in agricultural soils, due to the excess application of nitrogenous fertilizers to the soils. N₂O is the byproduct of the complete denitrification process and nitrification process, directly from NO reduction and hydroxylamine oxidation, respectively. However, some denitrifying strains were reported to lack N₂O reducing activity, causing N₂O be the final product of nitrate reduction, which were functional revealed by denitrifying fungal, common lacking *nos* genes in their genomes (Shoun et al., 1992). Besides, nitrifier denitrification process, carried out by some AOB possessing *nir* genes, was also reported as an important source to N₂O emission, in which N₂O produced from both hydroxylamine oxidation and NO reduction (Poth and Focht, 1985). Furthermore, a recent literature also noted that chemodenitrification process, combining abiotic reaction into denitrification process, significantly contributed to N₂O emission in paddy soils, which account for 6.8–67.6% of the total N₂O emission, depending on the concentrations of Fe(II), nitrite, nitrate, and organic carbon (Wang et al., 2020a). Similar results were also occurred on the batch experiment with an isolated bacterium, *Anaeromyxobacter dehalogenans*. On that, *A. dehalogenans* possesses uncomplete denitrification pathway due to the absence of the nitrite reductase genes, but it can also produce N₂O under the support of Fe(III) reduction (Onley

et al., 2018). Thus, abiotic reactions are also crucial parts for N₂O emission in natural environments. Apart from nitrifiers and denitrifiers, DNRA microbes were also reported to be a source for N₂O emission, but the mechanism has not yet been clarified so far (Giblin et al., 2013; Giles et al., 2012; Heo et al., 2020), indicating more potential N₂O generating pathways are still present but not illustrated.

Although multiple processes, including abiotic and biotic reactions, were reported to contribute to N₂O emission, N₂O reduction is limited to a sole microbial reaction, which is driven by the N₂O reductase (Nos) present among taxonomically diverse bacteria and archaea (Hallin et al., 2018). N₂O reduction to N₂ gas is the last step of denitrification process with the marked enzyme, NosZ, which also serves for energy conservation through anaerobic respiration, detoxification, or removal of excess electrons. However, not all denitrifiers have the ability to reduce N₂O, because part of them lack *nosZ* genes. Also, some phylogenetically diverse bacteria and archaea were reported to be N₂O reducers, but they are not denitrifiers, due to the absence of the nitrite reducing activity. In paddy soils, it has been well-recognized that strong denitrification activity is occurred, but N₂O emission was obvious lower than that from upland fields (Akiyama et al., 2006), indicating more active N₂O reducers are present in paddy soils. In order to explore these functional microbes, Ishii et al. (2011b) performed a paddy soil microcosm study and found that one of the denitrifier groups, *Herbaspirillum* sp. strains were the dominant active N₂O reducers using both culture-independent (SIP analysis) and culture-dependent (FSC isolation) methods, indicating the denitrifiers were the major player in N₂O reduction in paddy soils, although nondenitrifying strains were also detected.

1.4 Iron reduction in paddy soils

1.4.1 Natural features of iron

Iron (Fe) has a widespread distribution in the planet and is the fourth most abundant element, just less than O, Si and Al, in the Earth's crust, thus, plays a significant role controlling the geochemistry in soils, sediments, and aquatic systems. Iron is common present in many types of minerals, such as primary silicate minerals, pedogenic clay minerals, Fe(oxyhydr)oxides with different degrees of crystallinity, as well as in organic complexes, thus, consists an important biogeochemical cycle, connecting many other processes together in natural environments (Huang et al., 2018). Although only trace amounts of iron are required by most life, they are necessary elements for life, due to its special role of cofactor to many important enzymes (Cairo et al., 2006). In nature, iron is mainly present in two common oxidation states, iron(II) and iron(III), and their present states are mainly determined by the physicochemical properties of the conditions, such as pH, oxygen content, oxidation-reduction potential and so on (Ratering and Schnell, 2001). For example, iron(II) is existence and stability under anaerobic conditions, whereas iron(II) is easy to be oxidized into iron(III) under aerobic conditions (Cornell and Schwertmann, 2003). In paddy soils, the cyclically variation of redox potentials, triggered by the alternation of soil wetting and drying, makes iron reduction and oxidation cyclically occurred, which further contribute and accelerate the flow of carbon cycles and nitrogen cycles, causing much more greenhouse gas (CH_4 , N_2O) emitted (Frenzel et al., 1999; Zhang et al., 2019). Besides, several studies also reported that paddy soils showed higher profile differentiation of iron oxides and exhibited lower magnetic susceptibility than their well-drained counterparts in many regions of the world at an investigation to explore the changing status of iron oxides and magnetic properties development through a comparison with the initial parent material

(Han and Zhang, 2013; Huang et al., 2018). Thus, the special characteristics of paddy soils make multiple profiles and conditions of iron.

1.4.2 Microbial interaction with iron redox cycle

The redox transition between iron(II) and iron(III) valence states has been recognized as a fundamental role in modern environmental biogeochemistry and was perhaps an key biogeochemical process on early Earth. The abiotic mechanisms had always thought to dominate environmental iron redox chemistry, before microbially mediated iron redox reactions were discovered. Currently, it is commonly accepted that microbial metabolism mainly controls iron redox reactions on Earth (Weber et al., 2006). In this way, iron was found to be a necessary element in microbial energy metabolism and served as an crucial electron acceptor in the form of ferric iron [Fe(III)], or as an electron donor in the form of ferrous iron [Fe(II)] for a number of microorganisms (Rickard, 2012). In general, iron(II) oxidation and iron(III) reduction are commonly occurred in most environments by different microbial drivers. For example, the microbial oxidation of iron(II) coupled to the reduction of oxygen prefer to occur in aerobic environments at acidic and circumneutral pH values, whereas iron(III) reducing microbes are more active in the anoxic zone of neoteric environments at pH > 4.0, because iron(III) oxides are stable under this condition and provide an important electron sink for both chemical and biological processes [see review (Weber et al., 2006)]. Furthermore, iron oxidizing microbes have been found in 7 phyla of archaea and bacteria, especially the phylum *Proteobacteria*, harboring most of all iron oxidizing bacteria, but all of them did not show conserved phylogeny. Besides, iron oxidizing microbes were also found present in the phyla *Actinobacteria*, *Firmicutes*, *Chlorobi* and *Nitrosospirae*, as well as the phyla *Euryarchaeota* and *Chrenarcaeota* in the domain Archae (Emerson et al., 2010), indicating the phylogenetically diversity of iron oxidizing ability among

microbes. As for iron reducing microbes, they were firstly reported in 1988 by Lovley and Phillips (1986) in the sediment column. Since then, many organisms spread throughout both the bacteria and archaea have been gradually isolated. Although most of the iron reducing microbes are also phylogenetically diverse, similar as iron oxidizing microbes, they contain a large phylogenetically cohesive group, the *Geobacteraceae*, which oxidize acetate to CO₂ with iron(III) serving as the sole electron acceptor as well as the H₂-oxidizing iron(III) reducers (Röling, 2014). Besides, there are still numerous well-studied bacterial genera on iron reducing process, such as *Shewanella*, *Anaeromyxobacter*, *Geothrix* and so on (Weber et al., 2006). These functional microbes not only drive iron redox cycles in the environments, but also are the ideal research tools to make us understand how the iron transformed microbially.

1.4.3 Microbial iron reduction coupled with nitrogen cycles

Microbial iron redox is common occurred in most environments, coupling multiple biogeochemical cycles and accelerating the materials and elements flow along with electrons transformation as described above. Iron reduction, therein, in paddy soils is more common than iron oxidation, due to the second reserves of iron oxides and high propositions (58-79%) of electron transformation from iron reduction (Yao et al., 1999). Furthermore, iron oxide reduction was also reported as the second most important electron sink in paddy soils (Yao et al., 1999), although iron (II) oxidation under anoxic conditions is also occurred, coupling to nitrite or nitrate reduction (Straub et al., 1996), or to photosynthesis (Hegler et al., 2008), regenerating oxidized iron(III) to sustain the iron(III) cycle. Thus, numerous studies have focused on dissimilatory iron(III) reduction owing to its global significance.

Nitrogen cycles, as one of the key process of the biogeochemical cycles, are strongly coupled with iron cycles by many functional microbes. Wang et al.

(2020a) recently reported that iron reduction, triggering chemodenitrification, accelerate nitrate reduction and increase N₂O emission in paddy soils. Moreover, Li et al., (2020a) has noted that iron-reducing bacteria strengthened the biological nitrogen fixation in paddy soils illustrated by the metabolically active bacterial community in flooded paddy soils amended with glucose. Although these studies were based on the culture-independent analysis, the culture-dependent experiments also got similar results. For example, Onley et al. (2018) have reported that the iron-reducing bacterium, *Anaeromyxobacter dehalogenans*, utilized iron cycle to couple its incomplete denitrification process, and then, successfully accomplished denitrification process with N₂O and N₂ generated. Taken together, iron-reducing microbes also play important roles in nitrogen cycles in natura environments.

1.4.4 Iron reducing microbes in paddy soils

Although many iron-reducing microbes were gradually isolated from multiple environments, *Geobacter* spp. and *Anaeromyxobacter* spp. were common accepted to be the predominant drivers reducing iron(III) to iron(II) in paddy soils (Hori et al., 2010). Among them, *Geobacter* is the single and type genus in the family *Geobacteraceae* of the order *Desulfuromonadales*. The type species of this genus, *Geobacter metalireducens*, was the first isolated bacterium reported to reduce iron(III) to iron(II) in the river sediments (Lovley et al., 1993). After that, many *Geobacter* strains were gradually isolated from different terrestrial environments, such as forest soil, lotus field mud, freshwater sediments, and oil/metal-contaminated soils, but no one was isolated from paddy soils (Reguera and Kashefi, 2019). Apart from the common feature of genus *Geobacter* with the ability to reduce iron(III) to iron(II) along with the complete oxidation of acetate to CO₂, they can also utilize various metals, humic substances, alcohols, hydrogen, organic acids, and aromatic compounds as electron acceptors and/or electron

donors, leading to mobilization of metals and mineralization of organic compounds (Reguera and Kashefi, 2019).

Anaeromyxobacter is the single genus in the family *Anaeromyxobacteraceae*, currently belonging to the order *Polyangiales* and the class *Polyangia* (Waite et al., 2020). Now, the genus *Anaeromyxobacter* only contains one species with validly published name, *A. dehalogenans*, even if multiple strains have been isolated but not identified (<https://lpsn.dsmz.de/genus/anaeromyxobacter>). The type species *A. dehalogenans* 2CP-1^T was reported to be isolated from stream sediment with the capacities that reducing iron(III) as the electron acceptor for bacterial growth (Sanford et al., 2002). Besides, a paddy soil-derived *Anaeromyxobacter* strain, Fac12, also showed its dissimilatory iron-reducing ability (Treude et al., 2003) with culture experiments, indicating the ubiquitous ability of iron reduction for *Anaeromyxobacter* strains in different environments. Moreover, recent studies also reported that the two genera, *Geobacter* and *Anaeromyxobacter*, deeply participated in the nitrogen cycles, especially in nitrate reduction and nitrogen fixation, in paddy soils using the DNA- and RNA-based culture-independent analysis (Li et al., 2020a; Masuda et al., 2017; Wang et al., 2020b). Therefore, there may be a new possibility that the two groups of iron reducers work as a bridge, connecting metal reductions and nitrogen cycles together and strengthen the global biogeochemical cycles in paddy soils.

1.5 Research objective

Reductive nitrogen transformation (RNT), including nitrogen fixation, DNRA, and denitrification, in paddy soils is a microorganism-driven process as described above that is crucial for sustainable rice production and environmental conservation. In our previous metatranscriptomic and metagenomic studies of paddy soils in Japan, it was found that most of the gene transcripts involved in RNT are derived from the genera *Geobacter* and *Anaeromyxobacter*, both known

as iron-reducing bacteria. However, to date, no such bacteria with a validly published name have been isolated from paddy soils, and their ability to transform nitrogen also has yet to be confirmed. Thus, I performed this study to isolate paddy soil-derived *Geobacter*-like and *Anaeromyxobacter*-like strains and clarify their ecological roles in paddy soils.

The research purposes of this study are: 1) Isolation and identification of *Geobacter*-like and *Anaeromyxobacter*-like strains from rice paddy soil, 2) Characterization of special abilities related to nitrogen transformation of the isolates, 3) Clarification of the nitrogen metabolic pathways they are taking part involved in the nitrogen cycle of the paddy soils, 4) Exploration of application methods using these strains in paddy soils to improve rice production.

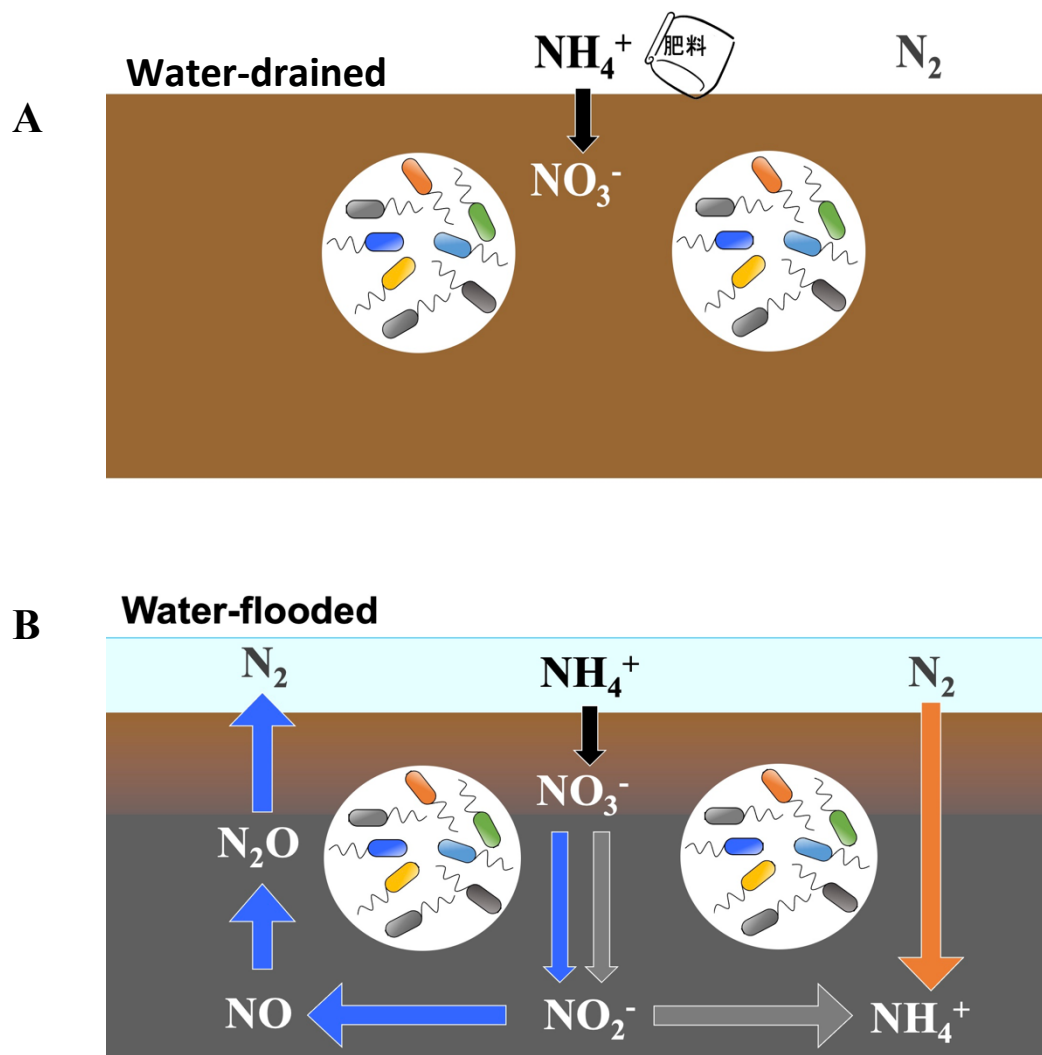


Fig. 1.1 Schematic description of the nitrogen cycle in paddy soils under water-drained condition (A) and water-flooded condition (B). The black arrow indicates nitrification process, oxidizing ammonium to nitrate. The blue arrows indicate denitrification process, reducing nitrate to N_2 . The grey arrows indicate DNRA process, reducing nitrate to ammonium. The orange arrow indicates nitrogen fixation process, fixing N_2 gas to ammonium.

Chapter 2: Isolation and identification of *Geobacter*-like and *Anaeromyxobacter*-like strains and reclassification of the family *Geobacteraceae*

2.1 Introduction

The family *Geobacteraceae*, first proposed by Holmes et al. (2004), was initially clustered into the domain Bacteria and the δ -subclass of Proteobacteria, but recently reassigned into the order *Geobacterales* and class *Desulfuromonadia* based on genome analysis (Waite et al., 2020). This family currently contains a single genus with a validly published name: *Geobacter*, which was first proposed by Lovley et al. in 1993 with a description of the type species, *Geobacter metallireducens* (Lovley et al., 1993). Before this study, the family *Geobacteraceae* contained 19 species with validly published names (<http://www.bacterio.net/geobacter.html>), which were isolated from different environmental sources, e.g., the type species *Geobacter metallireducens* GS-15^T was isolated from surficial bottom sediment (Lovley et al., 1993), *Geobacter daltonii* FRC-32^T from contaminated sediment (Prakash et al., 2010), *Geobacter toluenoxydans* TMJ1^T from tar-oil-contaminated sludge (Kunapuli et al., 2010), and *Geobacter sulfurreducens* PCA^T from wastewater biofilm (Caccavo et al., 1994). Besides these isolates, dozens of *Geobacteraceae* clone sequences have been reported from culture-independent analyses in various environments, such as contaminated sediments (Holmes et al., 2015), wastewater (Tejedor-Sanz et al., 2018), paddy soils (Hori et al., 2010), and freshwater lake sediments (Cummings et al., 2003), indicating that the *Geobacteraceae* family is one of the ubiquitous microbial groups in terrestrial and freshwater ecosystems.

Similar with the genus *Geobacter*, *Anaeromyxobacter* is also the single genus in the family *Anaeromyxobacteraceae*, which was initially assigned to the order *Myxococcales* and the class *Myxococcia* (Yamamoto et al., 2014), but

recently classified into the novel order *Polyangiales* and the class *Polyangia* (Waite et al., 2020). At the time of writing, the genus *Anaeromyxobacter* only contains one species with validly published name, *A. dehalogenans*, even if multiple strains have been isolated but not identified (<https://lpsn.dsmz.de/genus/anaeromyxobacter>). The type species *A. dehalogenans* 2CP-1^T was reported to be isolated from stream sediment with the special capacity that reduce 2-chlorophenol as the electron acceptor, which was a key process in environmental bioremediation (Sanford et al., 2002). Besides, several batch experiments using isolated *Anaeromyxobacter* strains also revealed their special abilities of nitrogen fixation, denitrification coupled with ferric iron reduction and arsenate reduction (Kudo et al., 2013; Masuda et al., 2020; Onley et al., 2018), suggesting *Anaeromyxobacter* strains also play important roles in natural biogeochemical processes.

Paddy soils, as the largest anthropogenic wetlands on Earth, represent a unique ecosystem that cycles between waterlogged and drained states during long-term paddy cultivation (Kögel- Knabner et al., 2010). Bacterial communities in paddy soils are therefore different from those occurring in other agricultural soils, particularly in terms of the abundance of facultative anaerobic or strictly anaerobic microbes. In our previous metatranscriptomic study of paddy soils in Japan, we found that most identified gene transcripts involved in reductive nitrogen transformation were derived from the order *Deltaproteobacteria*, specifically the genera *Geobacter* and *Anaeromyxobacter* (Masuda et al., 2017). Similar results were also described by Breidenbach et al. (2016), who noted that the genera *Geobacter* and *Anaeromyxobacter*, as potential iron reducers, are notably abundant in the rice rhizosphere environment. However, to date, a *Geobacter* or *Anaeromyxobacter* species with a validly published name isolated from paddy soil has not been described. Thus, in order to clarify the environmental roles of these dominant strains in paddy soil, an isolation

experiment, specially target to *Geobacter* and *Anaeromyxobacter* strains, is strongly needed.

In addition, numerous reports have highlighted the unique physiological traits of *Geobacter* species and pointed out their ubiquitous distribution in the terrestrial and freshwater ecosystems over past 30 years (Reguera and Kashefi, 2019), but few of them focus on the phylogenetic status of the genus *Geobacter* or the family *Geobacteraceae*. As introduced above, the family *Geobacteraceae* was proposed and reclassified based on the phylogenetic analysis of 16S rRNA gene and 5 housekeeping genes, similar with the propositions of all species in the genus *Geobacter*, that all of them were assigned to the genus based on the 16S rRNA gene similarities. 16S rRNA gene has been used as a universal phylogenetic marker for bacterial taxonomy more than 30 years, however, the phylogeny and overall genome related index based on the whole genome sequences were more robust and recently encouraged for bacterial taxonomy, especially with the development of next-generation high throughput sequencing technologies (Chun et al., 2018; Rosselló-Móra and Amann, 2015). Moreover, a recent review pointed out that taxonomic reassignment was necessary for all the species in the genus *Geobacter*, because a single species of *Pelobacter propionicus* was phylogenetically located in this genus but showed different physiological features (Reguera and Kashefi, 2019). Thus, a taxonomic reclassification work for the family *Geobacteraceae* is required.

In this chapter, I aim to isolate more *Geobacter*-like and *Anaeromyxobacter*-like strains from paddy soils and their nearby places and characterize them if they are novel species. Furthermore, based on the genome analysis, the taxonomic positions of all members in the family *Geobacteraceae* would also be revised.

2.2 Materials and Methods

2.2.1 Sampling sites, enrichment and isolation

Hundreds of paddy soils and the related environmental samples were collected from more than 30 sites all over the Japan (Fig. 2.1A). After collected, the soil or sediment samples were immediately stored in a portable incubator supplemented with ice and then brought to the Laboratory. All collected samples were treated for experiments once they arrived at the Laboratory or preserved in 4 °C for following studies. Partial of each sample (1.0-3.0 g) was picked up for the enrichment experiments as described as Fig. 2.1B. Detailly, in enrichment experiments for isolating strains named with “S”, 3.0 g of fresh paddy soil samples were added aseptically into 50 mL serum bottles containing 30 mL autoclaved modified freshwater medium supplemented with 20 mM fumarate and 20 mM acetate as electron acceptor and donor, respectively (Lovley et al., 1993). The modified freshwater medium contained the following (MFM; in L⁻¹): 2.0 g KHCO₃, 0.02 g MgSO₄·7H₂O, 0.3 g KH₂PO₄, 0.1 g MgCl₂·6H₂O, 0.08 g CaCl₂·2H₂O, 0.6 g NaCl, 9.52 g HEPES, 10.0 mL vitamin stock solution (in L⁻¹, 2 mg Biotin; 2 mg Folic acid; 10 mg Pyridoxine-HCl; 5 mg Thiamine-HCl; 5 mg Nicotinic acid; 5 mg Aminobenzoic acid; 5 mg Ca-pantothenate; 0.01 mg Vitamin B12; 5 mg Lipoic acid) and 10.0 mL mineral stock solution (in L⁻¹, 12.8 g Nitrilotriacetic acid; 1.35 g FeCl₃·6H₂O; 0.1 g MnCl₂·4H₂O; 0.024 g CoCl₂·6H₂O; 0.1 g CaCl₂·2H₂O; 0.1 g ZnCl₂; 0.025 g CuCl₂·2H₂O; 0.01 g H₃BO₃; 0.024 g Na₂MoO₄·2H₂O; 1g NaCl; 0.12 g NiCl₂·6H₂O; 4 mg Na₂SeO₃·5H₂O; 4 mg Na₂WO₄, pH 6.5). For the isolation of strains named with “Red”, such enrichment culture was performed using soil slurry (air-dried paddy soil/distilled water, 1/1.5) supplemented with only vitamin stock solution, in place of MFM with fumarate and acetate as described above. After bottle neck sealed and gas changed with N₂/CO₂ (80:20, v/v), the enrichment culture bottles were incubated at 30 °C without shaking till the soil color changed to grey. Then the enriched

cultures were collected using syringes and diluted serially in oxygen-free water (10^{-1} to 10^{-4}), 100 μ L samples of every serial dilution were spread on R2A agar (Difco, MA, USA) with 20 mM fumarate (modified R2A agar), this process was performed under sterile and oxygen-free condition. The plates were incubated in anaerobic jars equipped with AnaeroPacks (Mitsubishi Gas Chemical, Tokyo, Japan) and oxygen indicators (Mitsubishi Gas Chemical, Tokyo, Japan) at 30 °C for 10 days. After repeating this process many times with every collected samples, hundreds of red colonies were obtained. Notably, all reported *Geobacter* and *Anaeromyxobacters* strains were identified as red-pigment of colony color due to the presence of *c*-type cytochrome, so red-color of colonies were used as the primary feature for selection.

Moreover, it was also found that all of the isolated strains grew well in modified freshwater medium (MFM) supplemented with 20 mM fumarate as the electron acceptor and 20 mM acetate as the electron donor. All of the isolated strains were preserved at -80 °C in modified R2A broth with 10% (v/v) DMSO. *Geobacter bemidjiensis* DSM 16622^T and *Geobacter chapellei* DSM 13688^T, both obtained from the German Collection of Microorganisms and Cell Cultures (DSMZ), were used as reference strains through the identification work of *Geobacter*-like strains in this study, while *Anaeromyxobacter dehalogenans* ATCC BAA-258^T, obtained from the American Type Culture Collection (ATCC), was used as reference strain in parallel studies with *Anaeromyxobacter*-like strains.

2.2.2 16S rRNA gene amplification and analysis

After all isolated strains with red colored colonies were purified, the biomass for every strain were collected from the modified R2A plates and then mixed with 50 mM NaOH solution. After heating at 95 °C for 10 mins, the bacterial suspensions were directly used as the templates for colony PCR to obtain the near

complete 16S rRNA genes with the common primers 27F (5'-AGAGTTTGATCCTGGCTCAG-3') and 1492R (5'-GGTTACCTTGTTACGACTT-3'). The reaction mixture (50 uL) of colony PCR contains: Template (bacterial suspensions), 1.0 uL; Extag, 0.5 uL; Primers (27F/1492R, 20 uM): each 1.0 uL; 10X buffer, 5.0 uL; dNTP (2.5 mM), 4 uL; Water, 37.5 uL. The PCR reaction conditions were as follows: initial denaturation at 95 °C for 5 min; followed by 30 cycles of 95 °C for 30 s, 50 °C for 30 s, 72 °C for 60 s; 72 °C for 7 min, finally 4 °C for preservation. The PCR products were then detected by agarose electrophoresis using TAE buffer under 100 V for 20 min. The PCR products with single and light bands on agarose gel were purified using a PCR clean-up Kit (Promega, USA) according to the manufacturer's instructions, and then quantified by the NanoDrop™ 1000 Spectrophotometer (Thermo Fisher Scientific, MA, USA). The quantified PCR products were mixed with single primer 27F/1492R (PCR product: 50 ng; Primer: 30 umol; Total: 14 ul) and then sequenced at a company, FASMAC (Tokyo, Japan) using the sanger method. After the near complete 16S rRNA gene sequences of all isolated strains obtained, the similarities of 16S rRNA genes between all the isolated strains and other type species in the families *Geobacteraceae* and *Anaeromyxobacteraceae* were calculated using the identify service in the EzBioCloud Database (<https://www.ezbiocloud.net/identify>) (Yoon et al., 2017).

2.2.3 Genomic fingerprints

Although the phylogenetic positions of all isolated strains were initially determined using the 16S rRNA gene similarities, the repetitive isolates cannot be identified, as the accuracy of a single gene, such as 16S rRNA gene, is too low to distinguish repetitive strains. Thus, a genomic fingerprint study based on the bacterial whole genomes was further carried out. For the specific fingerprints, the bacterial suspensions of all isolates were used as the templates for PCR

amplification according to the methods of random amplified polymorphic DNA (RAPD) (primer: AGCAGCGTGG) (Yu and Pauls, 1992) and repetitive sequence-based PCR (rep-PCR) with ERIC primers (ERIC1/ERIC2) and BOX primer (BoxA1R) (Healy et al., 1994). Detailly, the reaction mixtures (50 μ L) contains: Template (bacterial suspensions), 2.0 μ L; Extag, 1.0 μ L; Primers (20 μ M/each): each 1.0 μ L; 10X buffer, 5.0 μ L; dNTP (2.5 mM), 4.0 μ L; Water, 36.0 μ L, with the reaction condition: initial denaturation at 94 °C for 3 mins; followed by 35 cycles of 94 °C for 30 s, 52 °C for 1 min, 68 °C for 8 min; then 68 °C for 16 min; finally 4 °C for sample preservation. Then 20 μ L of the PCR products were electrophoresed in a 1.5% agarose gel using 1 \times TAE buffer mixed with 3.0 μ L of ethidium bromide/mL under 100 V for 45 min.

The gel bands obtained from BOX primer were further sort out as the marker to separate the repetitive isolates, owing to its high-resolution ratio. The gel bands were digitized and matriculated with values 0 (no band) and 1 (band), and then a heatmap with the clustered isolates was generated using the “pheatmap” package of R version 3.5.2.

2.2.4 Genome sequencing and comparison

The genomic DNA samples of selected strains for further investigation were extracted from 3–5 days cultures grown on modified R2A agar using the DNeasy Blood and Tissue Kit (Qiagen, Germany), according to the manufacturer’s instructions for Gram-negative bacteria, while the purchased type strains were cultured using their reported mediums. The quality and quantity of all DNA samples were determined by NanoDrop™ 1000 Spectrophotometer (Thermo Fisher Scientific, MA, USA) and Qubit 2.0 Fluorometer (Invitrogen, MA, USA) with the corresponding reagents. Subsequently, the DNA samples were fragmented randomly by sonication to produce DNA fragments of less than 500 bp, and then end repair and the adapter ligation were carried out. After

amplification and purification, the qualified libraries with different indices were constructed and then sequenced using the Illumina HiSeq instrument (Illumina, CA, USA) with a 2x150 paired-end (PE) configuration at Genewiz Inc. (Suzhou, China). The raw data of the sequencing were quality checked and assembled to long contigs using the Velvet (Zerbino and Birney, 2008), and the gaps were filled with the SSPACE and GapFiller (Boetzer et al., 2010; Boetzer and Pirovano, 2012).

The assembled contigs with more than 100-fold coverage were used for genome annotation and analysis with different database and tools as following. The open reading frames prediction and functional genes annotation were performed based on SEED database of the RAST server (Aziz et al., 2008) and NCBI Refseq database (Pruitt et al., 2005), while the metabolic pathways were annotated with KEGG database (Kanehisa and Goto, 2000). Besides the genomes obtained from this study, those of other species in the family *Geobacteraceae* were retrieved from NCBI database and analyzed equally in the following steps. The DNA G+C contents of all analyzed species were calculated from the genome sequences as described by Meier-Kolthoff et al., (2014). The overall genome related index at the nucleotide level was usually revealed with the average nucleotide identity (ANI) and the digital DNA-DNA hybridization (dDDH). Therein, ANI values between all studied isolates and other type species in the family *Geobacteraceae* were calculated in silico using the JspeciesWS tool with the BLAST+ algorithm (Richter et al., 2016), while dDDH values were obtained using the Genome-to-Genome Distance Calculator 2.1 (GGDC) with recommended BLAST+ alignment and Formula 2. Moreover, at the amino acid level, the average amino acid identity (AAI) and percentage of conserved protein (POCP) were widely used to determine the genomic similarity (Konstantinidis and Tiedje, 2005; Qin et al., 2014). AAI and POCP values of each pairs among members in the families *Geobacteraceae* and *Anaeromyxobacteraceae* were

calculated using an online-tool (<http://enve-omics.ce.gatech.edu/>) and a Python script (<https://github.com/2015qyliang/POCP>), respectively.

2.2.5 Phylogenetic analysis

The 16S rRNA gene sequences of related strains were downloaded from the NCBI database and aligned using CLUSTAL W algorithm in MEGA X (Kumar et al., 2018). The phylogenetic trees were constructed using neighbour-joining, maximum-likelihood and maximum-parsimony methods with 1, 000 bootstrap replicates. In order to elucidate the exact taxonomic position of the isolated strains, a phylogenetic tree based on 92 concatenated core genes was also constructed using the up-to-date bacterial core gene (UBCG) pipeline (www.ezbiocloud.net/tools/ubcg) as described previously (Na et al., 2018). In addition, previous studies revealed that five housekeeping genes (*fusA*, *gyrB*, *nifD*, *recA* and *rpoB*) were better to define the phylogeny of the family *Geobacteraceae* (Holmes et al., 2004), so a multilocus sequence analysis (MLSA) of these five housekeeping genes was performed with the primers GYR48F/GYR1010R, NIFDF2/NIFDR2, RPO175F/RPO800R and two modified primer pairs for *recA* (*recF*: 5'-TGATCGAGATCTTCGGACCGGA-3'; *recR*: 5'-TCCTTGCCGTAGGAGAACCA-3') and *fusA* (*fusF*: 5'-CTNGACATCAAGATCTGCCC-3'; *fusR*: 5'-TTCGCCTCNACCTTGAAGTC-3'). The deduced amino acid sequences of five housekeeping genes were translated with standard codons using MEGA X software (Kumar et al., 2018). After the nucleotide sequences and amino acid sequences of the five housekeeping genes were respectively aligned and concatenated in order (*rpoB*–*recA*–*nifD*–*gyrB*–*fusA*), phylogenetic trees based on concatenated nucleic acid and amino acid sequences were generated using the maximum-likelihood method as described above.

2.2.6 Phenotypic characterization

Cell morphology and size were examined by transmission electron microscopy (model JEM-1400, JEOL) at 80 kV, after the cultures were negatively stained with ammonium molybdate. Colony size, shape and colour were determined after 3-5 days of incubation at 30 °C on modified R2A agar. The temperature and pH tests were performed in modified R2A broth at different temperatures (6, 10, 13, 16, 20, 25, 30, 33, 37, 40, and 45 °C) and different pH (adjusted from 5.0 to 9.0 in increments of 0.5 pH units) with 20 mM buffers (MES, pH 5.0–6.5; HEPES, pH 7.0–8.0, Tricine, pH 8.5–9.0). Growth was measured at OD₆₀₀ using a spectrophotometer (Jasco V550, Japan) after 1 week of culture. The requirement and tolerance to NaCl was tested on modified R2A agar supplemented with various concentrations of NaCl (adjusted from 0 to 1.0% with 0.1% increments). Electron donor and acceptor utilization tests were carried out using degassed MFM at 30 °C. Acetate (10 mM) was used as the electron donor for all electron acceptor tests while Fe(III)-NTA (5 mM) was the electron acceptor for all electron donor tests. The final concentrations of detected electron acceptors and donors were utilized as previously described (Nevin et al., 2005). Enzymatic activities of the four isolates and reference strain were detected using API ZYM strips (bioMérieux) based on the manufacturer's instructions. Cytochrome analysis of the four analysed strains was performed with cell grown in MFM with 20 mM fumarate and 20 mM acetate. Cultures (5 ml) were collected and resuspended in 2 ml of 20 mM PIPES buffer (pH 7.0). A dithionite-reduced minus air-oxidized difference spectrum of whole cells was obtained using a Jasco V550 spectrophotometer (Lovley et al., 1993).

2.2.7 Chemotaxonomic characterization

For fatty acid detection, biomass of all chose isolates and their reference strains was collected from cultures grown for 2-3 days at 30 °C in modified R2A

broth, when the bacteria were in the late exponential growth phase. After washed twice in autoclaved distilled water and freeze dried, the fatty acid was extracted as described previously (Kunapuli et al., 2010). The fatty acid profiles were determined using a gas chromatography mass spectrometry (GCMS-QP2010 ultra, Shimadzu, Japan) with the standard reagents for different fatty acids (Gunina et al., 2014). Biomass collection for respiratory quinones analysis was same as fatty acid detection, except cultured for 5 days to get more biomass. Extraction and purification were performed as described previously (Bligh et al., 1959) and Sep-Pak plus silica (Waters, USA) was employed for separation of quinones. Quinone profiles were determined using HPLC with ACQUITY UPLC H-Class system (Waters, USA), which was carried out by the TechnoSuruga Laboratory (Shizuoka, Japan).

2.2.8 Reclassification of the family *Geobacteraceae*

The five type species, *Geobacter pelophilus* DSM 12255^T, *Geobacter grbicum* DSM 13689^T, *Geobacter hydrogenophilus* DSM 13691^T, *Geobacter chapellei* DSM 13688^T and *Geobacter luticola* JCM 17780^T obtained from the German Collection of Microorganisms and Cell Cultures (DSMZ) and Japan Collection of Microorganisms (JCM), were cultured using MFM medium as described previously with 10 mM acetate as the electron donor and 5 mM Fe(III)-NTA as the electron donor. The genomic DNA samples were extracted from the collected biomass with the DNeasy Blood and Tissue Kit (Qiagen, Germany). The genomes were sequenced using the Illumina HiSeq instrument (Illumina, CA, USA) with a 2x150 paired-end (PE) configuration at Genewiz Inc. For details, see Chapter 2.2.4.

The process for genome annotation and comparison is same with that described in Chapter 2.2.4. ANI, AAI and POCP values were used to quantify the genomic

similarity. The visualization of the numerical correlation and matrix for ANI, ANI and POCP values was carried out by using R version 3.5.2.

The 16S rRNA gene of every species in the family *Geobacteraceae* were fetched from the corresponding genome sequences unless otherwise stated, and their similarities between each pair of all *Geobacteraceae* members were determined using the Identify service of EZBioCloud (Yoon et al., 2017). Phylogenetic analysis based on the 16S rRNA gene, MLSA and UBCG were same with those described in Chapter 2.2.5.

2.3 Results and discussion

2.3.1 Isolation of different *Geobacter*-like and *Anaeromyxobacter*-like strains

In this study, hundreds of red colonies were first isolated from paddy soils and nearby places collected in different places all over the Japan using enrichment culture combined with spread plate method. After purification and primary verification by the 16S rRNA sequencing, 71 isolates, similar with *Geobacter* spp, and 3 isolates, similar with *Anaeromyxobacter* spp., were identified (Fig. 2A). Given all *Anaeromyxobacter* strains showed obviously difference of 16S rRNA gene similarities (< 98%), only *Geobacter*-like strains with high 16S rRNA gene similarities were investigated using genomic fingerprint for repetition checking. As shown in Fig. 2B, the 63 of the 71 isolates are different strains due to the different fingerprint patterns. Subsequently, the 14 of the 63 different strains (S43^T, S62^T, Red32^T, Red51^T, Red53^T, Red69^T, Red88^T, Red96^T, Red100^T, Red111^T, Red276^T, Red330^T, Red736^T and Red745^T) belonging to the family *Geobacteraceae* and all the 3 *Anaeromyxobacter*-like strains (Red232^T, Red267^T and Red630^T) were sort out for a complete polyphasic taxonomy analysis.

2.3.2 Polyphasic taxonomy of *Geobacter*-like and *Anaeromyxobacter*-like strains

2.3.2.1 Phylogenetic analysis of all chosen strains

Nearly complete 16S rRNA gene sequences (> 1400 bp) were obtained for all chosen 14 *Geobacter*-like and 3 *Anaeromyxobacter*-like strains. Primary comparisons using Blastn tool of NCBI database suggested these strains belong to the families *Geobacteraceae* and *Anaeromyxobacteraceae*, respectively, with the high similarity values. In the phylogenetic tree based on the 16S rRNA gene sequences, all of the 14 *Geobacter*-like strains were located within the clade comprising species of the family *Geobacteraceae* (Fig. 2.3A), whereas 3 *Anaeromyxobacter*-like strains were fell within the cluster of species in the family *Anaeromyxobacteraceae* (Fig. 2.3B). However, the 14 novel *Geobacter*-like strains formed 2 coherent clusters (group 1 and group 2) among the species in the family *Geobacteraceae* based on the phylogenetic analysis. Therein, group 1 is consisted of 11 isolated strains, S43^T, S62^T, Red32^T, Red51^T, Red53^T, Red69^T, Red111^T, Red276^T, Red330^T, Red736^T and Red745^T, clustered with *G. bemidjiensis* Bem^T and *G. bremensis* Dfr1^T, while group 2 just includes strains Red88^T, Red96^T and Red100^T, with a bootstrap resampling value of 100% (Fig. 2.3A). This topological structure was further confirmed by the phylogenetic trees drawn using the UBCG and MLSA, which also placed the 14 strains in 2 independent and monophyletic branches in the family *Geobacteraceae* and showed high robustness (Fig. 2.4). These stable phylogenetic relationships suggest that the 2 novel clusters may consist of two novel taxa in the family *Geobacteraceae*.

Pairwise comparisons of the 16S rRNA gene sequences in group 1 revealed 96.1–99.8% similarity between each pair within the 11 isolated strains. *G. bemidjiensis* Bem^T and *G. bremensis* Dfr1^T were the most closely related strains

in the family *Geobacteraceae* to these 11 isolated strains and showed 16S rRNA gene sequence similarities of 96.7–98.3% and 96.8–98.0%, respectively. However, the 16S rRNA gene sequences similarity values are as low as 93.3% (mean value) when these isolated strains were in contrast with other valid *Geobacter* strains, except with *G. bemidjiensis* Bem^T and *G. bremensis* Dfr1^T (Table 2.1). Similar results were also occurred for the group 2, whose pairwise comparisons of the 16S rRNA gene sequences among the 3 strains are 99.0–99.9% similarities, but when they compared with other *Geobacter* species, the similarity values were lower than 95.7% with a mean similarity value of 93.9% (Table 2.1). In addition, Yarza et al., (2014) recently proposed that the generally used arbitrary genus threshold of 16S rRNA gene identity should be revised to a lower minimum value of 94.5% from the previous 95% with a confidence interval of 94.55–95.05 and median sequence identity of 96.4%. However, comparison of the 16S rRNA genes of strains in the 2 groups with the sequence of the type strain of the type species *G. metallireducens* showed similarity values ranging from 91.9–92.9%, which is clearly lower than the common threshold for genus differentiation. Thus, together with the distinct branches on the phylogenetic trees, the 14 isolated strains in 2 groups may be classified into 2 distinct genera from the type species *G. metallireducens*.

As described above, strain *A. dehalogenans* 2CP-1^T is the sole valid species in the genus *Anaeromyxobacter* and in the family *Anaeromyxobacteraceae* (Yamamoto et al., 2014). Pairwise comparisons of the 16S rRNA gene sequences among three *Anaeromyxobacter*-like isolates (Red232^T, Red267^T and Red630^T) and *A. dehalogenans* 2CP-1^T showed similarity values of 95.4–97.4% (Table 2.2), higher values than that of the genus threshold proposed by Yarza et al. (2014), but lower than the proposed species threshold (98.65%) (Kim et al., 2014). These findings indicate that these three *Anaeromyxobacter*-like isolates may represent three novel species in the genus *Anaeromyxobacter*.

2.3.2.2 Genomic characteristics and comparison

The draft genomes of the 14 *Geobacter*-like and 3 *Anaeromyxobacter*-like strains were sequenced with a high sequencing coverage ($> 150\times$). For the 14 *Geobacter*-like strains, the genome size was ranging from 3.6 – 5.5 Mb, with the DNA G+C content from 58.4 – 62.6 mol%. However, when compared the genomic characteristics among these 14 strains, it was found that the three strains, Red88^T, Red96^T and Red100^T in group 2 showed lower values in both genome size and G+C content than those of the 11 strains in the group 1, indicating the obvious genomic difference between these two groups. Notably, the G+C content values of the 11 strains in the group 1 are 60.3 – 62.6 mol%, which are evidentially higher than their three phylogenetic neighbors, *G. uraniireducens* Rf4^T, *G. daltonii* FRC-32^T and *G. toluenoxydans* TMJ1^T with values of 53.6 – 54.2 mol%. Previous literatures indicated that within-species variation in DNA G+C content is at most 5 mol% (Moreira et al., 2011), which demonstrated that the 11 isolates in the group 1 mostly represented a different genus from their three close neighbors. Similar results were also happened for the three strains in the group 2, that strains Red88^T, Red96^T and Red100^T in the group 2 showed the G+C content of 58.4, 59.0 and 59.7 mol%, respectively, but their two close phylogenetic neighbors, *G. lovleyi* SZ^T and *G. thiogenes* K1^T showed those of 54.8 and 52.8 mol%. These facts indicated that all of the strains in the two groups mostly represented two novel genera in the family *Geobacteraceae*. For the 3 *Anaeromyxobacter*-like strains, the draft genome sizes were ranging from 4.6 – 6.7 Mb with the DNA G+C content of 73.5 – 74.5 mol%, in line with the genomic characteristics of strain *A. dehalogenans* 2CP-1^T with genome size of 5.03 Mb and DNA G+C content of 74.8 mol%. More detailed genomic characteristics of these studied strains were listed in Table 2.3.

The genomic comparison was qualified at the nucleic acid level using ANI and GGDC values and at the amino acid level using AAI and POCP values. As shown

in Table 2.4 and 2.5, all of the 14 *Geobacter*-like strains shared similarity values ranging from 67.4 – 78.3 % of ANI and 17.0 – 22.8 % of GGDC with other valid reported *Geobacteraceae* species, which are well-below the defined thresholds for species delineation of 95 – 96% for ANI and 70% for GGDC (Chun et al., 2018), and further support the conclusion of the 14 *Geobacter*-like strains as novel taxa in the family *Geobacteraceae*. When the 14 *Geobacter*-like isolates were compared with each other, the ANI values and GGDC values were in the range of 69.8 – 95.6% and 44.9 – 64.6%, respectively (Table 2.4 and 2.5). Among them, the maximum relatedness values related to the isolated strains except strains Red53^T and Red88^T were 93.8% (ANI) and 61.7% (GGDC), which are lower than the threshold for delineation of bacterial species as described above, supporting the classification of these 12 isolates as 12 novel species. However, there was slightly more variability in two pairs of strains Red53^T - Red111^T and Red88^T - Red96^T in the ANI and GGDC values (95.3% and 64.6%), respectively; the values are located in the transition zone for novel species description of 95 – 96% for ANI and 60 – 70% for GGDC (Richter and Rosselló-Móra, 2009). Although the two pairs of strains Red53^T – Red111^T and Red88^T – Red96^T can be separated from other known *Geobacteraceae* species as novel species with lower ANI (Max. 93.8%) and GGDC (Max. 56.2%) values, their species status cannot be separated from each other in each pair based on their genomic relatedness. Given the obscure position of strains Red53^T and Red88^T, more comparisons were performed based on their physiological and biochemical characteristics. For the 3 *Anaeromyxobacter*-like strains, when they compared with each other or with the type species *A. dehalogenans*, the ANI and GGDC values of each pair were ranging from 75.3 – 79.5% and 19.6 – 21.7%, respectively (Table 2.6), which are obviously higher than the threshold for delineation of bacterial species, suggesting that these three *Anaeromyxobacter*-like isolates represent three different species from the known *A. dehalogenans*.

Because genomic relatedness with nucleotide sequences were not suitable for genera separation (Qin et al., 2014), we further determined AAI and POCP values, which are robust approaches based on amino acid sequences, to determine the genome distance between the 14 isolated strains and other known closely species in the family *Geobacteraceae* (Fig. 2.5). The 14 isolated strains shared similarities of 70.4 – 78.5% for AAI and 66.1 – 77.0% for POCP to *G. bemidjiensis* and *G. bremensis*, 57.1 – 64.9% for AAI and 44.3 – 62.8% for POCP to other known *Geobacteraceae* species (Table 2.7). Qin et al. (2014) proposed a threshold for genera delineation with the 50% of POCP, meaning the 11 isolated strains in the group 1 belong to different genera from *G. lovleyi*, *G. thiogenes* and *P. propionicus* of the family *Geobacteraceae*. However, based on 16S rRNA gene phylogenetic analysis (Fig. 2.3A), the type strains of *G. lovleyi*, *G. thiogenes* did not show the furthest genetic distance from the isolated strains in the group 1 within the family *Geobacteraceae*. The 50% boundary of POCP, hence, is not an appropriate metric for delineating genera within the family *Geobacteraceae*, as reported previously for the families *Methylococcaceae* (Orata et al., 2018), *Bacillaceae* (Aliyu et al., 2016), *Burkholderiaceae* (Lopes-Santos et al., 2017), *Neisseriaceae* (Li et al., 2017), and *Rhodobacteraceae* (Wirth and Whitman, 2018). Additionally, AAI, which delimits taxonomic ranks at the genus levels, has proposed a threshold range of 60 – 80% to separate different genera (Luo et al., 2014). However, because of the large range in genera separation, specific AAI boundaries have been proposed for several families for genera delineation. For example, the family *Methylococcaceae* used 71% AAI as the lower genus limit (Orata et al., 2018), the family *Methylothermaceae* used 70% 70% AAI as the threshold to separate its genera (Skenner et al., 2015), and ~80% AAI was reported for the family *Rhodobacteraceae* (Wirth and Whitman, 2018). Thus, the large difference from 64.9% AAI of maximum value within *Geobacter* species to 69.6% AAI of minimum value within the species in the group 1 or to 95.0% AAI of minimum value within the species in the group 2 is distinct enough to

define three different genera in the family *Geobacteraceae* (Table 2.7). Moreover, along with the separated branches in the phylogenetic trees, it was clearly proposed the thresholds separating different genera from the traditional genus, *Geobacter*, based on the similarity of amino acid sequences with values of 65% POCP and 68 – 70% AAI, which in turn confirmed the status of two novel genera of the strains in two groups (**Fig. 2.5**). Notably, the two thresholds proposed here to classify bacterial strains in the family *Geobacteraceae* are just concluded from the data analysis, rather than strict cut-off values, indicating a certain transition zone (ca. 2% of AAI) is also present for the proposed thresholds.

For the 3 *Anaeromyxobacter*-like strains, the AAI and POCP values of each pair among them are ranging from 63.4 – 66.6% and 50.1 – 59.0%, respectively (Table 2.8). When compared with the type species *A. dehalogenans*, strain Red232^T showed the highest similarity values of 72.2% AAI and 61.8% POCP, while strain Red630^T showed the smallest similarity values of 64.5% AAI and 57.2% POCP (Table 2.8). These POCP values are well-higher than the proposed threshold (50%) for genus separation, whereas the AAI values are located in the transition zone for novel genera description, indicating novel genera different from *Anaeromyxobacter* cannot be proposed evidently.

2.3.2.3 Morphological and physiological characterization

The 14 *Geobacter*-like isolates were characterized as Gram-stain negative, motile, and strictly anaerobic. Growth on the modified R2A plate were better than on the modified freshwater plate. TEM images of the 14 *Geobacter*-like isolates showed that the cells were rod-shaped, with 0.4 – 0.8 µm wide and 1.0 – 7.0 µm long and contained peritrichous flagella for motility (Fig. 2.6). Growth of the 14 isolated strains was observed under 42 °C with an optimum of 30 – 33 °C and at pH 5.0 – 8.0 with a relative optimum of pH 6.5. Notably, 2 strains of them, Red53^T and Red111^T can grow at the temperature of 10 °C, the lowest

temperature among all the isolated strains, indicating these paddy soil-derived strains are mesophilic bacteria and mainly working on non-frozen soils. All of the 14 strains can tolerate 0.4% (w/v) NaCl and grew well under 0.2%, whereas several strains such as strains S43^T, Red53^T, S62^T, Red69^T, Red111^T, Red736^T and Red100^T can tolerate a high concentration of 0.7% (w/v) NaCl. For enzyme activity detected with API ZYM strips, all analyzed strains contained leucine arylamidase, acid phosphatase, and naphthol-AS-BI- phosphohydrolase activities. Besides them, strains Red32^T, S43^T, Red51^T, Red53^T, S62^T, Red69^T, Red276^T, Red330^T, Red736^T and Red745^T contained esterase (C4) and esterelipase (C8) activities, strains Red53^T, Red330^T, Red745^T, Red88^T, Red96^T, and Red100^T also contained alkaline phosphatase (Table 2.9). The *c*-type cytochromes were present based on the different spectra of whole cells (Fig. 2.7). In detail, the *c*-type cytochromes for strains S43^T, S62^T, Red69^T, Red111^T, Red330^T, Red96^T and Red100^T have the same absorbance peaks of 424, 524, and 554 nm, indicating the same structure of cytochromes among these isolates, whereas other strains showed distinct differences of absorbance peaks, especially the comparison with the two reference strains, *G. bemidjiensis* DSM 16622^T (422, 522, and 555 nm) and *G. chapellei* DSM 13688^T (423, 526 and 553 nm) (Table 2.9). Similar to other species in the family *Geobacteraceae*, all of the isolated strains possessed ferric reducing ability, which reduced ferric iron [Fe(III)-NTA, ferrihydrite] to ferrous iron and utilized ferric iron as the electron acceptors for their anaerobic growth. Other phenotypic characteristics of the strains are presented in Table 2.9 along with the species description. Based on these physiological features, strains Red53^T and Red88^T showed clearly difference from their relative neighbors, detailly in different electron donors and enzyme activities between strains Red53^T and Red111^T and in distinct absorbance peaks of *c*-cytochrome between strains Red88^T and Red96^T, confirming the possible distinct species status of strains Red53^T and Red88^T from their closest genomic relatives.

For the 3 *Anaeromyxobacter*-like strains, they also showed similar characteristics with the *Geobacter*-like strains as described above, such as Gram-stain negative, strictly anaerobic and a better growth condition with modified R2A medium than MFM. Moreover, based on the TEM images, the three *Anaeromyxobacter*-like strains showed the long rod-shaped with 0.2 – 0.6 μm wide and 2.0 – 12.0 μm long. Strain Red267^T was determined with peritrichous flagella for motility, but other two strains, Red232^T and Red630^T did not have. Growth conditions of these three strains revealed the common temperature ranging from 20 – 40 °C (optimum 30 – 33 °C), pH ranging from 5.0 – 8.0 (optimum 7.0), and NaCl concentration ranging from 0% – 0.5% (optimum 0 – 0.1). However, the sole type species *A. dehalogenans* 2CP-1^T showed the growth conditions of temperature ranging from 15 – 42 °C, pH ranging from 5.5 – 8.5, and NaCl concentration ranging from 0 – 1.8%, distinct enough to separate it from the three novel isolates. Besides, the three novel isolates along with the type species *A. dehalogenans* also showed distinct characteristics related to electron donors/acceptors and enzyme activities between each pair within all of strains (Table 2.10). For instance, strains 2CP-1^T can use arginine as the electron donor and use oxygen as the electron acceptor, but other three isolates cannot, only strain Red630^T can degrade phenol and only Red267^T did not contain alkaline phosphatase. These findings of different characteristics among the four analyzed strains suggested the independent status of these four strains and further confirmed that strains Red232^T, Red267^T and Red630^T represent three novel species obviously different from the type species *A. dehalogenans*.

2.3.2.4 Chemotaxonomic characterization

For the 14 *Geobacter*-like isolates, the major fatty acids (>10% of the total fatty acids) present in most strains (> 7) were identified as iso-C_{15:0} and C_{16:0}, consistent with the two reference strains *G. bemidjiensis* DSM 16622^T and *G.*

chapelleyi DSM 13688^T. Moreover, several strains such as strains Red51^T, Red53^T, Red276^T, Red330^T and Red745^T contain C_{15:0} as the predominant composition, while strains Red276^T, Red330^T and Red745^T also contain C_{15:1} ω 5*c* as the predominant composition. However, the 3 strains in the group 2 of *Geobacter*-like isolates, Red88^T, Red96^T and Red100^T, contain C_{16:1} ω 7*c* as the predominant composition, which is much more than that of all strains in group 1, indicating C_{16:1} ω 7*c* may be an indicator to separate the two groups of all isolated strains (Table 2.11). Other moderate and minor amounts of all the strains showed no significant differences, as shown in Table 2.11. Notably, strains Red53^T and Red88^T showed different major fatty acid profiles from those of strain Red111^T and Red96^T, respectively, which further certified the separate species status of strains Red53^T and Red88^T. The respiratory quinone was also investigated for all 14 isolates and MK-8 was identified as the predominant quinone, in line with the quinone profiles of other reported *Geobacteraceae* species (Sun et al., 2014; Viulu et al., 2013; Zhou et al., 2014)

For the 3 *Anaeromyxobacter*-like isolates along with the reference strain *A. dehalogenans* 2CP-1^T, C_{16:0} was detected as the shared and predominant fatty acid for all strains. Besides that, strain Red232^T also contains iso-C_{15:0}, anteiso-C_{15:0}, and iso-C_{16:0}, strain Red267^T also contains iso-C_{15:0}, iso-C_{16:0} and iso-C_{17:0}, strain Red630^T also contains iso-C_{17:0} and anteiso-C_{17:0}, and strain 2CP-1^T also contains iso-C_{15:0} and unidentified C_{17:1} as the major profiles of fatty acid (Table 2.12). These distinct composition profiles present in the 4 *Anaeromyxobacter* strains revealed the obvious different physical characteristics among these strains, indicating different species status of the 4 strains. Similar with described *Geobacter*-like isolates, MK-8 was also the respiratory quinone of all analyzed *Anaeromyxobacter* strains.

2.3.3 Taxonomic conclusion

In this study, we isolated 17 novel iron-reducing strains, including 14 *Geobacter*-like strains and 3 *Anaeromyxobacter*-like strains, from paddy soils and the related environments collected from different places all over Japan. Phylogenetic analyses based on 16S rRNA genes, UBCG, and MLSA showed that the 14 *Geobacter*-like strains formed two robust and different groups in the family *Geobacteraceae*. The group 1 consisting 11 different isolated strains was phylogenetically clustered with two relatives (*G. bemidjiensis* and *G. bremensis*) and were obviously separate from other type strains of the family *Geobacteraceae*, while the group 2 consisting 3 strains formed an independent branch from their relatives. When all of the isolated strains were compared with each other or with their closest phylogenetic relatives, the genomic relatedness with ANI and GGDC values were less than the proposed threshold value for species delineation (Table 2.4 and 2.5), indicating that these isolated strains are not from a clonal origin and represent three novel species. This distinctiveness was also supported by the biochemical characteristics and fatty acid profile results (Table 2.9 and 2.11). When comparing strains Red53^T to Red111^T and Red88^T to Red96^T, although these two pairs showed high genomic relatedness in the transition zone for novel species classification, their physiological and biochemical characteristics clearly differed. Thus, the 14 isolates represented 14 novel species in the family *Geobacteraceae*. In addition, the 16S rRNA gene similarities between the 14 isolated strains and *G. metallireducens*, the type species of the genus *Geobacter*, showed a lower value than the common threshold for genus differentiation (Yarza et al., 2014). On the basis of the genomic G + C content, the 11 strains in the group 1 together with the two close relatives (*G. bemidjiensis* and *G. bremensis*) were separated clearly from their phylogenetic neighbors, *G. uraniireducens*, *G. daltonii* and *G. toluenoxydans* with > 5 mol% difference (Table 2.3). These facts, along with the robust phylogenetic positions

and the difference in AAI and POCP values, indicate that the 11 isolated strains in the group 1 represent a novel genus in the family *Geobacteraceae*. Therefore, we proposed a new genus, *Geomonas* gen. nov., which also includes the new combinations *Geomonas bemidjiensis* comb. nov. and *Geomonas bremensis* comb. nov., to accommodate *Geobacter bemidjiensis* and *Geobacter bremensis*. Similarly, the 3 isolated strains in the group 2 also showed lower values of genomic comparison than the common thresholds for genera/species separation, indicting three strains Red88^T, Red96^T and Red100^T also represented a novel genus, for which we named *Oryzomonas* gen. nov. Additionally, the phylogenetic trees based on gene and protein sequences strongly suggests that the remaining *Geobacter* is still paraphyletic (Fig. 2.3; Fig. 2.4). This proposition of the novel genera *Geomonas* and *Oryzomonas* is a pioneer but only a start of the taxonomic reclassification for the genus *Geobacter*. More taxonomic studies are still needed to overhaul *Geobacter* taxonomy.

For the three *Anaeromyxobacter*-like strains, phylogenetic analysis based on the 16S rRNA gene revealed that they are located in the family *Anaeromyxobacteraceae*, because they were clustered with the sole valid species in the *Anaeromyxobacteraceae*, *A. dehalogenans* 2CP-1^T, which was further confirmed by the comparisons at the 16S rRNA gene and the whole genome levels, that the 3 isolates strains shared the highest similarity values with *A. dehalogenans* 2CP-1^T. Besides, the similarity values based on the genomic comparison (ANI and GGDC) were much lower than the proposed threshold values for species delineation, indicating that these 3 isolates are different enough to be three novel species, which are further confirmed by the difference of physiological and biochemical characteristics, such as electron acceptors/donors, enzyme activities and fatty acid profiles. Hence, three novel species in the genus *Anaeromyxobacter*, *A. oryzae*, *A. diazotrophica* and *A. paludicola* are proposed.

2.3.4 Description of novel genera and novel species

Description of *Geomonas* gen. nov.

Geomonas (Ge.o.mo'nas. Gr. fem. n. *ge*, the earth; L. fem. n. *monas*, a unit, monad; N.L. fem. n. *Geomonas*, a monad from the earth).

Cells are Gram-stain negative, strictly anaerobic, chemoheterotrophic, non-spore-forming, rod-shaped, and motile by peritrichous flagella or non-motile. Colonies are red-pigmented due to the presence of c-type cytochromes. Able to use fumarate, Fe(III)-NTA, and ferrihydrite as the electron acceptors in the presence of a variety of electron donors, including yeast powder, tryptone, glucose, acetate, pyruvate, casamino acid, nicotinate, proline, mannitol and malate. The predominant quinone is MK-8; MK-7 and MK-9 are also present in some species. The genomic DNA G + C content is 60.3 – 62.6 mol%. The type species is *Geomonas oryzae*.

Description of *Geomonas oryzae* sp. nov.

Geomonas oryzae (o.ry'zae. L. gen. n. *oryzae*, of rice, referring to the isolation of the type strain from rice paddy soil).

Besides the characteristics that define the genus, the following characteristics are observed. Growth occurs at 13 – 42 °C (optimum, 30 – 33 °C), at pH 5.5 – 8.0 (optimum, 6.0 – 7.0), and with 0 – 0.7% (w/v) NaCl (optimum, 0 – 0.2%). With Fe(III)-NTA as electron acceptor, methanol, lactate, succinate, propionate, glutamine, glycerol, isopropanol, serine, naphthalene, salicylic acid, and arginine can also be utilized as electron donor, but phenol, butanol, toluene, benzyl alcohol, and benzaldehyde cannot be utilized as electron donor. With acetate as electron donor, malate, nitrite, and nitrate can also be utilized as electron acceptor, but Fe(III) pyrophosphate, Fe(III) citrate, sulfur, and MnO₂ cannot be utilized as electron acceptor. Esterase (C4), esterelipase (C8), leucine arylamidase, acid phosphatase, and naphthol-AS-BI-phosphohydrolase activities were present but

alkaline phosphatase, lipase (C14), valine arylamidase, cystine arylamidase, trypsin, α -chymotrypsin, α -galactosidase, β -galactosidase, β -glucuronidase, α -glucosidase, β -glucosidase, N-acetyl- β -glucosaminidase, α -mannosidase, and α -fucosidase activities are absent. The major fatty acids are iso-C_{15:0} and C_{15:0} 3-OH. MK-7 and MK-9 are present in minor amounts.

The type strain, S43^T (= MCCC 1K03691^T = JCM 33030^T), was isolated from paddy soil of a field in Niigata, Japan. The genomic DNA G + C content of type strain is 61.2 mol%.

Description of *Geomonas edaphica* sp. nov.

Geomonas edaphica (e.da'phi.ca. Gr. neut. n. edaphos, ground; L. fem. suff. -ica, adjectival suffix used with the sense of belonging to; N.L. fem. adj. *edaphica*, living in soil).

Besides the characteristics that define the genus, the following characteristics are observed. Growth occurs at 10 – 42 °C (optimum, 30 – 33 °C), at pH 5.5 – 8.0 (optimum, 6.0 – 7.0), and with 0 – 0.7% (w/v) NaCl (optimum, 0–0.2%). With Fe(III)-NTA as electron acceptor, lactate, succinate, propionate, glutamine, glycerol, isopropanol, serine, naphthalene, salicylic acid, and arginine can also be utilized as electron donor, but methanol, phenol, butanol, toluene, benzyl alcohol, and benzaldehyde cannot be utilized as electron donor. With acetate as electron donor, malate, nitrite, and nitrate can also be utilized as electron acceptor, but Fe(III) pyrophosphate, Fe(III) citrate, sulfur, and MnO₂ cannot be utilized as electron acceptor. Esterase (C4), esterelipase (C8), leucine arylamidase, alkaline phosphatase, acid phosphatase, and naphthol-AS-BI-phosphohydrolase activities were present but lipase (C14), valine arylamidase, cystine arylamidase, trypsin, α -chymotrypsin, α -galactosidase, β -galactosidase, β -glucuronidase, α -glucosidase, β -glucosidase, N-acetyl- β -glucosaminidase, α -mannosidase, and α -fucosidase activities are absent. The major fatty acids are iso-C_{15:0} and C_{15:0}. MK-7 and MK-9 are present in minor amounts.

The type strain, Red53^T (= MCCC 1K04027^T = NBRC 114064^T), was isolated from paddy soil of a field in Yamaguchi, Japan. The genomic DNA G + C content of type strain is 60.5 mol%.

Description of *Geomonas ferrireducens* sp. nov.

Geomonas ferrireducens (fer.ri.re.du'cens. L. neut. n. ferrum, iron; L. pres. part. reducens, converting to a different state; N.L. part. adj. *ferrireducens*, reducing ferric ions).

Besides the characteristics that define the genus, the following characteristics are observed. Growth occurs at 13 – 42 °C (optimum, 30 – 33 °C), at pH 5.5 – 8.0 (optimum, 6.0 – 7.0), and with 0 – 0.7% (w/v) NaCl (optimum, 0 – 0.2%). With Fe(III)-NTA as electron acceptor, methanol, lactate, succinate, propionate, glutamine, glycerol, isopropanol, serine, naphthalene, salicylic acid, and arginine can also be utilized as electron donor, but phenol, butanol, toluene, benzyl alcohol, and benzaldehyde cannot be utilized as electron donor. With acetate as electron donor, malate, nitrite, and nitrate can also be utilized as electron acceptor, but Fe(III) pyrophosphate, Fe(III) citrate, sulfur, and MnO₂ cannot be utilized as electron acceptor. Esterase (C4), esterases lipase (C8), leucine arylamidase, acid phosphatase, and naphthol-AS-BI-phosphohydrolase activities were present but alkaline phosphatase, lipase (C14), valine arylamidase, cystine arylamidase, trypsin, α -chymotrypsin, α -galactosidase, β -galactosidase, β -glucuronidase, α -glucosidase, β -glucosidase, N-acetyl- β -glucosaminidase, α -mannosidase, and α -fucosidase activities are absent. The major fatty acids are iso-C_{15:0} and C_{15:0} 3-OH. MK-7 and MK-9 are present in minor amounts.

The type strain, S62^T (= MCCC 1K04028^T = NBRC 114031^T), was isolated from paddy soil of a field in Niigata, Japan. The genomic DNA G + C content of type strain is 60.7 mol%.

Description of *Geomonas terrae* sp. nov.

Geomonas terrae (ter'rae. L. gen. n. *terrae* of/from soil).

Besides the characteristics that define the genus, the following characteristics are observed. Growth occurs at 10 – 42 °C (optimum, 30 – 33 °C), at pH 5.5 – 8.0 (optimum, 6.0 – 7.0), and with 0 – 0.7% (w/v) NaCl (optimum, 0 – 0.2%). With Fe(III)-NTA as electron acceptor, methanol, lactate, succinate, propionate, glutamine, glycerol, isopropanol, serine, naphthalene, salicylic acid, and arginine can also be utilized as electron donor, but phenol, butanol, toluene, benzyl alcohol, and benzaldehyde cannot be utilized as electron donor. With acetate as electron donor, malate, nitrite, and nitrate can also be utilized as electron acceptor, but Fe(III) pyrophosphate, Fe(III) citrate, sulfur, and MnO₂ cannot be utilized as electron acceptor. Leucine arylamidase, acid phosphatase, and naphthol-AS-BI-phosphohydrolase activities were present but esterase (C4), esterase lipase (C8), alkaline phosphatase, lipase (C14), valine arylamidase, cystine arylamidase, trypsin, α -chymotrypsin, α -galactosidase, β -galactosidase, β -glucuronidase, α -glucosidase, β -glucosidase, N-acetyl- β -glucosaminidase, α -mannosidase, and α -fucosidase activities are absent. The major fatty acids are iso-C_{15:0} and C_{15:0} 3-OH. MK-7 and MK-9 are present in minor amounts.

The type strain, Red111^T (= MCCC 1K04029^T = NBRC 114026^T), was isolated from paddy soil of a field in Yamaguchi, Japan. The genomic DNA G + C content of type strain is 61.0 mol%.

Description of *Geomonas silvestris* sp. nov.

Geomonas silvestris (sil.ves'tris. L. fem. adj. *silvestris* pertaining to the forest soil from which the type strain was isolated).

Besides the characteristics that define the genus, the following characteristics are observed. Growth occurs at 20 – 40 °C (optimum, 30–33 °C), at pH 5.5 – 7.5 (optimum, 6.5 – 7.0), and with 0 – 0.4% (w/v) NaCl (optimum, 0 – 0.1%). With Fe(III)-NTA as electron acceptor, arginine, lactate, isopropanol, glycerol, propionate and ethanol can also be utilized as electron donor, but succinate,

phenol, butanol, toluene, benzyl alcohol, and benzaldehyde cannot be utilized as electron donor. With acetate as electron donor, malate can also be utilized as electron acceptor, but Fe(III) pyrophosphate, sulfur, and MnO₂ cannot be utilized as electron acceptor. Esterase (C4), esteraselipase (C8), alkaline phosphatase, leucine arylamidase, acid phosphatase, and naphthol-AS-BI-phosphohydrolase activities were present but lipase (C14), valine arylamidase, cystine arylamidase, trypsin, α -chymotrypsin, α -galactosidase, β -galactosidase, β -glucuronidase, α -glucosidase, β -glucosidase, N-acetyl- β -glucosaminidase, α -mannosidase, and α -fucosidase activities are absent. The major fatty acids are C_{15:0}, C_{15:1} ω 5c and C_{16:0}.

The type strain, Red330^T (= MCCC 1K03949^T = NBRC 114028^T), was isolated from paddy soil of a field in Nagano, Japan. The genomic DNA G + C content of type strain is 62.6 mol%.

Description of *Geomonas paludis* sp. nov.

Geomonas paludis (pa.lu'dis. L. gen. n. *paludis* of a marsh, referring to paddy soil where the type strain was isolated).

Besides the characteristics that define the genus, the following characteristics are observed. Growth occurs at 20 – 40 °C (optimum, 30 – 33 °C), at pH 5.0 – 7.5 (optimum, 6.0 – 6.5), and with 0 – 0.4% (w/v) NaCl (optimum, 0 – 0.1%). With Fe(III)-NTA as electron acceptor, succinate, serine, arginine, lactate, isopropanol, glycerol, propionate and ethanol can also be utilized as electron donor, but phenol, butanol, toluene, benzyl alcohol, and benzaldehyde cannot be utilized as electron donor. With acetate as electron donor, malate can also be utilized as electron acceptor, but Fe(III) pyrophosphate, sulfur, and MnO₂ cannot be utilized as electron acceptor. Esterase (C4), esteraselipase (C8), leucine arylamidase, acid phosphatase, and naphthol-AS-BI-phosphohydrolase activities were present but alkaline phosphatase, lipase (C14), valine arylamidase, cystine arylamidase, trypsin, α -chymotrypsin, α -galactosidase, β -galactosidase, β -glucuronidase, α -

glucosidase, β -glucosidase, N-acetyl- β -glucosaminidase, α -mannosidase, and α -fucosidase activities are absent. The major fatty acids are iso-C_{15:0} and C_{16:0}.

The type strain, Red736^T (= MCCC 1K03950^T = NBRC 114029^T), was isolated from paddy soil of a field in Okinawa, Japan. The genomic DNA G + C content of type strain is 62.4 mol%.

Description of *Geomonas limicola* sp. nov.

Geomonas limicola (li.mi'co.la. L. masc. n. *limus*, mud; L. suff. *-cola* from L. masc. or fem. n. *incola* dweller; N.L. fem. n. *limicola* mud-dweller, referring to waterlogged paddy soil where the type strain was isolated).

Besides the characteristics that define the genus, the following characteristics are observed. Growth occurs at 20 – 40 °C (optimum, 30 – 33 °C), at pH 5.0 – 7.5 (optimum, 6.0 – 6.5), and with 0 – 0.4% (w/v) NaCl (optimum, 0 – 0.1%). With Fe(III)-NTA as electron acceptor, succinate, arginine, lactate, glycerol, propionate and ethanol can also be utilized as electron donor, but phenol, butanol, isopropanol, toluene, benzyl alcohol, and benzaldehyde cannot be utilized as electron donor. With acetate as electron donor, malate can also be utilized as electron acceptor, but Fe(III) pyrophosphate, sulfur, and MnO₂ cannot be utilized as electron acceptor. Esterase (C4), esteraselipase (C8), alkaline phosphatase, leucine arylamidase, acid phosphatase, and naphthol-AS-BI-phosphohydrolase activities were present but lipase (C14), valine arylamidase, cystine arylamidase, trypsin, α -chymotrypsin, α -galactosidase, β -galactosidase, β -glucuronidase, α -glucosidase, β -glucosidase, N-acetyl- β -glucosaminidase, α -mannosidase, and α -fucosidase activities are absent. The major fatty acids are C_{15:0}, C_{15:1} ω 5*c* and C_{16:0}.

The type strain, Red745^T (= MCCC 1K03951^T = NBRC 114030^T), was isolated from paddy soil of a field in Yamaguchi, Japan. The genomic DNA G + C content of type strain is 61.8 mol%.

Description of *Geomonas bemidjiensis* comb. nov.

Geomonas bemidjiensis (be.mid.ji.en'sis. N.L. fem. adj. *bemidjiensis* from Bemidji, MN, United States, where sediment samples were taken from which the type strain was isolated). Basonym: *Geobacter bemidjiensis* Nevin et al., 2005.

Besides the characteristics that define the genus, the following characteristics are observed. Growth occurs at 15 – 37 °C (optimum, 30 °C) with the optimum pH, 7.0. With Fe(III)-NTA as electron acceptor, yeast powder, mannitol, glucose, tryptone, casamino acid, nicotinate, glycerol, isopropanol, serine, and proline can also be utilized as electron donor, but methanol, phenol, butanol, toluene, benzyl alcohol, arginine and benzaldehyde cannot be utilized as electron donor. With acetate as electron donor, malate, MnO₂ and Fe(III) citrate can also be utilized as electron acceptor, but Fe(III) pyrophosphate, nitrate and sulfur cannot be utilized as electron acceptor. Leucine arylamidase, acid phosphatase, esterase (C4) and naphthol-AS-BI-phosphohydrolase activities were present, but esterelipase (C8), alkaline phosphatase, lipase (C14), valine arylamidase, cystine arylamidase, trypsin, α -chymotrypsin, α -galactosidase, β -galactosidase, β -glucuronidase, α -glucosidase, β -glucosidase, N-acetyl- β -glucosaminidase, α -mannosidase, and α -fucosidase activities are absent. The major fatty acids are iso-C_{15:0}, C_{16:0} and C_{15:0} 3-OH.

The type strain is Bem^T (= ATCCBAA-1014^T = DSM16622^T), isolated from subsurface sediments collected in Bemidji, MN, United States. The genomic DNA G + C content of type strain is 60.3 mol%.

Description of *Geomonas bremensis* comb. nov.

Geomonas bremensis (bre.men'sis. N.L. fem. adj. *bremensis*, pertaining to Breme, in northern Germany, where samples for enrichment cultures were taken).

Basonym: *Geobacter bremensis* Straub and Buchholz-Cleven, 2001

As described by Straub and Buchholz-Cleven (2001), optimum growth occurs at 30 – 32 °C with the optimum pH, 5.5 – 6.7. The majority of the cells are non-motile and tend to form aggregates. With ferrihydrite as electron acceptor,

hydrogen, formate, acetate, propionate, butyrate, pyruvate, lactate, malate, succinate, fumarate, benzoate, ethanol, propanol and butanol can be utilized as electron donor. With acetate as electron donor, Fe(III), Mn(IV), sulfur, fumarate and malate can be utilized as electron acceptor. No vitamins required.

The type strain is Dfr1^T (= ATCC BAA-607^T = DSM 12179^T), isolated from a freshwater ditch in Bremen, Germany. The genomic DNA G + C content of type strain is 60.0 mol%.

Description of *Oryzomonas* gen. nov.

Oryzomonas (O.ry.zo.mo'nas. Gr. fem. n. *oryza*, rice; L. fem. n. *monas*, a unit, monad; N.L. fem. n. *Oryzomonas*, a monad from rice soil).

Cells are strictly anaerobic, Gram-stain negative, and rod-shaped. Colonies on R2A agar plates supplementary with 5 mM fumarate are smooth, spherical and red-pigmented. Able to use Fe(III) citrate, Fe(III)-NTA, ferrihydrite and fumarate as the electron acceptors along with a variety of different electron donors, including yeast powder, acetate, tryptone, succinate, glucose, pyruvate, glycerol, propionate, methanol, and malate. The predominant fatty acids are iso-C_{15:0}, and C_{16:1} ω 7c. The major quinone is MK-8. The type species is *Oryzomonas japonicum*.

Description of *Oryzomonas japonicum* sp. nov.

Oryzomonas japonicum (ja.po'ni.ca. N.L. fem. adj. *japonica* Japanese, pertaining to Japan).

Displays the following properties besides those given in the genus description. Cells are rod shaped with light curve in appearance (0.4 – 0.8 μ m wide, 1.0 – 3.0 μ m long) and motile with peritrichous flagella. Strains display good growth on R2A agar plus 5 – 20 mM fumarate and freshwater medium. Growth occurs at 16 – 40 °C (optimum, 30 – 33 °C), at pH 5.0 – 7.5 (optimum, 5.5 – 6.5), and with 0% – 0.7% (w/v) NaCl (optimum, 0 – 0.1%). Can also utilize lactate, mannitol,

ethanol, casamino acid, nicotinate, glutamine, arginine, serine, and proline as electron donors in the presence of Fe(III)-NTA as electron acceptor, but not phenol, isopropanol, toluene, butanol, benzaldehyde or benzyl alcohol. Can also utilize Fe(III) pyrophosphate, Fe(III)-EDTA and MnO₂ as electron acceptors in the presence of acetate as electron donor, but not sulfur, nitrite or nitrate. Alkaline phosphatase, acid phosphatase, leucine arylamidase, and naphthol-AS-BI-phosphohydrolase activities were present but valine arylamidase, esterase (C4), trypsin, esterelipase (C8), lipase (C14), cystine arylamidase, α -glucosidase, α -chymotrypsin, α -galactosidase, α -mannosidase, β -galactosidase, β -glucuronidase, β -glucosidase, N-acetyl- β -glucosaminidase, and α -fucosidase activities are absent. The predominant fatty acids are iso-C_{15:0} and C_{16:1} ω 7c.

The type strain, Red96^T (=NBRC 114286^T = MCCC 1K04376^T), was isolated from paddy soil collected from Niigata, Japan. The DNA G + C content of type strain is 59.0 mol%.

Description of *Oryzomonas sagensis* sp. nov.

Oryzomonas sagensis (sa.gen'sis. N.L. fem. adj. *sagensis*, of or pertaining to the Saga Prefecture of Japan).

Displays the following properties besides those given in the genus description. Cells are rod shaped with light curve in appearance (0.4 – 0.8 μ m wide, 1.0 – 2.5 μ m long) and motile with peritrichous flagella. Strains display good growth on R2A agar plus 5 – 20 mM fumarate and freshwater medium. Growth occurs at 16 – 40 °C (optimum, 30 – 33 °C), at pH 5.0 – 7.5 (optimum, 6.0 – 7.0), and with 0 – 0.5% (w/v) NaCl (optimum, 0 – 0.1%). Can also utilize glutamine, mannitol, nicotinate, casamino acid, arginine, serine, and proline as electron donors in the presence of Fe(III)-NTA as the electron acceptor, but not toluene, isopropanol, phenol, lactate, butanol, benzyl alcohol, ethanol, or benzaldehyde. Can also utilize Fe(III)-EDTA and Fe(III) pyrophosphate as electron acceptor in the presence of acetate as electron donor, but not sulfur, MnO₂, nitrite or nitrate.

Alkaline phosphatase, naphthol-AS-BI-phosphohydrolase, acid phosphatase and leucine arylamidase activities were present but esterase (C4), trypsin, lipase (C14), valine arylamidase, esterelipase (C8), cystine arylamidase, α -chymotrypsin, α -glucosidase, α -fucosidase, α -galactosidase, α -mannosidase, β -galactosidase, β -glucosidase, β -glucuronidase, and N-acetyl- β -glucosaminidase activities are absent. The predominant fatty acids are iso-C_{15:0}, C_{16:1} ω 7c and C_{16:0}.

The type strain, Red100^T (= NBRC 114287^T = MCCC 1K04377^T), was isolated from paddy soil collected from Saga, Japan. The DNA G + C content of type strain is 59.7 mol%.

Description of *Oryzomonas ruber* sp. nov.

Oryzomonas ruber (ru'bra. L. fem. adj. *rubra*, red).

Displays the following properties besides those given in the genus description. Cells are rod shaped with light curve in appearance (0.4 – 0.8 μ m wide, 1.0 – 3.0 μ m long) and motile with peritrichous flagella. Strains display good growth on R2A agar supplemented with 5–20 mM fumarate and freshwater medium. Growth occurs at 16 – 40 °C (optimum, 30 – 33 °C), at pH 5.0 – 7.5 (optimum, 5.5 – 6.5), and with 0 – 0.5% (w/v) NaCl (optimum, 0 – 0.1%). Can also utilize mannitol, lactate, nicotinate, casamino acid, ethanol, glutamine, arginine, serine, and proline as electron donors in the presence of Fe(III)-NTA as electron acceptor, but not phenol, isopropanol, benzyl alcohol, butanol, benzaldehyde or toluene. Can also utilize Fe(III)-EDTA, Fe(III) pyrophosphate, MnO₂ and nitrate as electron acceptor in the presence of acetate as electron donor, but not sulfur. Alkaline phosphatase, naphthol-AS-BI-phosphohydrolase, acid phosphatase and leucine arylamidase activities were present but esterase (C4), trypsin, lipase (C14), valine arylamidase, esterelipase (C8), cystine arylamidase, α -chymotrypsin, α -fucosidase, α -glucosidase, α -galactosidase, α -mannosidase, β -glucuronidase, β -galactosidase, β -glucosidase, and N-acetyl- β -glucosaminidase activities are absent. The predominant fatty acids are iso-C_{15:0}, C_{16:1} ω 7c and C_{16:0}.

The type strain, Red88^T (= MCCC 1K03694^T = JCM 33033^T), was isolated from sediment of a pond in Niigata, Japan. The DNA G + C content of type strain is 58.4 mol%.

2.4 Chapter Conclusion

In order to obtain isolated iron-reducing bacteria from the paddy soil for following studies, hundreds of paddy soils or related samples were collected from all over of Japan. After multiple enrichment processes under anaerobic condition, 63 different *Geobacter*-like strains and 3 different *Anaeromyxobacter*-like strains were successfully isolated. Through a polyphasic taxonomy analysis, the 14 of the 63 *Geobacter*-like isolates were identified as novel species and belong to 2 novel genera in the family *Geobacteraceae*, for which we proposed the names as *Geomonas* gen. nov., including 11 novel species and two reclassified species, *Geobacter bremensis* and *Geobacter bemidjiensis*, and *Oryzomonas* gen. nov., including 3 novel species, while the 3 *Anaeromyxobacter*-like strains were characterized as novel species.

Table 2.1 16S rRNA gene similarities between each pair within all species in the family *Geobacteraceae*

	1	2	3	4	5	6	7	8	9	10	11	12	13	14	15	16	17
1. <i>G. paludicola</i> Red32	100																
2. <i>G. sediminis</i> Red276	98.31	100															
3. <i>G. silvestris</i> Red330	97.12	97.33	100														
4. <i>G. limicola</i> Red745	97.19	97.13	98.46	100													
5. <i>G. bemidjiensis</i> Bem	97.05	97.41	97.83	97.63	100												
6. <i>G. bremensis</i> Dfr1	96.69	96.92	97.61	97.84	99.11	100											
7. <i>G. azotofixans</i> Red51	96.69	96.42	97.05	97.12	97.96	97.89	100										
8. <i>G. paludis</i> Red736	96.83	96.91	97.26	96.43	96.72	96.78	98.52	100									
9. <i>G. diazotrophicus</i> Red69	96.77	96.63	97.12	97.19	98.04	98.03	99.79	98.5	100								
10. <i>G. oryzae</i> S43	96.35	96.28	97.05	96.84	98.25	97.96	98.39	97.7	98.6	100							
11. <i>G. terrae</i> Red111	96.42	96.07	96.42	96.35	97.4	97.12	98.17	98.17	98.31	98.95	100						
12. <i>G. edaphica</i> Red53	96.49	96.21	96.63	96.56	97.61	97.26	98	97.89	97.82	99.16	99.44	100					
13. <i>G. ferrireducens</i> S62	96.63	96.35	96.77	96.7	97.75	97.4	97.89	97.89	97.96	99.3	99.58	99.8	100				
14. <i>G. uraniireducens</i> Rf4	95.37	95.73	95.93	95.32	95.6	95.8	96.13	96.09	95.99	96.07	96.91	96.63	96.49	100			
15. <i>G. daltonii</i> FRC-32	94.52	94.83	95.37	94.7	95.3	95.4	95.37	94.83	95.23	95.65	96.07	95.79	95.65	98.2	100		
16. <i>G. toluenoxydans</i> TMJ1	94.66	94.82	95.15	94.55	95.3	95.3	95.22	94.75	95.08	95.58	95.99	95.71	95.57	98.2	99.8	100	
17. <i>G. luticola</i> OSK6	94.1	94.62	94.03	93.92	94.6	94.3	94.45	93.92	94.38	94.45	95.15	95.01	94.94	95.5	96.1	96.1	100
18. <i>G. lovleyi</i> SZ	93.61	93.85	93.82	93.36	94.2	93.9	93.68	93.57	93.75	93.61	93.68	93.82	93.82	93.8	93.9	93.9	94.1
19. <i>G. thiogenes</i> K1	92.84	93.15	93.05	92.87	93.7	93.4	93.18	93.15	93.25	92.84	93.05	93.05	93.05	93.2	93.4	93.4	93.8
20. <i>O. rubra</i> Red88	93.53	93.75	93.75	92.97	93.82	93.46	93.68	93.52	93.61	93.4	93.68	93.68	93.54	94.1	94.59	94.73	94.6
21. <i>O. japonica</i> Red96	93.47	93.82	93.82	93.04	93.89	93.53	93.75	93.59	93.68	93.47	93.75	93.75	93.61	93.82	94.31	94.44	94.46
22. <i>O. sagensis</i> Red100	93.4	93.82	93.61	92.9	94.03	93.53	93.68	93.52	93.61	93.26	93.54	93.54	93.4	94.03	94.52	94.66	94.67
23. <i>G. psychrophilus</i> P35	92.39	92.43	92.61	92.78	92.8	93	93.16	92.22	93.09	93.03	93.1	93.24	93.1	92.9	93.4	93.2	93.5
24. <i>P. propionicus</i> DSM2379	92.28	92.66	93.05	92.52	93.3	93.1	92.76	91.96	92.69	92.84	92.56	92.84	92.7	92.9	93.4	93.5	93.6

25. <i>G. chapellei</i> 172	93.01	92.62	93.23	93.26	93.3	93.4	93.5	92.7	93.29	93.23	93.37	93.58	93.44	93.3	93.8	93.7	94.1
26. <i>G. pelophilus</i> Dfr2	92.97	93.28	92.91	92.73	93.1	93	93.46	92.66	93.39	92.97	93.18	93.18	93.04	93.8	94.3	94.3	95.4
27. <i>G. argillaceus</i> G12	92.62	92.51	92.55	92.23	92.1	92.5	92.54	91.89	92.47	91.91	92.19	92.19	92.12	93.2	93.1	92.9	94
28. <i>G. pickeringii</i> G13	93.05	93.15	92.63	93.15	93.3	93.2	93.11	92.24	93.11	92.77	92.77	92.77	92.7	93.6	93.8	93.9	94
29. <i>G. anodireducens</i> SD-1T	92.2	92.16	91.85	92.1	92.3	92.1	91.91	91.54	92.05	91.92	91.99	91.92	92.06	92.1	92.1	92.1	92.5
30. <i>G. soli</i> GSS01	92.13	92.1	91.78	92.03	92	92.1	91.85	91.47	91.99	91.85	91.99	91.92	92.06	92.1	92.1	92.1	92.5
31. <i>G. sulfurreducens</i> PCA	92.42	92.66	92.42	92.03	93.1	92.9	92.34	91.96	92.55	92.63	92.63	92.63	92.63	92.6	93.2	93.2	93.2
32. <i>G. hydrogenophilus</i> H-2	92.86	92.65	92.06	92.49	92.9	92.6	92.49	91.98	92.57	92.28	92.28	92.28	92.28	92.7	92.5	92.4	93.3
33. <i>G. grbicum</i> TACP-2	92.7	92.52	92.28	92.24	93.2	93	92.55	91.96	92.62	92.49	92.49	92.49	92.49	93	93	92.9	93.3
34. <i>G. metallireducens</i> GS-15	92.77	92.59	92.21	92.17	92.9	92.7	92.48	91.89	92.55	92.42	92.42	92.42	92.42	92.9	92.8	92.8	93.2

	18	19	20	21	22	23	24	25	26	27	28	29	30	31	32	33	34
1. <i>G. paludicola</i> Red32																	
2. <i>G. sediminis</i> Red276																	
3. <i>G. silvestris</i> Red330																	
4. <i>G. limicola</i> Red745																	
5. <i>G. bemidjiensis</i> Bem																	
6. <i>G. bremensis</i> R1																	
7. <i>G. azotofixans</i> Red51																	
8. <i>G. paludis</i> Red736																	
9. <i>G. diazotrophicus</i> Red69																	
10. <i>G. oryzae</i> S43																	
11. <i>G. terrae</i> Red111																	
12. <i>G. edaphica</i> Red53																	
13. <i>G. ferrireducens</i> S62																	
14. <i>G. uraniireducens</i> Rf4																	
15. <i>G. daltonii</i> FRC-32																	

16. <i>G. toluenoxydans</i> TMJ1																			
17. <i>G. luticola</i> OSK6																			
18. <i>G. lovleyi</i> SZ	100																		
19. <i>G. thiogenes</i> K1	98.6	100																	
20. <i>O. rubra</i> Red88	95.66	95.59	100																
21. <i>O. japonica</i> Red96	95.45	95.52	99.79	100															
22. <i>O. sagensis</i> Red100	95.73	95.66	99.37	99.44	100														
23. <i>G. psychrophilus</i> P35	93.3	93.7	94.66	94.38	94.73	100													
24. <i>P. propionicus</i> DSM2379	93.9	94.1	95.66	95.38	95.73	96.3	100												
25. <i>G. chapellei</i> 172	94.5	94.3	95.64	95.36	95.71	97.3	97.1	100											
26. <i>G. pelophilus</i> Dfr2	93	93.1	93.68	93.4	93.75	94.2	94.3	94.6	100										
27. <i>G. argillaceus</i> G12	93.1	92.5	93.26	92.91	93.19	93.8	93.3	94.9	94.8	100									
28. <i>G. pickeringii</i> G13	92.5	92.2	92.84	92.77	93.12	92.6	93.6	93.5	95.3	94.2	100								
29. <i>G. anodireducens</i> SD-1	92.1	92.3	92.07	92.07	92	92	93	92.5	92.9	93.5	94.3	100							
30. <i>G. soli</i> GSS01	92.1	92.3	92.08	92.08	92.01	92	93	92.5	92.9	93.5	94.3	100	100						
31. <i>G. sulfurreducens</i> PCA	92.8	92.7	92.22	92.01	92.22	93.1	93.7	93.1	93.8	93.4	94.3	98.5	98.5	100					
32. <i>G. hydrogenophilus</i> H-2	93	92.2	92.44	92.29	92.44	93.5	93.1	93.7	93.4	94.3	95.4	95.1	95.3	95.1	100				
33. <i>G. grbicum</i> TACP-2	93.4	92.6	92.43	92.29	92.5	93.3	93.4	93.7	93.2	94.3	95.1	94.7	94.7	95.2	99.3	100			
34. <i>G. metallireducens</i> GS-15	92.8	92	92.36	92.22	92.43	93	93.2	93.4	93.1	94.2	95	94.6	94.6	95.1	99.2	99.6	100		

Table 2.2 16S rRNA gene similarities between each pair within all species in the genus *Anaeromyxobacter*

	1	2	3	4
1. <i>A. oryzae</i> Red 232	100			
2. <i>A. diazotrophicus</i> Red267	96.14	100		
3. <i>A. paludicola</i> Red630	95.59	97.2	100	
4. <i>A. dehalogenans</i> 2CP-1	97.31	96.49	95.37	100

Table 2.3 Genome characteristics of all genome-sequenced validated species in the family *Geobacteraceae* and the genus *Anaeromyxobacter*. Asterisks indicates the species were genome sequenced in this study. Type species of different genera are shown in bold. NA, Not available.

	Accession number	Contig number	Coverage	Genome size	N50	GC content	ORF numbers	RNAs number	integrity
<i>Geobacteraceae</i>									
<i>G. paludicola</i> Red32*	NA	23	207	5.4	507624	62.2	4580	62	Draft
<i>G. sediminis</i> Red276*	NA	137	351	5.5	135987	62.5	4560	74	Draft
<i>G. silvestris</i> Red330*	BLXX01000000	45	339	5.1	357369	62.6	4315	60	Draft
<i>G. limicola</i> Red745*	BLXZ01000000	40	375	5.2	526827	61.8	4387	56	Draft
<i>G. bemidjiensis</i> Bem	NC_011146.1	1	NA	4.6	4615150	60.3	3969	76	Complete
<i>G. bremensis</i> R1	AUGE01000001.1	82	NA	4.7	114026	60.3	4001	60	Draft
<i>G. azotofixans</i> Red51*	NA	18	236	5	1028531	62.4	4202	60	Draft
<i>G. paludis</i> Red736*	BLXY01000000	47	348	5.1	475719	62.4	4251	67	Draft
<i>G. diazotrophicus</i> Red69*	NA	58	360	4.7	260083	61.9	3955	70	Draft
<i>G. oryzae</i> S43*	SRSC00000000	8	324	4.7	1057769	61	3959	57	Draft
<i>G. terrae</i> Red111*	RAHW00000000	18	158	4.9	578332	61.2	4170	64	Draft
<i>G. edaphica</i> Red53*	SSYB00000000	17	756	4.8	1148776	60.5	4072	61	Draft
<i>G. ferrireducens</i> S62*	SSYA00000000	16	647	4.8	1386104	60.7	4098	64	Draft
<i>G. uraniireducens</i> Rf4	NC_009483.1	1	NA	5.1	5136364	54.2	4398	61	Complete
<i>G. daltonii</i> FRC-32	NC_011979.1	1	10	4.3	4304501	53.5	3774	59	Complete
<i>G. toluenoxydans</i> TMJ1	BBCJ01000001.1	77	NA	4.2	122019	53.6	4531	51	Draft
<i>G. luticola</i> OSK6*	NA	61	456	3.7	497364	58.2	3344	51	Draft
<i>G. lovleyi</i> SZ	NC_010814.1	2	NA	4	3917761	54.8	3627	54	Complete
<i>G. thiogenes</i> K1	FUWR01000042.1	44	NA	3.6	149898	52.8	3237	65	Draft
<i>O. rubra</i> Red88*	SRSD00000000	23	271	3.8	353860	58.4	3523	53	Draft

<i>O. japonica</i> Red96*	VZQZ00000000	31	808	3.6	336264	59	3363	53	Draft
<i>O. sagensis</i> Red100*	VZRA00000000	21	958	3.6	620468	59.7	3322	54	Draft
<i>P. propionicus</i> DSM2379	NC_008609.1	3	NA	4.2	4008000	58.5	3796	69	Draft
<i>G. chappellei</i> 172*	NA	80	476	3.9	218010	51.1	3708	49	Draft
<i>G. pelophilus</i> Dfr2*	NA	42	452	4.4	511291	53.1	4047	59	Draft
<i>G. argillaceus</i> G12	VLLN00000000.1	71	253	4.4	139,136	58.2	3912	55	Draft
<i>G. pickeringii</i> G13	CP009788.1	1	110	3.6	3618700	62.3	3211	65	Complete
<i>G. anodireducens</i> SD-1	CP014963.1	1	261	3.7	3555507	61.5	2839	59	Complete
<i>G. soli</i> GSS01	JXBL00000000.1	18	163	3.7	567723	61.8	3257	59	Draft
<i>G. sulfurreducens</i> PCA	NC_002939.5	1	NA	3.8	3814128	60.9	3430	58	Complete
<i>G. hydrogenophilus</i> H-2*	NA	70	495	4	325008	59.6	3569	49	Draft
<i>G. grbicum</i> TACP-2*	NA	84	405	4.2	186775	59.5	3792	52	Draft
<i>G. metallireducens</i> GS-15	NC_007517.1	2	NA	4	3997420	59.5	3539	60	Complete
<i>Anaeromyxobacter</i>									
<i>A. oryzae</i> Red 232*	NA	17	274	6.7	872500	73.5	5795	50	Draft
<i>A. diazotrophicus</i> Red267*	NA	17	319	4.8	545166	74.5	3995	51	Draft
<i>A. paludicola</i> Red630*	NA	15	449	4.6	1199586	74.1	3821	51	Draft
<i>A. dehalogenans</i> 2CP-1	NC_011891.1	1	NA	5	5029329	74.8	4434	59	Complete

Table 2.4 Genome similarities based on nucleotide sequences (ANI) between each pair within all species in the family *Geobacteraceae*.

	1	2	3	4	5	6	7	8	9	10	11	12	13	14	15	16	17
1. <i>G. paludicola</i> Red32	-																
2. <i>G. sediminis</i> Red276	90.4	-															
3. <i>G. silvestris</i> Red330	74.8	75.1	-														
4. <i>G. limicola</i> Red745	74.7	74.9	86.6	-													
5. <i>G. bemidjiensis</i> Bem	75.0	75.1	75.3	75.0	-												
6. <i>G. bremensis</i> R1	74.8	75.1	75.1	75.0	95.2	-											
7. <i>G. azotofixans</i> Red51	75.4	75.5	75.7	75.5	77.9	78.1	-										
8. <i>G. paludis</i> Red736	75.5	75.7	76.0	75.7	78.2	78.4	87.5	-									
9. <i>G. diazotrophicus</i> Red69	75.4	75.6	75.7	75.2	78.2	78.3	87.2	87.0	-								
10. <i>G. oryzae</i> S43	74.7	74.8	75.1	75.0	77.1	77.2	80.8	80.7	81.0	-							
11. <i>G. terrae</i> Red111	74.9	75.0	75.4	74.9	77.5	77.6	81.0	80.9	81.2	91.8	-						
12. <i>G. edaphica</i> Red53	74.6	74.8	75.0	74.8	77.0	77.2	80.8	80.5	80.7	95.3	91.2	-					
13. <i>G. ferrireducens</i> S62	74.7	74.9	75.1	74.9	77.2	77.3	80.8	80.7	80.9	93.6	91.8	93.2	-				
14. <i>G. uraniireducens</i> Rf4	70.8	71.0	70.8	70.7	71.0	71.1	71.0	71.1	71.1	70.5	70.7	70.5	70.7	-			
15. <i>G. daltonii</i> FRC-32	69.5	69.5	69.3	69.3	69.5	69.9	69.6	69.6	69.6	69.0	69.4	69.2	69.4	73.6	-		
16. <i>G. toluenoxydans</i> TMJ1	70.0	70.1	69.9	69.9	70.2	70.6	70.1	70.2	70.0	69.6	69.8	69.7	69.8	74.5	94.7	-	
17. <i>G. luticola</i> OSK6	71.1	71.3	70.9	71.0	71.1	70.8	71.1	71.2	71.1	70.8	70.8	70.7	70.8	72.5	70.7	72.1	-
18. <i>G. lovleyi</i> SZ	68.1	68.4	68.1	68.3	68.3	68.1	68.3	68.4	68.3	68.0	67.9	68.0	67.9	68.6	68.1	68.5	70.4
19. <i>G. thiogenes</i> K1	67.5	67.9	67.8	67.9	67.7	67.4	67.8	67.9	67.7	67.39	67.5	67.4	67.5	68.4	67.7	68.3	69.8
20. <i>O. rubra</i> Red88	70.2	70.4	70.5	70.3	70.3	70.0	70.6	70.76	70.3	69.9	70.0	69.9	69.94	70.6	69.1	69.9	71.5
21. <i>O. japonica</i> Red96	70.1	70.4	70.4	70.2	70.12	70.0	70.5	70.7	70.2	69.8	69.9	69.79	69.9	70.6	69.28	70.2	71.5
22. <i>O. sagensis</i> Red100	70.4	70.5	70.52	70.42	70.3	70.2	70.73	70.9	70.5	70.0	70.0	70.0	70.0	70.6	69.4	70.2	71.5

24. <i>P. propionicus</i> DSM2379	69.3	69.4	69.3	69.5	69.4	69.1	69.6	69.7	69.6	69.0	69.2	68.9	68.9	69.9	68.7	69.3	71.3
25. <i>G. chapellei</i> 172	67.5	67.6	67.4	67.5	67.7	67.4	67.7	67.8	67.7	67.37	67.4	67.4	67.5	68.7	68.0	68.6	68.8
26. <i>G. pelophilus</i> Dfr2	68.5	68.5	68.5	68.6	68.6	68.5	68.6	68.82	68.71	68.3	68.4	68.3	68.5	69.9	68.8	69.6	70.5
27. <i>G. argillaceus</i> G12	71.0	71.1	70.8	70.7	71.1	70.9	71.0	71.2	71.0	70.4	70.7	70.5	70.8	72.0	70.9	71.9	72.5
28. <i>G. pickeringii</i> G13	71.4	71.6	71.3	71.3	71.43	71.4	71.6	71.7	71.6	71.1	71.2	71.1	71.23	71.6	70.2	71.2	73.1
29. <i>G. anodireducens</i> SD-1	70.7	70.9	70.5	70.6	70.5	70.3	70.8	71.0	70.7	70.25	70.2	70.3	70.4	70.8	69.75	70.7	72.4
30. <i>G. soli</i> GSS01	70.7	70.8	70.5	70.6	70.5	70.3	70.8	71.0	71.1	70.2	70.3	70.3	70.4	70.5	69.2	70.8	72.5
31. <i>G. sulfurreducens</i> PCA	70.3	70.6	70.2	70.6	70.2	70.0	70.44	70.7	70.3	70.0	70.0	70.1	70.1	70.7	69.4	70.7	72.3
32. <i>G. hydrogenophilus</i> H-2	71.0	71.2	70.6	70.6	71.0	70.8	70.9	71.0	71.0	70.5	70.6	70.6	70.7	71.4	73.6	71.2	73.1
33. <i>G. grbicum</i> TACP-2	70.9	71.1	70.6	70.8	70.9	71.0	71.0	71.2	70.9	70.5	70.83	70.5	70.7	71.1	70.7	71.2	72.87
34. <i>G. metallireducens</i> GS-15	70.9	71.0	70.6	70.8	70.9	71.0	70.9	71.2	70.9	70.5	70.68	70.5	70.8	71.2	70.5	71.1	72.96

	1	2	3	4	5	6	7	8	9	10	11	12	13	14	15	16
1. <i>G. paludicola</i> Red32																
2. <i>G. sediminis</i> Red276																
3. <i>G. silvestris</i> Red330																
4. <i>G. limicola</i> Red745																
5. <i>G. bemidjensis</i> Bem																
6. <i>G. bremensis</i> R1																
7. <i>G. azotofixans</i> Red51																
8. <i>G. paludis</i> Red736																
9. <i>G. diazotrophicus</i> Red69																
10. <i>G. oryzae</i> S43																
11. <i>G. terrae</i> Red111																
12. <i>G. edaphica</i> Red53																
13. <i>G. ferrireducens</i> S62																
14. <i>G. uraniireducens</i> Rf4																

15. <i>G. daltonii</i> FRC-32																
16. <i>G. toluenoxydans</i> TMJ1																
17. <i>G. luticola</i> OSK6																
18. <i>G. lovleyi</i> SZ	-															
19. <i>G. thiogenes</i> K1	82.9	-														
20. <i>O. rubra</i> Red88	70.8	70.3	-													
21. <i>O. japonica</i> Red96	70.7	70.3	95.6	-												
22. <i>O. sagensis</i> Red100	70.6	70.0	94.6	94.2	-											
24. <i>P. propionicus</i> DSM2379	70.3	69.8	73.9	73.8	74.0	-										
25. <i>G. chapellei</i> 172	69.1	68.8	71.4	71.3	71.3	70.8	-									
26. <i>G. pelophilus</i> Dfr2	69.4	68.8	69.7	69.7	69.7	69.1	68.3	-								
27. <i>G. argillaceus</i> G12	69.4	68.8	71.5	71.4	71.5	70.3	68.7	70.6	-							
28. <i>G. pickeringii</i> G13	69.1	68.6	71.5	71.5	71.6	70.4	68.4	69.7	72.9	-						
29. <i>G. anodireducens</i> SD-1	69.1	68.3	70.9	70.8	71.0	70.2	68.1	69.2	71.8	76.1	-					
30. <i>G. soli</i> GSS01	69.1	68.5	71.0	71.0	71.1	70.4	68.0	69.4	71.8	76.1	99.4	-				
31. <i>G. sulfurreducens</i> PCA	69.0	68.2	70.8	70.6	70.8	70.3	68.0	69.5	71.5	75.6	91.9	91.9	-			
32. <i>G. hydrogenophilus</i> H-2	69.2	68.8	71.1	71.0	71.3	70.6	68.5	70.2	72.6	77.5	76.2	76.5	76.2	-		
33. <i>G. grbicum</i> TACP-2	69.21	68.58	70.84	70.8	70.94	70.6	68.14	69.74	72.53	77.36	76.03	76.3	76.1	90.6	-	
34. <i>G. metallireducens</i> GS-15	68.75	68.28	70.81	70.71	70.93	70.2	68.08	69.35	72.49	77.3	76.06	76.4	75.8	90.9	95.7	-

Table 2.5 Genome similarities based on nucleotide sequences (GGDC) between strains isolated in this study and other type species in the family *Geobacteraceae*.

	S43	S62	Red32	Red51	Red53	Red69	Red111	Red276	Red330	Red736	Red745	Red88	Red96	Red100
<i>G. oryzae</i> S43	100													
<i>G. ferrireducens</i> S62	47.5	100												
<i>G. paludicola</i> Red32	21.5	21.2	100											
<i>G. azotofixans</i> Red51	25.5	25.3	21.9	100										
<i>G. edaphica</i> Red53	44.9	54.4	21.2	25.2	100									
<i>G. diazotrophicus</i> Red69	25.3	25.1	21.8	34.0	24.9	100								
<i>G. terrae</i> Red111	47.2	56.2	21.3	25.2	64.6	25.0	100							
<i>G. sediminis</i> Red276	21.6	21.5	42.2	21.9	21.6	22.0	21.6	100						
<i>G. silvestris</i> Red330	21.5	21.4	21.6	21.8	21.4	21.8	21.5	21.7	100					
<i>G. paludis</i> Red736	25.5	25.5	22.0	34.9	25.1	33.6	25.1	22.1	21.9	100				
<i>G. limicola</i> Red745	21.4	21.2	21.5	21.8	21.2	21.7	21.2	17.6	33.3	21.9	100			
<i>O. rubra</i> Red88	19.3	19.5	19.8	19.3	19.3	19.4	19.2	19.7	19.4	20.1	19.0	100		
<i>O. japonica</i> Red96	19.3	19.3	19.7	19.2	19.2	19.4	19.0	19.9	19.6	19.9	19.1	67.5	100	
<i>O. sagensis</i> Red100	19.4	19.2	20.2	19.2	19.1	19.4	19.3	19.8	19.4	20.0	19.1	61.7	58.2	100
<i>G. bemidjiensis</i> Bem	22.6	22.3	21.4	22.9	22.3	23.2	22.2	22.0	21.4	23.2	21.6	19.9	19.8	19.8
<i>G. bremensis</i> R1	22.8	22.4	21.5	23.0	22.5	23.0	22.3	22.0	21.5	23.2	21.6	19.9	19.9	19.9
<i>G. lovleyi</i> SZ	18.7	19.3	20.4	19.0	18.9	20.4	17.0	19.3	18.9	19.3	19.1	19.8	19.8	19.9
<i>G. chapellei</i> 172	21.5	202.	21.4	19.1	19.3	19.8	19.5	20.8	19.9	19.9	20.7	18.6	18.8	18.7
<i>G. thiogenes</i> ATCC BAA-34	19.8	19.7	21.5	19.0	18.9	20.4	17.5	20.8	19.1	19.2	20.2	19.7	19.2	20.0

<i>G. luticola</i> OSK6	19.0	20.2	20.1	19.0	19.1	19.9	18.9	19.7	19.2	20.2	18.8	20.6	20.9	20.4
<i>G. metallireducens</i> GS-15	19.4	19.1	19.7	19.4	19.3	19.2	18.9	19.3	19.1	19.2	20.2	20.2	20.2	19.9
<i>G. uraniireducens</i> Rf4	20.1	19.2	19.8	19.8	19.1	19.9	18.8	19.6	19.8	19.9	19.4	20.3	20.2	20.6
<i>G. toluenoxydans</i> TMJ1	23.2	21.4	19.4	19.0	21.4	19.0	22.8	19.4	17.8	18.3	17.8	19.3	20.0	20.5
<i>G. daltonii</i> FRC-32	19.4	18.8	19.5	19.2	19.3	18.4	18.4	18.8	18.4	18.7	18.6	20.6	20.3	22.2
<i>G. grbiciae</i> TACP-2	19.3	19.3	19.8	19.4	19.2	19.4	18.9	19.6	19.3	19.5	19.7	20.0	20.1	19.9
<i>G. hydrogenophilus</i> H2	19.4	19.2	19.5	19.3	19.1	19.7	18.8	19.4	19.1	19.5	19.1	19.9	20.3	20.4
<i>G. sulfurreducens</i> PCA	18.6	18.6	19.9	18.9	18.3	19.2	18.4	19.9	19.0	19.5	19.0	20.2	20.0	20.5
<i>G. anodireducens</i> SD-1	18.7	18.7	19.9	18.9	18.5	18.9	18.5	19.4	19.2	19.1	19.1	20.0	19.7	20.2
<i>G. pickeringii</i> G13	19.3	19.6	19.7	19.3	19.2	19.8	19.2	19.7	19.5	19.8	19.7	20.6	20.3	20.7
<i>G. soli</i> GSS01	18.7	18.7	19.8	18.9	18.4	19.0	18.4	19.4	19.3	19.0	19.2	20.1	19.8	20.3
<i>G. argillaceus</i> G12	19.1	18.7	19.6	19.4	18.5	19.9	18.8	19.9	19.4	19.5	19.4	20.6	20.3	20.2
<i>G. pelophilus</i> Dfr2	20.7	19.7	21.0	19.4	20.2	20.1	18.5	20.9	19.4	20.0	19.2	20.8	20.1	20.7
<i>P. propionicus</i> DSM 2379	19.6	19.10	20.0	19.3	19.0	19.4	18.5	20.0	19.1	19.8	19.5	21.1	20.6	21.1

Table 2.6 Genome similarities based on nucleotide sequences between each pair within all species in the family *Geobacteraceae*. Genome-to-Genome-Distance Calculator (GGDC) and average nucleotide identity (ANI) values were listed in the upper-right and lower-left part of the table, respectively.

	1	2	3	4
1. <i>A. oryzae</i> Red 232	100	19.9	19.6	21.7
2. <i>A. diazotrophicus</i> Red267	75.8	100	20.3	19.8
3. <i>A. paludicola</i> Red630	75.3	76.6	100	19.8
4. <i>A. dehalogenans</i> 2CP-1	79.5	76.5	76.2	100

Table 2.7 Genome similarities based on ammino acid sequences between each pair within all species in the family *Geobacteraceae*. Average ammino acid identity (AAI) values and percentage of conserved proteins (POCP) values were listed in the upper-right and lower-left part of the table, respectively.

	1	2	3	4	5	6	7	8	9	10	11	12	13	14	15	16	17
1. <i>G. paludicola</i> Red32	-	92.4	69.8	69.6	70.4	70.4	70.2	70.1	71.1	70.1	70.2	70.1	70.1	63.9	62.7	62.2	62.9
2. <i>G. sediminis</i> Red276	86.0	-	70.0	70.0	70.6	70.6	70.5	70.3	71.0	70.2	70.4	70.3	70.4	64.0	62.5	62.1	62.9
3. <i>G. silvestris</i> Red330	68.1	67.8	-	90.1	71.3	71.1	71.1	70.9	71.7	70.8	71.0	71.0	71.1	64.7	63.4	63.0	63.6
4. <i>G. limicola</i> Red745	67.6	67.2	84.9	-	71.1	71.1	71.1	70.8	71.6	71.0	71.0	70.9	71.1	64.2	63.1	63.0	63.1
5. <i>G. bemidjiensis</i> Bem	66.5	66.5	69.7	68.6	-	95.9	78.0	77.9	78.5	77.2	77.5	77.3	77.4	64.8	64.0	63.5	63.6
6. <i>G. bremensis</i> R1	66.1	65.5	68.8	68.1	87.5	-	77.8	77.8	78.4	77.2	77.4	77.2	77.7	64.6	64.6	63.9	63.3
7. <i>G. azotofixans</i> Red51	67.7	67.8	68.7	69.5	76.6	75.2	-	90.3	89.6	82.8	82.8	82.9	82.8	64.6	63.4	62.9	63.8
8. <i>G. paludis</i> Red736	66.1	66.4	67.9	68.0	76.5	74.3	84.8	-	89.5	82.5	82.6	82.6	82.7	64.6	63.2	63.2	63.7
9. <i>G. diazotrophicus</i> Red69	68.4	68.6	70.0	70.5	77.0	76.5	84.1	81.9	-	83.1	83.2	83.0	83.0	64.8	63.5	63.3	64.1
10. <i>G. oryzae</i> S43	67.1	67.3	69.1	69.2	76.8	77.0	81.2	78.8	82.0	-	94.7	96.5	95.8	64.6	62.8	62.5	63.2
11. <i>G. terrae</i> Red111	67.0	67.4	68.5	68.7	76.1	75.7	81.1	78.7	82.6	88.1	-	94.0	94.4	64.4	63.5	63.1	63.4
12. <i>G. edaphica</i> Red53	67.1	67.5	69.8	69.6	76.9	75.8	81.7	78.9	82.1	89.4	87.8	-	95.2	64.9	63.2	62.9	63.7
13. <i>G. ferrireducens</i> S62	67.1	67.6	69.3	68.7	76.7	75.6	80.4	78.3	81.9	88.1	88.3	88.7	-	64.6	63.4	63.2	63.4
14. <i>G. uraniireducens</i> Rf4	54.5	55.2	54.9	53.6	57.8	57.5	56.3	55.2	56.9	56.1	56.3	56.1	56.4	-	72.7	72.0	68.4
15. <i>G. daltonii</i> FRC-32	54.6	54.9	56.5	56.2	61.8	62.8	59.0	57.4	58.4	57.6	58.3	58.4	58.6	63.9	-	94.0	66.4
16. <i>G. toluenoxydans</i> TMJ1	50.2	50.5	51.3	50.9	56.1	56.7	53.6	53.0	53.0	52.2	52.8	52.3	53.1	58.5	80.5	-	66.2
17. <i>G. luticola</i> OSK6	53.7	53.5	55.0	53.7	56.6	56.2	55.9	55.2	57.4	54.8	55.4	55.4	55.7	57.4	58.1	52.5	-
18. <i>G. lovleyi</i> SZ	46.6	47.2	47.3	47.1	48.6	48.5	48.4	47.2	49.8	48.4	48.4	49.0	48.6	47.9	48.1	43.5	51.2
19. <i>G. thiogenes</i> K1	45.9	46.4	46.6	46.2	48.5	47.4	47.9	46.6	48.8	47.1	47.3	47.6	47.7	47.2	47.9	42.6	49.1

20. <i>O. rubra</i> Red88	55.8	55.0	55.9	55.0	56.1	55.5	56.0	54.7	57.1	56.7	56.4	56.7	56.1	53.1	53.3	47.8	54.7
21. <i>O. japonica</i> Red96	57.4	57.0	56.9	56.1	56.8	56.4	57.7	55.6	58.7	58.1	57.4	57.9	57.7	54.5	55.2	49.4	55.4
22. <i>O. sagensis</i> Red100	56.0	55.2	56.8	55.8	56.1	55.7	56.3	54.7	57.3	56.2	56.4	56.5	56.3	53.8	54.7	49.0	55.4
24. <i>P. propionicus</i> DSM2379	44.3	44.5	45.4	45.7	47.0	46.8	46.6	46.2	47.5	46.5	46.3	47.0	46.8	45.9	45.1	41.1	47.2
25. <i>G. chappellei</i> 172	53.5	53.9	55.1	54.5	57.0	56.8	55.3	55.1	56.1	55.1	54.6	55.0	55.1	53.2	55.4	50.2	55.8
26. <i>G. pelophilus</i> Dfr2	52.1	51.8	52.7	52.7	54.5	54.2	53.4	52.1	53.9	52.9	53.0	53.0	52.9	55.5	54.9	50.0	56.0
27. <i>G. argillaceus</i> G12	53.5	53.1	53.4	53.7	56.8	58.4	55.2	53.1	55.0	53.9	54.7	54.3	55.5	59.3	60.0	55.5	57.0
28. <i>G. pickeringii</i> G13	57.0	56.0	58.6	57.4	61.3	60.4	58.2	57.1	59.1	58.1	58.5	58.0	58.4	62.4	61.7	54.8	62.9
29. <i>G. anodireducens</i> SD-1	54.2	54.2	55.6	54.8	57.5	57.4	57.1	55.7	57.9	56.7	56.8	56.5	57.1	57.5	57.8	51.7	61.7
30. <i>G. soli</i> GSS01	55.0	54.8	56.4	55.6	58.8	58.8	57.9	56.3	58.7	57.4	57.7	57.3	58.0	58.4	58.9	52.1	62.1
31. <i>G. sulfurreducens</i> PCA	56.6	56.3	57.9	57.0	58.6	58.3	58.9	57.5	59.7	58.8	58.7	59.0	58.7	58.8	59.2	53.1	63.1
32. <i>G. hydrogenophilus</i> H-2	54.8	54.6	56.5	55.4	58.9	59.1	57.5	56.1	57.7	56.2	56.8	56.5	57.1	58.6	61.5	55.3	62.1
33. <i>G. grbicum</i> TACP-2	53.4	53.2	54.7	53.6	57.1	58.1	55.0	53.8	55.5	54.7	54.7	54.3	55.5	58.1	60.7	54.5	59.8
34. <i>G. metallireducens</i> GS-15	55.0	54.8	56.6	55.4	59.6	60.4	57.2	55.6	57.6	56.6	57.3	56.5	57.5	60.3	63.7	56.5	61.5

	18	19	20	21	22	24	25	26	27	28	29	30	31	32	33	34
1. <i>G. paludicola</i> Red32	57.4	57.1	60.6	60.7	60.8	57.5	59.4	60.4	62.0	63.2	60.8	61.7	61.7	61.8	61.9	61.9
2. <i>G. sediminis</i> Red276	57.8	57.5	60.3	60.7	60.7	57.4	59.5	60.4	61.9	62.9	61.0	61.6	61.6	61.5	61.7	61.7
3. <i>G. silvestris</i> Red330	58.1	57.8	60.8	61.0	61.2	57.5	60.4	60.9	62.4	63.4	61.4	62.2	62.3	62.5	62.3	62.5
4. <i>G. limicola</i> Red745	58.0	57.6	66.7	60.9	60.9	57.8	59.9	60.7	62.2	63.3	61.4	62.2	62.2	62.0	62.0	62.3
5. <i>G. bemidjiensis</i> Bem	57.8	57.6	60.5	60.6	60.6	57.6	60.0	60.8	62.5	63.6	61.4	62.0	62.1	62.7	62.4	62.5
6. <i>G. bremensis</i> R1	57.7	57.5	60.1	60.4	60.5	57.7	60.3	60.6	63.1	63.3	61.5	62.3	62.1	62.9	63.1	63.0
7. <i>G. azotofixans</i> Red51	58.2	57.9	60.7	61.0	60.7	57.9	60.1	60.7	62.2	63.1	61.5	62.1	62.1	62.5	62.1	62.5
8. <i>G. paludis</i> Red736	57.9	57.5	60.2	60.6	60.4	57.1	60.2	60.8	62.0	63.1	61.5	62.1	62.1	62.1	61.8	61.8
9. <i>G. diazotrophicus</i> Red69	58.5	58.0	60.8	61.3	61.0	58.1	60.4	61.0	62.6	63.4	62.0	62.6	62.6	62.8	62.5	62.4
10. <i>G. oryzae</i> S43	58.1	57.7	60.4	60.5	60.5	57.6	59.6	60.9	62.1	63.0	61.3	61.8	61.8	62.3	62.1	62.1

11. <i>G. terrae</i> Red111	58.2	57.8	60.6	60.8	60.7	58.0	59.7	60.9	62.1	63.1	61.7	62.0	62.0	62.6	62.0	62.3
12. <i>G. edaphica</i> Red53	58.2	57.6	60.7	61.0	60.9	57.9	60.0	61.1	62.0	63.1	61.4	62.0	61.9	62.5	62.0	62.1
13. <i>G. ferrireducens</i> S62	58.0	57.6	60.5	60.8	60.7	57.7	60.1	61.2	62.3	63.3	61.7	62.2	62.2	62.8	62.5	62.4
14. <i>G. uraniireducens</i> Rf4	58.6	58.9	62.3	62.9	62.2	58.9	61.6	64.0	65.5	67.4	64.1	65.3	65.3	66.4	66.0	66.2
15. <i>G. daltonii</i> FRC-32	58.1	57.9	60.7	61.3	61.1	57.6	60.8	62.6	65.2	67.7	63.0	64.0	64.0	65.6	65.5	65.7
16. <i>G. toluenoxydans</i> TMJ1	57.5	57.3	60.5	61.0	60.8	57.5	60.4	61.9	65.1	65.0	62.4	63.6	63.9	65.1	65.0	65.1
17. <i>G. luticola</i> OSK6	61.4	60.7	62.9	62.9	63.2	60.6	62.3	64.9	65.8	67.7	65.7	66.6	66.7	67.5	67.1	67.2
18. <i>G. lovleyi</i> SZ	-	85.7	63.3	63.6	63.5	61.4	62.8	60.4	59.5	59.9	58.8	59.9	60.1	60.1	60.0	59.6
19. <i>G. thiogenes</i> K1	73.9	-	63.2	63.8	63.5	61.1	62.3	59.9	59.2	59.7	58.3	59.0	59.4	59.4	59.8	59.3
20. <i>O. rubra</i> Red88	53.9	53.4	-	96.3	95.2	66.4	69.7	61.8	62.5	63.3	61.4	62.3	62.3	62.2	61.8	62.0
21. <i>O. japonica</i> Red96	55.5	55.5	85.0	-	95.0	66.6	69.6	62.0	62.9	63.2	61.5	62.5	62.6	62.6	62.2	62.3
22. <i>O. sagensis</i> Red100	54.4	54.4	83.5	86.0	-	66.6	69.7	61.7	62.7	63.2	61.3	62.3	62.7	62.6	61.9	62.3
24. <i>P. propionicus</i> DSM2379	50.5	50.7	50.8	52.6	51.8	-	66.3	58.6	58.7	59.4	58.3	59.0	59.5	59.6	59.2	58.8
25. <i>G. chappellei</i> 172	52.5	51.6	59.7	61.4	60.6	50.2	-	60.6	62.3	62.0	60.5	61.4	61.3	61.7	61.4	61.5
26. <i>G. pelophilus</i> Dfr2	50.7	49.3	53.6	55.1	54.1	47.0	52.5	-	64.8	63.7	61.6	62.9	63.5	64.1	63.6	63.2
27. <i>G. argillaceus</i> G12	49.5	49.4	54.8	56.1	55.8	46.9	54.4	57.4	-	66.3	63.2	64.6	64.4	66.3	66.2	66.5
28. <i>G. pickeringii</i> G13	51.1	51.0	60.2	61.5	61.4	48.3	59.4	57.4	64.7	-	73.8	74.5	74.5	76.0	75.6	75.8
29. <i>G. anodireducens</i> SD-1	51.7	50.3	57.1	58.0	57.6	45.8	57.6	56.2	58.0	70.2	-	98.6	93.0	73.2	73.1	73.4
30. <i>G. soli</i> GSS01	52.6	51.7	58.2	59.2	58.8	48.1	58.3	57.0	58.9	71.7	89.6	-	93.8	74.3	74.2	74.4
31. <i>G. sulfurreducens</i> PCA	54.0	52.3	59.4	60.8	60.1	49.8	58.7	59.1	59.0	71.9	85.5	85.4	-	74.8	74.3	74.3
32. <i>G. hydrogenophilus</i> H-2	52.3	50.7	56.3	57.9	57.5	48.8	58.0	58.3	62.2	71.8	68.3	69.1	69.9	-	91.5	91.7
33. <i>G. grbicum</i> TACP-2	50.9	49.7	54.2	55.3	55.0	47.3	55.8	56.7	62.1	70.3	67.3	67.7	67.5	79.2	-	96.3
34. <i>G. metallireducens</i> GS-15	51.5	51.2	56.6	57.9	57.4	47.0	58.5	57.7	64.2	73.9	69.3	70.5	69.9	81.3	85.0	-

Table 2.8 Genome similarities based on ammino acid sequences between each pair within all species in the genus *Anaeromyxobacter*. Ammino acid identity (AAI) values and percentage of conserved proteins (POCP) values were listed in the upper-right and lower-left part of the table, respectively.

	1	2	3	4
1. <i>A. oryzae</i> Red 232	100	50.6	50.1	61.8
2. <i>A. diazotrophicus</i> Red267	64.1	100	59.0	57.6
3. <i>A. paludicola</i> Red630	63.4	66.6	100	57.2
4. <i>A. dehalogenans</i> 2CP-1	72.2	64.8	64.5	100

Table 2.9 Differential characteristics among strains isolated in this study and the type strains of phylogenetically related species of the family *Geobacteraceae*. All data in this table come from this study. +, Positive; –, negative. Nd, no data available.

Characteristic	Red32	S43	Red51	Red53	S62	Red69	Red111	Red276
Isolation origin	Paddy soil	Paddy soil	Paddy soil	Paddy soil	Paddy soil	Paddy soil	Paddy soil	Sediments
Location	Joetsu, Niigata	Nagaoka, Niigata	Yukuhashi, Fukuoka	Mine, Yamaguchi	Nagaoka, Niigata	Kanzaki, Saga	Kasumigaura, Ibaraki	Joetsu, Niigata
Growth temperture (optimum)	20–40°C (30–33°C)	13–42°C (30–33°C)	13–42°C (30–33°C)	10–42°C (30–33°C)	13–42°C (30–33°C)	15–42°C (30–33°C)	10–42°C (30–33°C)	15–40°C (30–33°C)
Growth pH (optimum)	5.0–8.0 (5.5–6.5)	5.5–8.0 (6.0–7.0)	5.5–8.0 (6.5–7.0)	5.5–8.0 (6.0–7.0)	5.5–8.0 (6.0–7.0)	5.5–8.0 (6.5–7.0)	5.5–8.0 (6.0–7.0)	4.5–7.0 (6.0–6.5)
Growth NaCl% (optimum)	0–0.6 (0–0.2)	0–0.7 (0–0.2)	0–0.6 (0–0.2)	0–0.7 (0–0.2)	0–0.7 (0–0.2)	0–0.8 (0–0.2)	0–0.7 (0–0.2)	0–0.4 (0–0.1)
Motility	+	+	+	+	+	+	+	+
Electron donors:								
Methonal (20 mM)	-	+	+	-	+	+	+	-
Arginine (5 mM)	-	+	+	+	+	+	+	-
Lactate (10 mM)	-	+	+	+	+	+	+	-
Succinate (10 mM)	+	+	+	+	+	+	+	+
Isopropanol (10 mM)	+	+	+	+	+	+	+	-
Glycerol (6 mM)	+	+	+	+	+	+	+	-
Propionate (10 mM)	+	+	+	+	+	+	+	-
Serine (10 mM)	-	+	+	+	+	+	+	+
Ethanol (10 mM)	+	+	+	+	+	+	+	-
Electron acceptors:								
Nitrate (10 mM)	-	+	+	+	+	+	+	+

MnO ₄	-	-	-	-	-	-	-	-
Enzymatic activities:								
Alkaline phosphatase	-	-	-	+	-	-	-	-
Esterase (C4)	+	+	+	+	+	+	-	+
Esterase lipase (C8)	+	+	+	+	+	+	-	+
Lipase (C14)	-	-	-	-	-	-	-	-
Leucine arylamidase	+	+	+	+	+	+	+	+
Absorbance peaks of cytochrome <i>c</i> (nm)	427, 523, 553	424, 524, 554	426, 524, 554	424, 522, 554	424, 524, 554	424, 524, 554	424, 524, 554	428, 525, 555

Characteristic	Red330	Red736	Red745	DSM 16622	Red88	Red96	Red100	DSM 13688
Isolation origin	Forest soil	Paddy soil	Paddy soil	Sediments	Sediments	Paddy soil	Paddy soil	Sediments
Location	Kamiminochi-gun, Nagano	Ishigaki, Okinawa	Mine, Yamaguchi	Bemidji, USA	Nagaoka, Niigata	Nagaoka, Niigata	Kanzaki, Saga	South Carolina, USA
Growth temperature (optimum)	20–40°C (30–33°C)	20–42°C (30–33°C)	20–40°C (30–33°C)	15–37°C (30°C)	16–40°C (30–33°C)	16–40°C (30–33°C)	16–40°C (30–33°C)	Nd
Growth pH (optimum)	5.0–7.5 (6.5–7.0)	5.5–7.5 (6.0–7.0)	5.0–7.5 (6.0–6.5)	5.0–7.5 (6.0–6.5)	5.5–8.0 (7.0)	5.0–7.5 (5.5–6.5)	5.0–7.5 (6.0–7.0)	Nd
Growth NaCl% (optimum)	0–0.4 (0–0.1)	0–0.8 (0–0.2)	0–0.4 (0–0.1)	0–0.8 (0–0.2)	0–0.5 (0–0.1)	0–0.5 (0–0.1)	0–0.7 (0–0.1)	Nd
Motility	+	+	+	-	+	+	+	-
Electron donors:								
Methional (20 mM)	-	-	-	-	+	+	+	+
Arginine (5 mM)	+	+	+	+	+	+	+	+
Lactate (10 mM)	+	+	+	+	+	+	-	+
Succinate (10 mM)	-	+	+	+	+	+	+	+

Isopropanol (10 mM)	+	+	-	+	-	-	-	-
Glycerol (6 mM)	+	+	+	+	+	+	+	-
Propionate (10 mM)	+	+	+	+	+	+	+	+
Serine (10 mM)	-	+	-	+	+	+	+	+
Ethanol (10 mM)	+	+	+	+	+	+	-	-
Electron acceptors:								
Nitrate (10 mM)	+	+	+	-	+	-	-	-
MnO ₄	-	-	-	+	+	+	-	-
Enzymatic activities:								
Alkaline phosphatase	+	-	+	-	+	+	+	-
Esterase (C4)	+	+	+	+	-	-	-	+
Esterase lipase (C8)	+	+	+	+	-	-	-	+
Lipase (C14)	-	-	-	-	-	-	-	-
Leucine arylamidase	+	+	+	+	+	+	+	-
Absorbance peaks of cytochrome <i>c</i> (nm)	424, 524, 554	424, 525, 553	424, 524, 553	422, 522, 555	418, 522, 552	424, 524, 554	424, 524, 554	423, 526, 553

Table 2.10 Differential characteristics of strains in the genus *Anaeromyxobacter*. All data in this table come from this study. +, Positive; –, negative.

Characteristic	2CP-1	Red232	Red267	Red630
Growth condition:				
Temp range	15-42	20-40	20-40	20-40
Optimal Temp	30	30-33	30-33	30-33
pH range	5.5-8.5	5.8-8.0	5.0-7.5	5.0-8.0
Optimal pH	6.5-7.0	7.0-7.5	6.0-7.0	6.0-7.0
NaCl concentration range (%)	0-1.8	0-0.5	0-0.5	0-0.5
Optimal NaCl concentration (%)	0-0.2	0-0.1	0-0.1	0-0.1
Electron donors:				
Arginine	+	-	-	-
Glucose	+	+	+	-
Lactate	+	-	+	-
Succinate	+	-	-	-
Casamino acid	+	+	+	-
Mannitol	-	-	+	+
Isopropanol	+	+	+	-
Propionate	+	+	+	-
Phenol	-	-	-	+
Electron acceptors:				
Oxygen	+	-	-	-
Fe(III) citrate	-	+	+	+
Enzyme activities:				
Alkaline phosphatase	+	+	-	+

Table 2.11 Fatty acid compositions of all strains isolated in this study and the reference strains *Geobacter bemidjensis* DSM 16622^T and *Geobacter chapellei* DSM 13688^T. All data listed in this table derived from this study, only those accounting for 0.1% or more of the total in one or more of the strains are given. tr, trace quantities (< 0.1%). -, not detected. * The double bond position could not be identified (except for C_{15:1} ω5c, C_{16:1} ω5c, C_{16:1} ω7c, and C_{17:1} ω7c). Unidentified fatty acid with a retention time of 12.1 and 15.4 min, respectively.

	Red32	S43	Red51	Red53	S62	Red69	Red111	Red276	Red330	Red736	Red745	DSM 16622	Red88	Red96	Red100	DSM 13688
C _{12:0}	-	-	-	-	-	-	-	-	-	-	-	-	0.1	-	-	1.9
iso-C _{13:0}	0.5	2.9	0.5	tr	8.5	0.4	2.8	0.3	0.1	0.3	0.2	-	0.3	0.2	0.3	2.6
C _{13:0}	0.2	0.2	2.0	0.5	0.5	0.2	0.1	1.0	3.0	0.5	2.3	-	-	-	-	-
iso-C _{14:0}	1.3	1.6	2.1	1.5	1.2	1.1	1.2	0.9	1.6	2.4	1.8	0.6	-	-	-	-
C _{14:0}	5.9	5.3	3.9	5.6	6.4	8.7	5.1	8.1	9.1	14.4	6.2	1.7	10.0	5.5	9.4	4.5
iso-C _{15:0}	41.4	19.6	17.2	43.5	22.3	30.3	37.7	20.5	2.5	14.4	3.2	29.7	33.5	52.1	40.4	19.1
anteiso-C _{15:0}	0.3	0.7	0.1	0.5	tr	1.0	0.4	0.8	0.9	6.3	2.3	0.1	0.5	0.7	0.5	0.8
Unidentified 1	0.4	1.6	0.4	-	0.3	-	1.5	0.6	-	0.4	-	0.4	-	-	-	-
C _{15:0}	3.2	2.6	19.7	12.8	9.1	4.2	1.3	11.5	20.1	4.5	17.2	2.3	0.4	0.4	0.6	0.4
C _{15:1} ω5c	1.6	1.9	0.4	6.5	0.1	6.5	1.3	10.5	23.8	4.7	25.6	1.3	1.3	1.4	1.3	0.4
3OH-C _{14:0}	-	-	6.6	-	3.0	0.2	-	0.5	-	-	0.3	-	-	-	-	-
iso-C _{16:0}	3.9	1.5	0.7	1.5	0.9	1.0	0.7	1.2	1.0	2.9	1.0	2.0	0.8	1.7	0.8	1.3
C _{16:1} *	2.0	2.2	1.4	2.6	1.3	4.1	2.1	1.9	1.7	10.6	2.9	1.6	0.4	1.9	0.5	1.9
C _{16:0}	12.1	7.6	3.1	8.2	9.4	13.4	4.5	17.0	11.8	17.7	13.8	15.0	13.8	7.4	10.8	20.1
C _{16:1} ω7c	8.6	7.1	3.3	0.8	5.5	12.1	6.3	8.4	2.9	8.4	4.2	8.7	26.0	19.2	22.2	32.9
10-Me C _{16:0}	-	5.0	2.2	0.3	0.8	-	-	-	-	-	-	6.4	0.8	0.9	0.6	-
C _{16:1} ω5c	1.1	1.6	0.5	0.8	0.8	1.0	1.2	0.5	0.7	0.8	1.5	1.4	1.0	0.7	0.6	2.1

iso-C _{17:0}	1.7	1.1	0.3	0.6	0.9	-	0.4	-	-	-	-	3.9	0.8	1.5	0.9	0.9
Unidentified 2	-	1.4	0.1	-	0.3	1.6	0.9	-	-	-	-	0.7	-	-	-	-
anteiso-C _{17:0}	0.6	1.0	0.1	-	0.3	-	0.6	-	-	-	-	0.3	0.1	0.1	0.1	0.2
C _{17:0}	0.4	0.2	0.8	0.5	0.6	0.4	-	0.8	1.7	0.9	0.8	0.6	-	-	-	-
C _{17:1} *	-	-	3.0	-	-	4.5	-	4.8	0.5	7.9	4.4	6.5	0.5	1.6	0.6	0.3
C _{17:1} ω7c	1.1	1.1	0.3	2.8	2.0	-	0.6	0.7	-	-	-	1.3	-	-	-	-
C _{18:1} ω7c	0.3	tr	0.1	tr	-	-	0.2	0.2	-	-	-	0.6	1.0	1.5	1.1	0.4
C _{18:0}	0.4	-	0.1	-	-	-	-	1.5	-	4.0	1.3	-	0.6	0.3	0.6	1.1
3-OH C _{14:0}	2.0	1.5	1.1	1.0	2.1	-	2.3	-	-	-	-	1.0	-	-	-	-
3-OH C _{15:0}	2.6	20.6	15.2	9.1	10.8	0.9	19.8	2.8	5.8	0.4	6.2	11.5	-	-	-	-
3-OH C _{17:0}	5.5	6.6	8.3	0.4	7.3	-	6.8	-	-	-	-	4.9	-	-	-	-
3-OH C _{16:0}	0.8	1.3	3.7	-	5.1	2.3	-	3.8	1.3	1.7	1.7	-	7.4	2.2	7.0	7.3
3-OH C _{18:0}	1.2	2.5	0.5	-	0.8	2.5	1.3	-	-	-	-	2.8	-	-	-	-

Table 2.12 Fatty acid compositions of all species in the genus *Anaeomyxobacter*. All data listed in this table derived from this study, only those accounting for 0.1% or more of the total in one or more of the strains are given. -, not detected. * The double bond position could not be identified (except for C_{15:1} ω 5c, C_{16:1} ω 5c, C_{16:1} ω 7c, and C_{17:1} ω 7c).

	2CP-1	Red232	Red267	Red630
3-OH C _{10:0}	-	-	0.3	0.2
iso-C _{13:0}	0.1	0.3	0.7	0.1
iso-C _{14:0}	0.6	2.1	0.9	0.1
C _{14:0}	3.1	3.2	3.3	2.4
C _{15:1} *	0.6	-	0.5	-
iso-C _{15:0}	17.0	17.1	19.0	4.6
anteiso-C _{15:0}	5.1	15.2	3.8	3.8
C _{15:1} ω 5c	0.3	0.2	1.4	0.8
C _{15:0}	2.0	1.1	2.8	3.5
C _{16:1} *	3.7	-	3.9	2.4
iso-C _{16:0}	9.9	19.7	11.0	4.9
C _{16:1} ω 7c	4.0	2.0	1.0	9.6
C _{16:1} ω 5c	0.2	0.3	0.5	0.8
C _{16:0}	18.3	10.7	15.1	19.1
3-OH C _{15:0}	0.3	0.3	-	-
C _{17:1} *	10.3	8.6	7.8	8.4
iso-C _{17:0}	6.1	8.0	15.1	18.1
anteiso-C _{17:0}	4.8	6.5	3.9	11.4
C _{17:1} *	1.4	0.5	3.2	4.9
C _{17:0}	1.5	0.6	3.8	2.7
3-OH C _{16:0}	2.8	1.7	-	0.6
iso-C _{18:0}	0.2	0.3	0.2	0.5
C _{18:1} ω 9c	0.5	0.2	0.4	-
C _{18:1} ω 7c	0.5	0.2	0.2	0.9
C _{18:0}	0.3	-	0.5	0.4
3-OH C _{17:0}	5.9	1.1	-	-

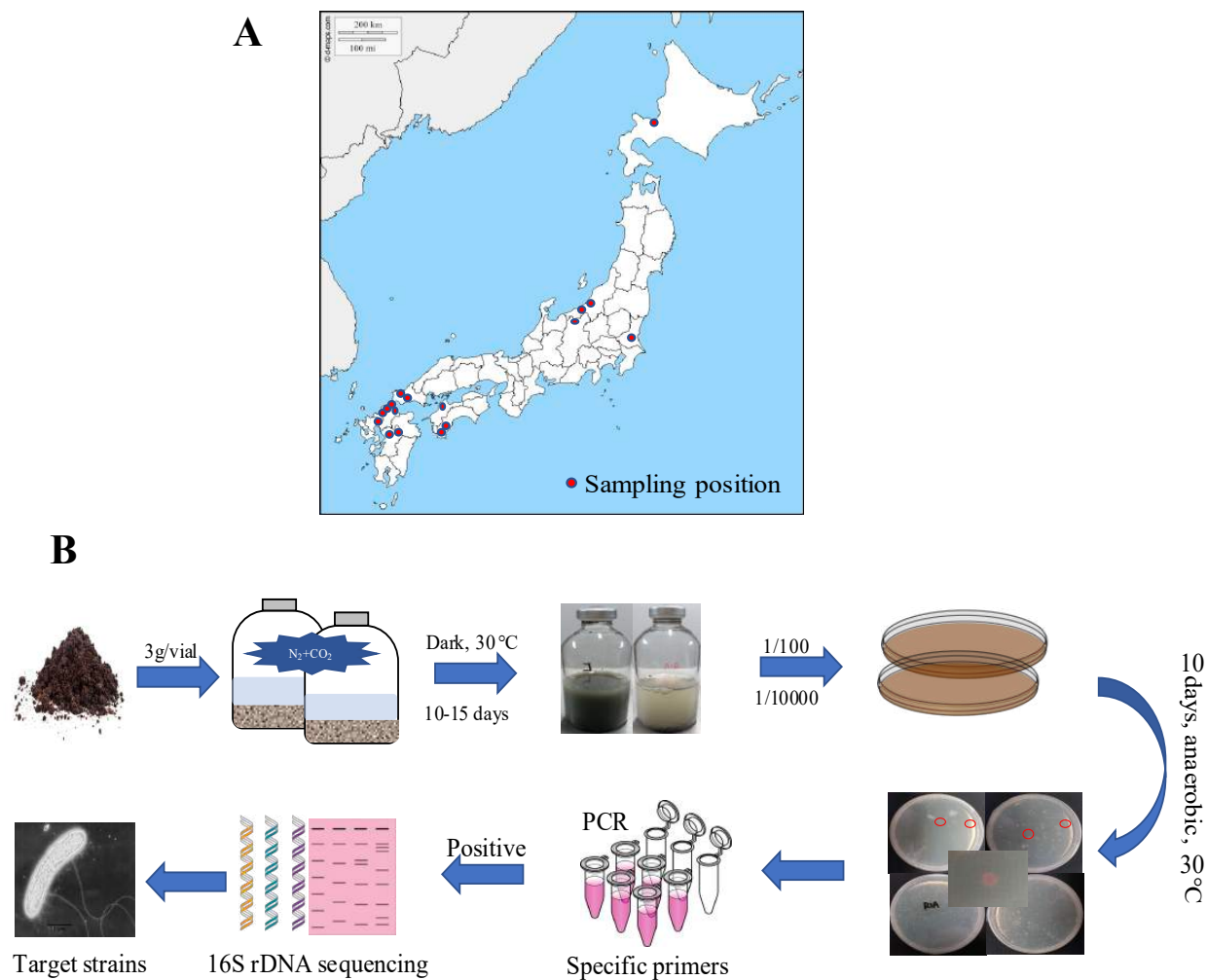


Fig. 2.1 The geographical map of the sampling positions (A) and the procedure chart of *Geobacte*-like and *Anaeromyxobacter*-like strains isolation (B).

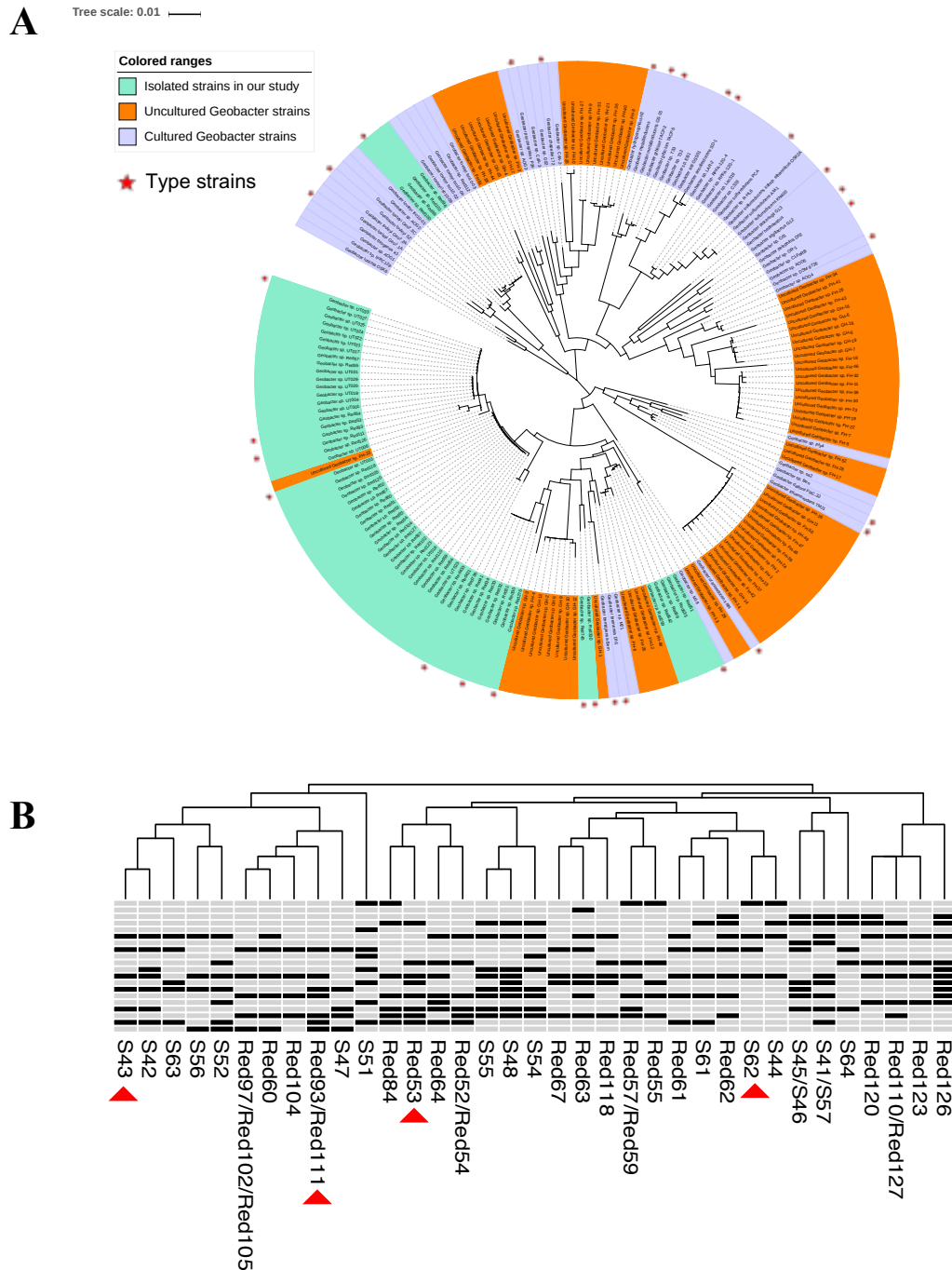


Fig. 2.2 Relationship of all isolated *Geobacter*-like strains. **A**, Neighbor-joining (NJ) phylogenetic tree based on the nearly full-length of 16S rRNA gene (> 1200 bp) of all *Geobacteraceae* strains. The tree was reconstructed using MEGA 7.0 with Kimura 2-parameter model. Bar, 0.01 substitutions per nucleotide position. **B**, BOX-PCR fingerprinting based on agarose gel profiles. The different strains were clustered using the default parameter of complete clustering method. The red triangles indicated the selected strains for next characterization.

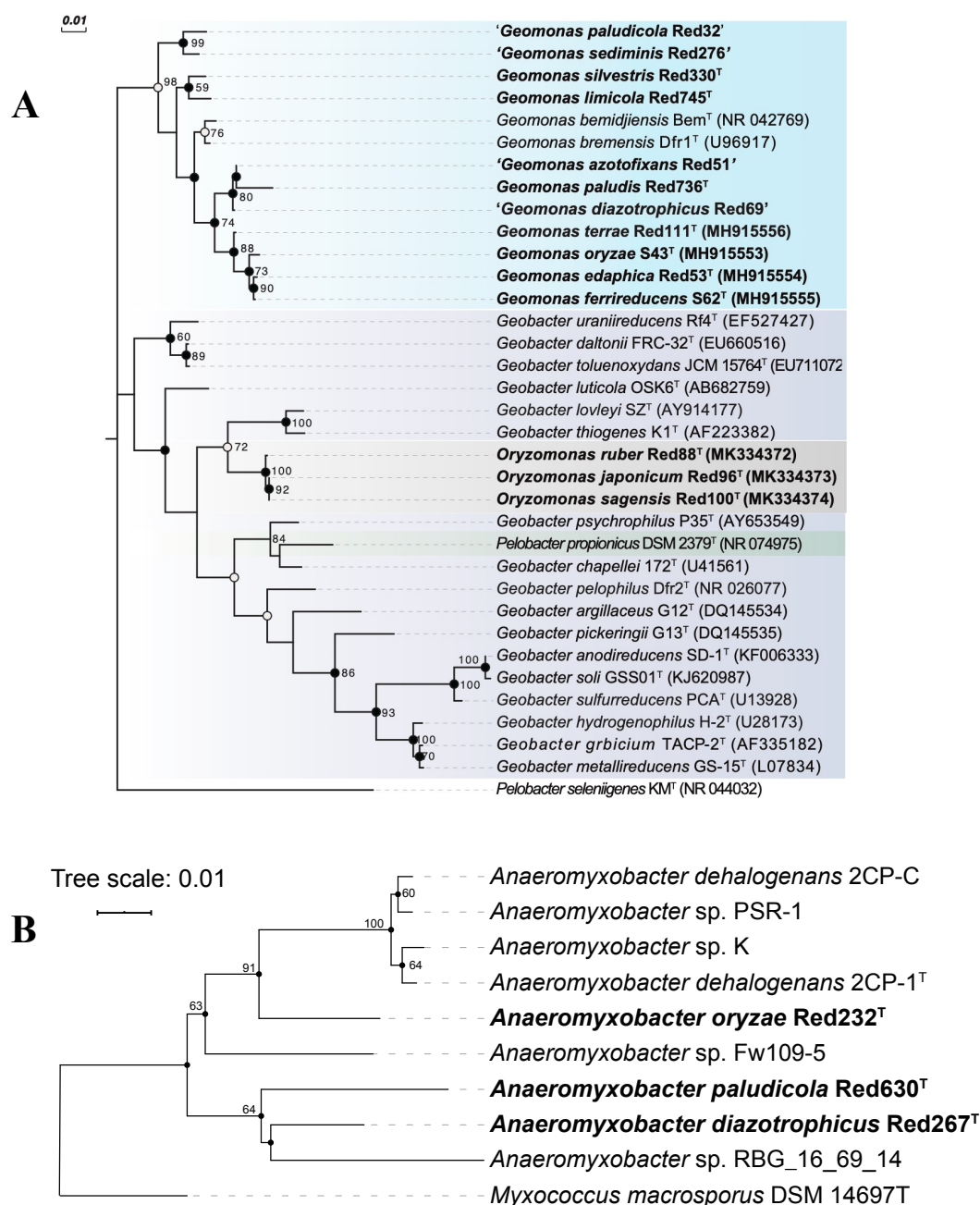


Fig. 2. 3 Phylogenetic trees of species in the family *Geobacteraceae* (A) and *Anaeromyxobacteraceae* (B) based on 16S rRNA sequence divergence. The both trees were inferred by the neighbor-joining (NJ) algorithm using MEGA X with Kimura 2-parameter model. Filled circles indicate that the corresponding nodes were also recovered in ML and MP algorithm. Open circles indicate that the corresponding nodes were also recovered in either the ML or MP algorithm. The background colors represent different bacterial genera. Bootstrap values (expressed as percentages of 1000 replications) over 50% are shown at branching nodes. Bar, 0.01 substitutions per nucleotide position.

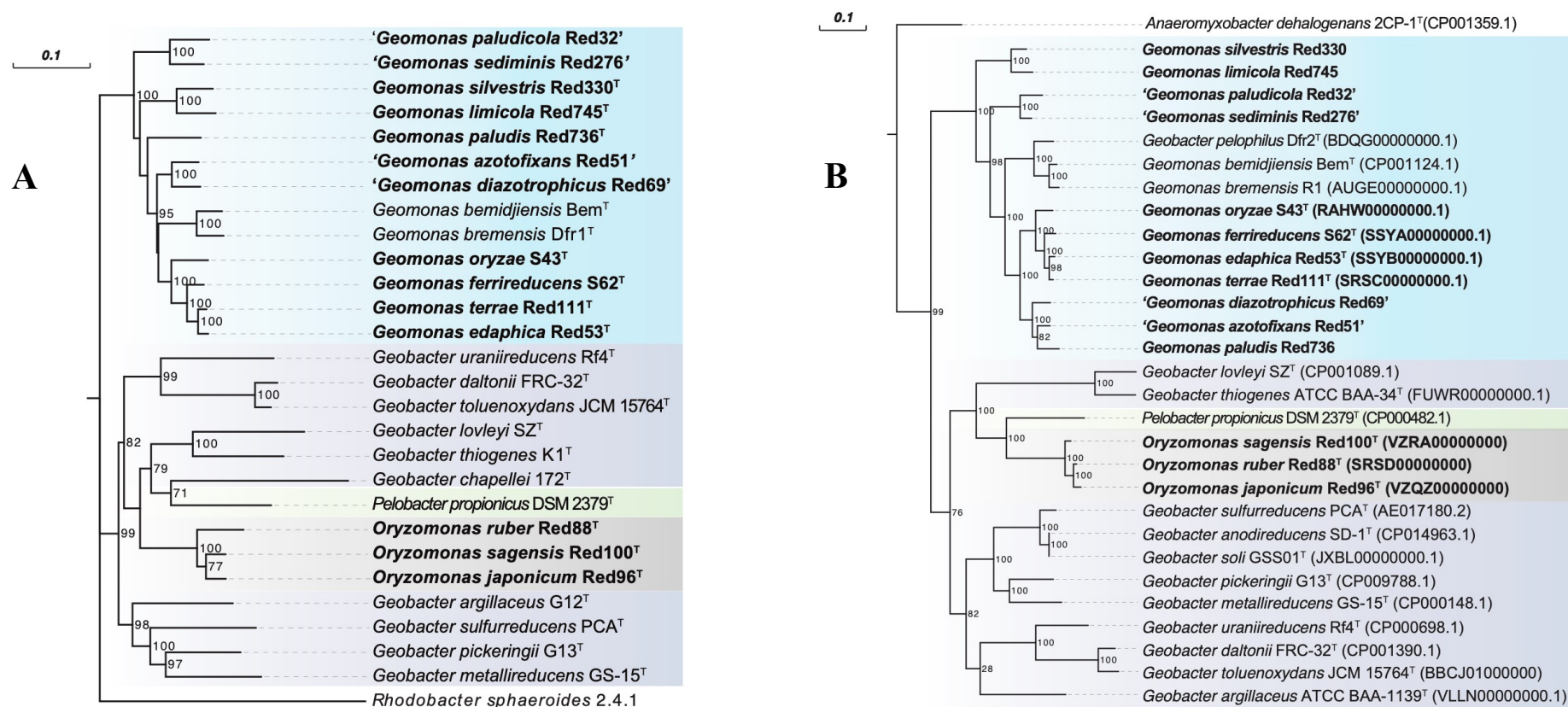


Fig. 2.4 Maximum-likelihood (ML) phylogenetic trees of species in the family *Geobacteraceae* based on the MLSA (A) and UBCG (B). MLSA tree was constructed based on the sequences of five concatenated housekeeping gene: *fusA* (1–650 bp), *gyrB* (651–1591 bp), *nifD* (1592–2359 bp), *gyrB* (2360–3022 bp) and *fusA* (3023–3618 bp), using MEGA X with LG + G model. UBCG tree was constructed using RAXML tool with GTR + CAT model based on concatenated alignment of 92 core genes. Bootstrap values on both trees over 50% are shown at branching nodes. Bar, 0.1 substitutions per amino acid position.

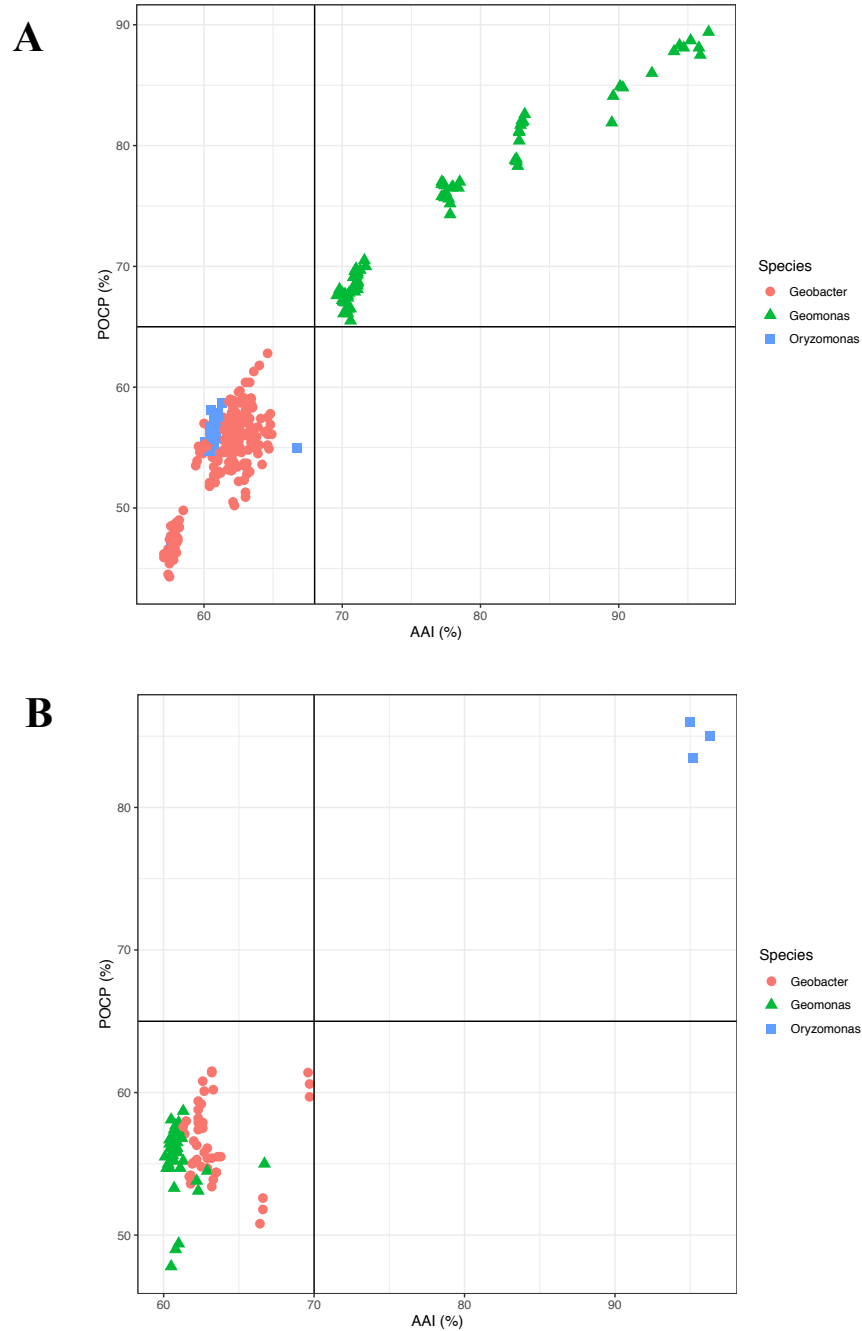


Fig. 2.5 Pairwise whole-genome comparisons of genomic similarities based on AAI and POCP values. The points represent comparison values between *Geomonas* strains (**A**) or *Oryzomonas* strains (**B**) and their close relatives in the family *Geobacteraceae*. A total of 28 genomes were included in this analysis.

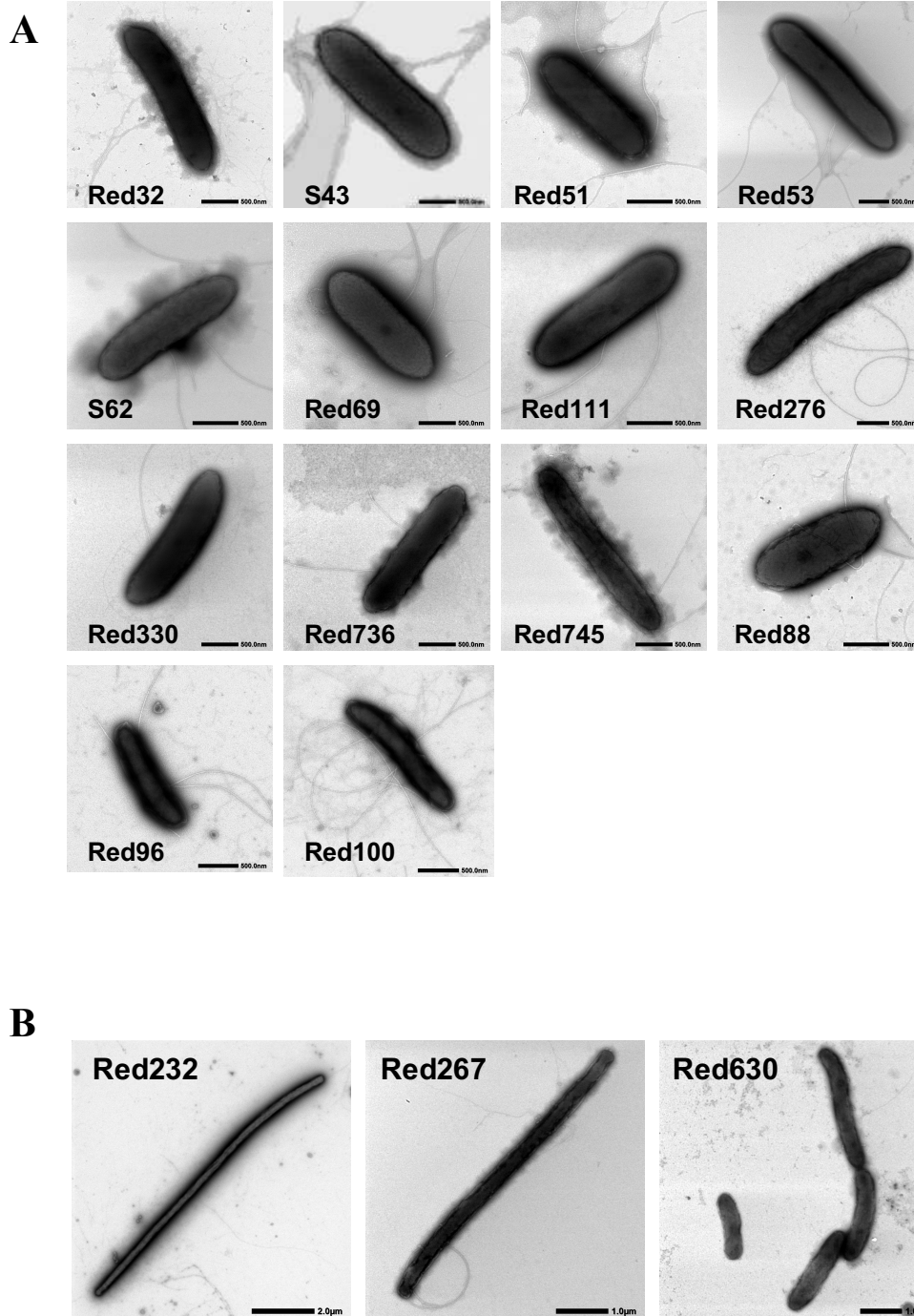


Fig. 2.6 Cellular transmission electron micrograph of the isolated *Geomonas* and *Oryzomonas* strains (A) and *Anaeromyxobacter* strains (B). Cells were grown on R2A agar supplemented with 10 mM fumarate at 30 °C for 3-5 days.

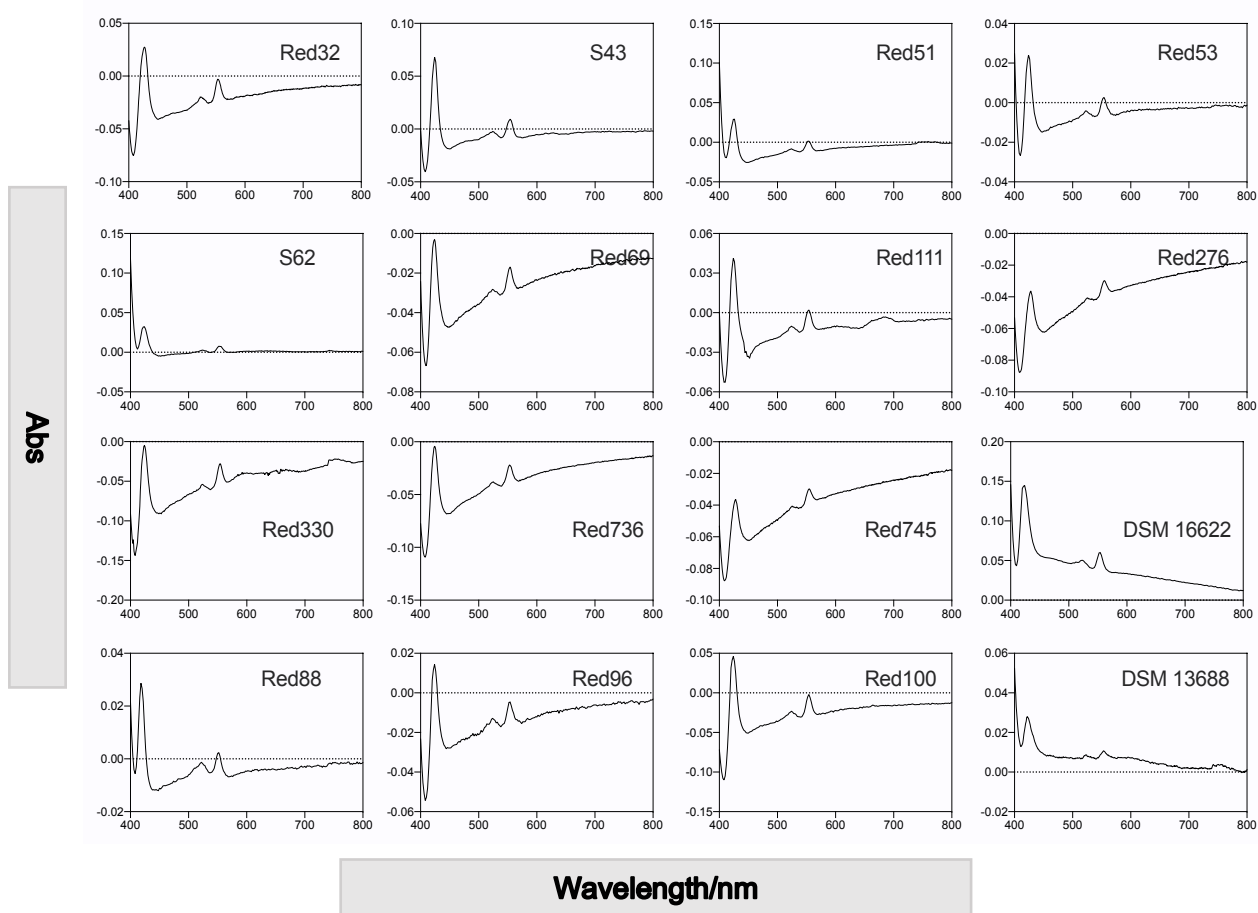


Fig. 2.7 Difference spectra of whole cells for all isolated *Geomonas* and *Oryzomonas* species and their reference strains in the wavelength range of 400 – 800 nm.

Chapter 3: Habitat preferences and biogeochemical roles of *Geomonas* and *Oryzomonas* strains

3.1 Introduction

Geomonas and *Oryzomonas*, two novel bacterial genera in the family *Geobacteraceae*, were proposed to differ the genus *Geobacter* in the Chapter 2. All of strains in these two genera were isolated from paddy soils or nearby places, except for the two reclassified ones, *G. bemidjiensis* Bem and *G. bremensis* Dfr1, which were both isolated from the freshwater sediments (Nevin et al., 2005; Straub and Buchholz-cleven, 2001). However, all of other strains in the family *Geobacteraceae* excluding *Geomonas* and *Oryzomonas* strains have been reported to be isolated from different environments, such as sediments, freshwater, polluted soils and so on, but no one was isolated from paddy soils. Moreover, a distribution survey focusing on the *Geobacter* strains using RT-qPCR method with special primers in different soil types indicated that *Geobacter* strains preferred to inhabit in paddy soils, due to the higher abundance than those in upland soils and river sediments (Masuda et al., 2017). These facts suggested that the inhabitation preference of different genera or groups in the family *Geobacteraceae* may be different. Additionally, before the proposition of the two genera, *Geomonas* and *Oryzomonas*, all of the strains that should belong to the *Geomonas* or *Oryzomonas* were annotated as *Geobacter* cluster, causing the overestimated abundance of the *Geobacter* species and the complete ignorance of the *Geomonas* or *Oryzomonas* species. Thus, to understand well for the role of the *Geomonas* or *Oryzomonas* strains in natural conditions, a new distribution survey of inhabitation preference for strains belonging to different genera in the family *Geobacteraceae* is required.

In addition, as described before, *Geobacteraceae* is a functional family containing multiple strains with special abilities, such as iron reduction, sulfur reduction, extracellular electron transfer and dechlorinating activity (Lovley et al., 2011). Besides, in the previous metatranscriptomic study, it was also found that *Geobacter* and *Anaeromyxobacter* were key drivers related to nitrogen cycles, particularly in nitrogen fixation and nitrate reduction in paddy soils (Masuda et al., 2017). However, as for the two novel genera with strains isolated from paddy soils, little is known for their special functions relate to nitrogen/carbon utilization and biogeochemical reactions because they were first isolated without any related reports introducing them before. Although the metagenomic or metatranscriptomic analysis give us information related to certain microbes based on functional genes annotation, there are still questions that if the target microbes really possess the ability as the meta-analysis annotated, which indicted that isolated strains are necessary to investigate the microbial ability. Besides, the development of microbe cultivation, also named as culturomics, has confirmed many errors between real bacterial functions and genome annotated functions (Lagier et al., 2018), indicating the method defects of common annotation tools in meta-analysis and the strong demand for microbe isolation.

Thus, based on the isolated *Geomonas* and *Oryzomonas* strains, I performed the following study to explore their distribution preference and relative abundance in the original environment and determine their real functions related to biogeochemical processes.

3.2 Materials and methods

3.2.1 Meta-analysis for distribution and relative abundance of

Geomonas and *Oryzomonas* species

The distribution of species of the genera *Geomonas* and *Oryzomonas* in different environments was tested using a special ProkAtlas database (<https://msk33.github.io/prokatlas.html>), which was constructed based on the Earth Microbiome Project (Thompson et al., 2017), with the default parameters (Mise and Iwasaki, 2020). The relative abundance, indicated by microbial habitat preference scores, of target species in different environments was calculated using the local blast+ with the 16S rRNA gene sequences of target species as the query file and the sequences in the ProkAtlas database as the database file. The operating parameters were set up with 98.5% of sequence similarity threshold and 150 bp of alignment length threshold.

The distribution and relative abundance of species of the family *Geobacteraceae* related to nitrogen cycle in paddy soils were calculated based on the metagenome data, which was retrieved and analyzed using metagenomics RAST server (MG-RAST) (Meyer et al., 2008). After a primary search, 10 sites of paddy fields all over Japan with raw reads exceeding 10^5 were sort out for further analysis. According to our previous metagenomic and metatranscriptomic results, the species in the family *Geobacteraceae* mainly take part in the nitrogen fixation and DNRA processes of nitrogen cycle in the paddy soils with the representative genes, *nif*, *nar*, *nor* and *nrf* (Masuda et al., 2017). Thus, we downloaded all of annotated sequences of *nifH*, *narG*, *norB/norZ* and *nrfA* genes from the metagenome data of the 10 sites, respectively, and named them as DBm, containing 5 subgroups. In view of the low accurate ratio of MG-RAST annotation, the 5 functional gene sequences from all bacteria, which were genome annotated with these 5 genes, were also downloaded from the GTDB database

using the AnnoTree server (Mendler et al., 2019). The misannotated sequences in DBm were eliminated by comparison with the verified 5 functional genes sequences with the threshold of e -value $1e-5$. The number of sequences classified to the target species in the DBm was determined by the local blast+ with the query files containing the functional gene sequences of target species.

The presence and absence of functional genes related to nitrogen cycle for the species in the family *Geobacteraceae* were determined based on the whole genomes. The whole genome sequences of all studied strains were retrieved from NCBI database and re-annotated by BlastKOALA server of KEGG database (Kanehisa et al., 2016). The heatmap figure was generated with the “pheatmap” package of R (version: 3.6.0).

3.2.2 Ferric iron reduction

Fe(III)-NTA stock solution: 10 N NaOH was added to the mix of 200 mM Nitrilotriacetic acid (NTA) and 200 mM $\text{FeCl}_3 \cdot 6\text{H}_2\text{O}$ until the pH reached a value of 7.0, then autoclaved and preserved in vials under N_2/CO_2 gas (80:20, v/v) condition.

Ferrihydrite stock solution: 1 M NaOH was added quickly to 200 mM $\text{FeCl}_3 \cdot 6\text{H}_2\text{O}$ with vigorously stirring until the pH reached a value of 6.5; the NaOH addition was continued slowly until the pH reached a value of 7.5. The precipitates were repeatedly washed with distilled water and preserved in vials under N_2/CO_2 gas (80:20, v/v) condition. The accuracy and purity of the produced ferrihydrite were determined by X-ray Diffraction (XRD).

Fe(III)-citrate stock solution: 200 mM commercial Fe(III)-citrate (Wako, Osaka, Japan) dissolved in hot water, and further sterilized with a 0.22 μm Millipore filter, then preserved in vials under N_2/CO_2 gas (80:20, v/v) condition.

The ability of ferric iron reduction of the selected strains in the genus *Geomonas* and *Oryzomonas* was determined using 20 mL MFM in 50 ml serum

bottles supplemented with 10 mM acetate as the electron donor under an 80:20 mixture gas of N₂:O₂. The vessels were incubated at 30 °C without shaking and every set of experiments were performed in triplicate. Three different type of ferric irons, Fe(III)-NTA (5 mM), Fe(III)-citrate (20 mM) and ferrihydrite (5 mM), were independently used as the electron acceptor to determine the iron reduction ratio. After cultured samples were collected at different sampling time, the soluble ferrous concentration was detected immediately using a ferrozine buffer as described by Onley et al., (2018), as well as total iron content after mixed with an equal volume of 10% (w/v) hydroxylamine hydrochloride solution. The soluble ferric concentration was calculated by subtracting the amount of ferrous from the total iron amount. Absorbance was measured using a Jasco V550 spectrophotometer at a wavelength of 562 nm. Standards were prepared with ferrous ammonium sulfate hexahydrate spanning a concentration range of 0.1 mM to 10 mM ferrous. The composition of the black mineral produced from ferrihydrite reduction was determined using XRD. XRD patterns were obtained with a Gandolfi camera of 114.6 mm in diameter employing Ni-filtered CuK α radiation. Simulation of powder XRD patterns was performed using DIFFaX (version 1.812) (Treacy et al., 1991), which calculates diffraction patterns from layered materials with various stacking sequences.

3.2.3 Carbon source utilization

The major compositions of rice straw, the most abundant carbon source in paddy fields, are cellulose, xylan, and lignin (Syafrika and Matsumura, 2018). In order to determine the capacity of rice straw degradation of the selected strains, the bacterial strains were cultured using 20 mL MFM in 50 mL serum bottles containing 0.1% cellulose, xylan, or lignin as the carbon sources and electron donors, Fe(III)-NTA (5 mM) as the electron acceptor. The vessels were incubated at 30 °C under an 80:20 mixture gas of N₂:O₂ without shaking and every set of

experiments were performed in triplicate. The changed color of the cultural bottles was used as the indicator to primitively show if the target strains contain the ability of rice straw degradation. The enzymatic activity to degrade polysaccharide derived from rice straw of the target strains was quantified by detecting the produced reducing sugar using a modified 3,5-dinitrosalicylic acid (DNS) method, as described previously (Xu et al., 2020b), modified to use 100 μ L of the bacterial broth as the reaction solution. The MFM containing cellulose or xylan without bacteria incubation was used as the negative control. Besides, acetate, usually the intermediate of carbon source utilization, was also checked using HPLC system with UV detector (LaChrom Elite; Hitachi, Tokyo, Japan) equipped with a Aminex HPX-87H column (300 mm \times 7.8 mm) (Bio-Rad, CA, USA) that maintained at 50°C in a column oven. The mobile-phase solution system comprised 10 mM sulfuric acid at a flow rate of 0.7 ml/min

3.2.4 Determination of nitrogen-fixing ability

The ability of nitrogen fixation of the selected strains in the genus *Geomonas* and *Oryzomonas* was assayed using 20 mL MFM in 50 mL serum bottles, followingly incubated at 30 °C without shaking and every set of experiments were performed in triplicate. Cells of target strains were first cultured under N₂/CO₂ gas (80:20, v/v) condition using different combinations of electron donors and acceptors. After preculturing for about 2 days till the bacteria were in the middle exponential growth phase, the N₂/CO₂ gas in serum bottles were totally exchanged to Ar/C₂H₂ gas (90:10, v/v). Then the bacteria in the serum bottles were continuedly cultured for 6 h under the same cultural conditions for C₂H₂ reduction. The traditional acetylene reduction assay (ARA) method based on C₂H₂ reduction into C₂H₄ by nitrogenase was used to measure the nitrogen fixation activity (Postgate, 1972). C₂H₄ production in the gaseous phase was measured by gas chromatography (GC-17A, Shimadzu, Japan) equipped with a

fused-silica column (RT-U PLOT; Restek, USA) as described previously (Nakajima et al., 2012). The negative control was set up using pure Ar gas in replacement of Ar/C₂H₂ gas. The cell number was monitored by plate count method for unclear medium and direct counting of the cells using a Multisizer 3 (Beckman Coulter, CA, USA) for clear medium. The effects of different concentrations of Fe(III)-NTA or ferrihydrite on nitrogen fixation activity were evaluated based on ARA as described above on cultures incubated at 30 °C in MFM with 20 mM acetate as the electron donor, while the effects of different carbon sources on nitrogen fixation activity were evaluated in MFM with 10 mM fumarate as the electron acceptor. The phylogenetic tree based on the concatenated genes of *nifH*, *nifD* and *nifK* was constructed similar to the process of MLSA as described above (See 2.2.1.5).

3.3 Results and discussion

3.3.1 Distribution of *Geobacteraceae* strains in various environments

Through a comparison against the ProkAtlas database, it was found that all of the species in the family *Geobacteraceae* were distributed widely in different type of environments, such as freshwater, termite gut, rice paddy, wetland and so on (Fig. 3.1). Although similar sequences of the species in the family *Geobacteraceae* were also found in seawater, the lowest habitat preference scores in seawater suggested that the terrestrial and freshwater ecosystems are the dominant habitats for these species (Fig. 3.1). It was also found that similar sequences of the species in the family *Geobacteraceae* are present in activated sludge and seawater, but none were classified into the genera *Geomonas* and *Oryzomonas*. Among these detected environments, rice paddy was determined as the highest relative abundant one not only for the species in the family *Geobacteraceae*, but also for those in the genus *Geomoans* (Fig. 3.1), which was consistent with the previous studies that the strains belonging to the family

Geobacteraceae consisted a dominant bacterial group in the paddy soils (Breidenbach et al., 2016; Masuda et al., 2017). In addition, based on the relative abundance between the genus *Geomonas* and the family *Geobacteraceae*, it was found that the genus *Geomonas* accounted for about or more than half of all sequences annotated to the family *Geobacteraceae* in most environments, such as freshwater, sediment, terrestrial, lake water, subsurface, rice paddy, and so on. Given the multiple genera of the family *Geobacteraceae* we proposed in Chapter 2, we concluded that the genus *Geomonas* is the most abundant group of the family *Geobacteraceae* in most different environments.

However, the more biomass of target bacteria in an environment does not equal to the major functional player of the bacteria related to biogeochemical processes. Thus, we sorted out 10 sites of paddy fields in Japan (Fig. 3.2A) and analyzed the relative abundance of functional genes related to nitrogen cycles using the metagenome data. As shown in Fig. 3.2B, 5 function genes, representing two nitrogen metabolic pathways, nitrogen fixation and DNRA, were present with different proportion in all 10 sites. Therein, the relative abundance of *nif* gene, classified to the family *Geobacteraceae* accounting for 10–35% of all *nif* genes in the environments, indicating the strains in the family *Geobacteraceae* are the major drivers who fix nitrogen to ammonium to supply nitrogen source for bacterial growth and plant nutrition. For the *nar/nap* and *nrf* genes, marker genes of the DNRA process, their relative abundance of the family *Geobacteraceae* is about 10% of all those genes in the paddy soils, which imply that the strains in the family *Geobacteraceae* consisted an important group taking part in the nitrate reduction process in the paddy soils.

Moreover, the relative abundance of target genera, *Geomonas*, *Oryzomonas* and no-reclassified *Geobacter* were also calculated (Fig. 3.2B). It was found that the relative abundance of the novel genus *Oryzomonas* was evidently lower than those of genera *Geomonas* and *Geobacter*, indicating the less contribution of strains in the genus *Oryzomonas* for nitrogen transformation in paddy soils in

contrast to other two groups. On the other hand, compared with the genus *Geobacter* of 17 species now, the genus *Geomonas* showed higher relative abundances of the 5 functional genes, especially for the genes *nor* and *nrf*, key genes of the processes NO reduction to N₂O and nitrite reduction to ammonium, respectively, showing significant difference between the two genera ($p < 0.05$) (Fig. 3.2C). These findings, along with the high habitat preference scores in different environments, indicated that the genus *Geomonas* would be the predominate group in the family *Geobacteraceae* related to nitrogen transformation in paddy soils.

Besides, the number of functional genes involved in the nitrogen metabolic processes of the isolated strains in the family *Geobacteraceae* was investigated with their whole genomes, to clarify the nitrogen transformation preference of different genera in the family *Geobacteraceae*. As shown in Fig. 3.3, all of studied strains, except for strains *G. soli* GSS01^T and *G. anodireducens* SD-1^T, possess the nitrogen fixing ability, due to the presence of the gene cluster, *nifDHK*. Notably, the strains in the genus *Oryzomonas* may possess a higher ability to fix nitrogen than the other two genera, because they contained multi-copy genes of nitrogenase. This fact would explain that the higher relative abundance of the genus *Oryzomonas* in the *nif* gene distribution than those in the other gene's distribution of the selected 10 sites (Fig. 3.2B). Furthermore, it was obviously shown that the strains in the genus *Geomonas* have the more potentials to reduce nitrate and NO than those strains in the genus *Geobacter*, because all of the studied *Geomonas* strains contain complete genetic pathways for nitrate and NO reduction, but only partial *Geobacter* strains contain genes of target pathways (Fig. 3.3).

There are many reports based on the shotgun sequencing of DNA/RNA in paddy soils have highlighted the importance and irreplaceability of strains in the genus *Geobacter*, due to their abilities, such as metal reduction, nitrogen transformation and extracellular electron transfer (Breidenbach et al., 2016;

Lovley et al., 2011; Masuda et al., 2017; Nojiri et al., 2020). However, in our studies of isolating *Geobacter*-like strains, two novel genera *Geomonas* and *Oryzomonas*, which were derived but phylogenetically independent from the traditional *Geobacter* group, were proposed (Xu et al., 2019, 2020a). Then, these three genera consist the family *Geobacteraceae*. To further determine the bacterial function on the genus level, this part of work with the meta-analysis was carried out and the results indicated the novel genus *Geomonas*, rather than the traditional genus *Geobacter*, was determined as the predominant group, playing key role in nitrogen transformation in paddy soils. Also, the results clarified the ecological role of strains in the *Geomonas*, as well as highlighted their contribution of nitrogen cycle in paddy soils. Taken together, these findings improved our understanding of diversity of predominant members in paddy soils, particularly showing the importance of the *Geomonas* and *Oryzomonas*, providing a reference for following culture-independent studies.

3.3.2 Ferric irons reduction

Because the four strains of the genus *Geomonas*, S43, Red53, S62 and Red111 cannot use Fe(III)-citrate as the electron acceptor, only Fe(III)-NTA was used to evaluate their Fe(III) reducing ability. For the three strains from the genus *Oryzomonas*, Red96, Red100 and Red88, both Fe(III)-citrate and Fe(III)-NTA were tested, while Fe(III)-citrate, Fe(III)-NTA and ferrihydrite were assayed for strains Red51 and Red69, two novel species in the genus *Geomonas*. The Fe(III) reducing ability of the selected nine strains was visualized by the color change from dark red to colorless after bacteria incubation (Fig. 3.4). The Fe(III) reducing ability was qualified by the decrease of ferric iron concentration and increase of ferrous iron concentration (Fig. 3.5). Although the selected strains belong to different genera and species, all of them showed a similar reducing ratio that all of added Fe(III)-citrate and Fe(III)-NTA were totally reduced within 10

days, indicating the similar Fe(III) reducing pathways were present among these strains.

Ferrihydrite is the most abundant form of amorphous Fe(III) in the environment. When ferrihydrite was used as the electron acceptor to culture the target strains, an interesting phenomenon was occurred that the total concentration of dissolved Fe(III) and Fe(II) was obviously lower at the final stage of bacterial cultivation than that at the first day of bacteria incubation. This finding indicated that more ferrihydrite in the medium was transformed into undissolved matters by the bacteria. The undissolved and black matters, adhered on the wall of the serum bottles, were collected and analyzed using XRD. The result showed that a different mineral, vivianite, was produced in the medium from ferrihydrite by the bacteria (Fig. 3.6). Vivianite ($\text{Fe}^{2+}\text{Fe}^{2+}_2(\text{PO}_4)_2 \cdot 8\text{H}_2\text{O}$), a hydrated iron phosphate mineral, is commonly found in a number of geological environments, such as marine sediments and freshwater, and in terrestrial systems such as hydrothermal deposits, waterlogged soils, bogs, and archaeological settings as well as in wastewater sludges (Rothe et al., 2016), which suggested that these strains isolated from paddy soils are deeply take part in the biogeochemical processes, especially for mineral production in natural environments.

There are two known bacterial gene clusters involved in the ferric reduction; the porin-cytochrome genes (*pcc*) cluster and metal-reducing gene (*mtr*) cluster, which have originally elucidated in *Geobacter sulfurreducens* and *Shewanella oneidensis*, respectively (Shi et al., 2016). In genomes of strains of the genera *Geomonas* and *Oryzomonas*, we found *pcc* homologous including constitutive genes encoding outer membrane- (*OmcB/C*–*OmbB/C*–*OmaB/C*), periplasmic- (*PpcA*), and cytoplasmic membrane- proteins (*CbcL*), suggesting that these strains reduce Fe(III) oxide by using the porin-cytochrome system as well as *Geobacter* spp. (Cai et al., 2018). Moreover, their genomes also harbored genes involved in the synthesis of electrically conductive pili (e-pili), including *pilA*

coding an e-pili assembler (Holmes et al., 2016). e-pili plays a key role in long-range extracellular electron transport, which allows for an electron exchange with farther minerals and microorganisms (Lovley and Walker, 2019). Therefore, from the viewpoint of efficient electron transfer, microorganisms having e-pili are popular research targets in the field of bioelectrochemistry and biogeochemistry, such as the development of microbial fuel cells and the bioremediation of heavy metal contaminations (Malvankar and Lovley, 2014). However, e-pili synthesis genes have been found in the genomes of limited bacterial groups (Walker et al., 2018). These strains would be novel candidates as valuable microbial resources in applied biochemistry research.

3.3.3 Carbon source utilization

The two type strains, S43 and Red96, belong to the genera, *Geomonas* and *Oryzomonas*, respectively, and two strains, Red267 and PSR-1, in the genus *Anaeromyxobacter* were used to assay the ability of rice straw degradation. The primitive results based on the color change showed that both *Geobacteraceae* strains, S43 and Red96, can use cellulose and xylan as carbon source and electron donors, but not lignin, whereas *Anaeromyxobacter* strain Red267 cannot use any one of degradation products of rice straw, strain PSR-1 can use cellulose only (Table 3.1). These facts suggested that the bacterial strains in the genera *Geomonas* and *Oryzomonas* can directly obtain carbon source from rice straw for growth, while *Anaeromyxobacter* strains are versatile, although all of them were isolated from the paddy soils.

The enzymatic activity to degrade cellulose and xylan of the two represent strains was further quantified, but no reducing sugar was detected using DNS method. Besides, there was no acetate detected during the bacterial growth using cellulose or xylan as the carbon source. Genome annotation also did not show function genes corresponding to cellulose or xylan utilization. These results,

along with the phenotypic features that cellulose and xylan can support bacterial growth, indicated a new but unknown metabolic pathway to utilize cellulose and xylan may present in studied *Geomonas* strains. Thus, more studies are needed to illustrate this result.

3.3.4 Determination of nitrogen fixing ability

Five *Geomonas* strains and three *Oryzomonas* strains were sort out to evaluate the nitrogen fixing ability under different combinations of electron donors and acceptors. All of the selected strains showed the nitrogen fixing ability coupled with the different carbon source, acetate, cellulose and xylan, with values ranging from 0.08 to 4.1 nmol/h/10⁹ cells (Table 3.2), indicating these bacterial strains can survive with nitrogen gas as the nitrogen source and rice straw as the carbon source. The nitrogen gas and degradation products of rice straw are common and abundant resource in paddy soils and independent of fertilizer addition, this may be one reason to explain why these strains showed a high preference of inhabitation in paddy soils and had a high relative abundance to be the dominant strains. Besides, when using fumarate as the electron acceptor, the strains in the genus *Oryzomonas* showed a relative higher C₂H₄ production than those strains in the genus *Geomonas*, which verified the genetic hypothesis as we proposed above that *Oryzomonas* strains contain a higher nitrogen fixing ability due to more copy numbers of nitrogenase genes. Furthermore, compared with conditions that Fe(III)-NTA as the electron acceptor in the medium, much more C₂H₄ in the gaseous phase of the vials was produced when fumarate as the electron acceptor, but the nitrogen fixing ability of single cell under the Fe(III)-NTA condition was significantly higher than that under the fumarate condition, because much more bacteria were present in the medium under the fumarate condition (Table 3.2). This result suggested that the presence of Fe(III) increased

the nitrogen fixing ability of single cells, but caused less bacterial biomass in the medium.

In order to clarify the Fe(III) effect on nitrogen fixation, two different Fe(III) types, Fe(III)-NTA and ferrihydrite with different concentrations were used to culture the selected strains. The results revealed that the high concentration of Fe(III)-NTA increased bacterial nitrogen fixing ability (Fig. 3.7A), whereas ferrihydrite showed a different influence that increasing the ability at low concentration and then decreasing at high concentration (Fig. 3.7B). Both Fe(III) reducing and nitrogen fixing reactions are electron consuming enzyme processes: $\text{N}_2 + 6\text{e}^- + 6\text{H}^+ \rightarrow 2\text{NH}_3$; $\text{Fe}^{3+} + \text{e}^- \rightarrow \text{Fe}^{2+}$, which indicated that these two reactions would be competed with each other for electrons during the whole bacterial growth phase. However, both Fe(III) and nitrogen gas are necessary source for bacterial growth, so these two reactions simultaneously use electrons from the electron donor, acetate, causing more acetate is served as electron donor, rather than carbon source for bacterial breed. This would explain less biomass in the medium if using Fe(III) as the electron acceptor. Besides, different Fe(III) type showed a different effect on bacterial nitrogen fixing ability. Fe(III)-NTA is a complex of Fe(III) and NTA, providing the electron acceptor, Fe(III), and carbon source, NTA, to bacterial growth, while ferrihydrite only supplies the electron acceptor, Fe(III). Furthermore, the key enzyme of nitrogen fixation in *Geobacteraceae* strains is annotated as iron-rich nitrogenase, which imposes a high demand for iron on diazotrophs (Mark Moore et al., 2009; Mills et al., 2004). Along with the fact as described above that the bacterial Fe(III) reducing and nitrogen fixing reactions require more electron acceptors and carbon source, high concentration of Fe(III)-NTA is reasonable to improve the bacterial nitrogen fixing ability. As for ferrihydrite, the presence of Fe(III) under low concentration enhanced the nitrogenase activity with a relative less carbon source. If the concentration of Fe(III) increased in the medium, the electron donor and carbon source, acetate, would be the limited factor to inhibit the bacterial nitrogen

fixating process. These results may explain why the bacterial nitrogen fixing ability increased at low concentration of ferrihydrite, but decreased at high concentration.

Based on the genomic annotation, these studied strains possessed a complete nitrogen fixing pathway, including genes in construction of nitrogenase (*nifHDK*), and biosynthesis of FeMo cofactor (*nifBENX*). Although three different types of nitrogenase are present in different bacteria based on three distinct cofactors, FeMo, Fe and V, representing by the gene names *nif*, *anf* and *vnf*, respectively, the FeMo nitrogenase (Nif) has been found to be more specific for and more efficient in binding dinitrogen and reducing it to ammonia than either of the alternative nitrogenases (in the order Nif > Vnf > Anf) (Raymond et al., 2004). This fact revealed the great nitrogen fixing potentials of the *Geobacteraceae* strains in their original environments. All these genes shared high similarity among these target strains and their phylogenetic neighbors in the family *Geobacteraceae*, suggesting the conserved gene sequences and similar enzyme features of nitrogen fixation in all diazotrophic *Geobacteraceae* strains. Besides, the phylogenetic analysis based on the concatenated *nifDHK* was constructed and showed a similar phylogenetic structure to that of the 16S rRNA gene tree, except for three *Geomonas* strains, Red32, Red276 and Red736, whose positions in *nifDHK* gene tree were located at the cluster of *Geobacter* and showed distance from their phylogenetic neighbors of 16S rRNA gene tree (Fig. 3.8). These findings may imply that the evolution of functional genes is mainly conserved and synchronized with the evolution of bacterial species, but genetic variation of some function genes is also occurred in the genus *Geomonas*.

3.4 Chapter conclusion

In this part of work, I checked the distribution preference and special functions of the isolated *Geomonas* and *Oryzomonas* strains. Although the members of the

family *Geobacteraceae* reported previously were mostly isolated from sediments, especially contaminated terrestrial environments, the two novel genera *Geomonas* and *Oryzomonas* prefer paddy soils with high preference ratio. Next, a meta-analysis based on the metagenomic data derived from the paddy soils was carried out and the results revealed the genus *Geomonas* should be the predominant group related to nitrogen cycle at the genus level in the paddy soil. Previous publications have highlighted the importance of *Geobacter* in different biogeochemical processes in different environments, but the genus *Geobacter* in those publications represent a family-level group including all of the members in the family *Geobacteraceae*, except *Pelobacter propionicus*, due to the recognized but unrevised paraphyletic problem of the genus *Geobacter* (Reguera and Kashefi, 2019). In the Chapter 2, two novel genera *Geomonas* and *Oryzomonas* were firstly proposed from the traditional *Geobacter* group. Besides, the genus *Geobacter* was reclassified into 7 groups at the genus level as described above. Taken together, the genus *Geomonas* should be the largest group at genus level in the family *Geobacteraceae*, and is reasonable to be the predominant group taking part in biogeochemical reactions in paddy soils.

Many reports recently showed that the group of *Geobacter* strains was one of the keystone taxa in microbial network coupling nitrogen-fixing and Fe(III)-reducing reactions in paddy soils (Li et al., 2020a, 2020b). Thus, based on the isolated *Geomonas* and *Oryzomonas* strains, the nitrogen-fixing and Fe(III)-reducing abilities were tested. The results revealed that all of the studied strains derived from paddy soils and nearby environments possess high activities to fix nitrogen and reduce Fe(III). Moreover, the presence of relatively low concentration of Fe(III) increased the nitrogenase activity in studied strains. Along with the mineral transformation of *Geomonas* strains from ferrihydrite to vivianite, it was concluded that the strains of the genera *Geomonas* and *Oryzomonas* deeply participate in the biogeochemical cycle in paddy soils. In addition, the studied strains were also verified that they can directly use cellulose

and xylan, the major compositions of rice straw, for growth. This finding demonstrated *Geomonas* and *Oryzomonas* strains have evolved a good-value survival stratagem that using nitrogen and rice straw as the nitrogen and carbon source, respectively, in paddy soils.

In conclusion, the strains in the genera *Geomonas* and *Oryzomonas*, derived from paddy soils and nearby places, showed their habitat preference of paddy soil and their special capacities related to nitrogen cycle and metal reduction, as well as the utilization of rice straw decomposed products. These special characteristics help them colonize and grow well and grab the ecological niche in their original environments, which further explained their ecological role as the dominant species and key drivers involved in biogeochemical processes. Although I have verified several special features of the strains in the genera *Geomonas* and *Oryzomonas*, it is just a start to recognize these bacterial strains. More special characteristics are still needed to explore in the following research.

Table 3.1 The utilization of carbon sources derived from rice straw by the type strains in the family *Geobacteraceae* and the genus *Anaeromyxobacter*. +, Positive; -, negative.

	<i>Geobacteraceae</i>		<i>Anaeromyxobacter</i>	
	S43	Red96	Red267	PSR-1
Cellulose	+	+	-	+
Xylan	+	+	-	-
Lignin	-	-	-	-
Acetate	+	+	+	+

Table 3.2 Nitrogen fixing activity of strains in the genera *Geomonas* and *Oryzomonas* under different culture conditions. The culture medium is MFM supplemented with different electron donors and acceptors: A. acetate (10 mM) and fumarate (10 mM); C. cellulose (1 g/L) and fumarate (10 mM); X. xylan (1 g/L) and fumarate (10 mM); Fe. Fe(III)-NTA (5 mM) and acetate (10 mM).

		C ₂ H ₄ production per vial (nmol/h)	Biomass per vial (10 ⁹)	C ₂ H ₄ production per cell (nmol/h/10 ⁹)
<i>Geomonas</i>	Red111-A	8.91 ± 2.44	108.09 ± 13.51	0.08 ± 0.01
	Red745-A	3.74 ± 1.02	59.37 ± 8.44	0.06 ± 0.01
	Red32-A	7.29 ± 2.42	37.27 ± 2.32	0.19 ± 0.05
	S43-A	24.51 ± 7.72	112.35 ± 8.23	0.22 ± 0.05
	Red51-A	15.57 ± 6.93	100.19 ± 7.74	0.15 ± 0.06
	Red32-C	5.53 ± 1.51	48.06 ± 1.64	0.11 ± 0.03
	Red111-X	6.07 ± 2.55	19.63 ± 5.61	0.30 ± 0.06
	Red32-Fe	0.69 ± 0.21	0.18 ± 0.08	4.10 ± 0.85
	Red51-Fe	0.78 ± 0.29	0.36 ± 0.07	2.13 ± 0.46
	Red111-Fe	0.57 ± 0.14	0.48 ± 0.09	1.18 ± 0.09
	Red745-Fe	0.47 ± 0.15	0.53 ± 0.15	0.88 ± 0.12
	Red88-A	1.57 ± 0.58	37.33 ± 4.52	0.08 ± 0.01
<i>Oryzomonas</i>	Red96-A	48.84 ± 26.42	127.90 ± 10.03	0.37 ± 0.18
	Red100-A	91.31 ± 19.58	96.37 ± 17.75	0.95 ± 0.08
	Red88-C	1.06 ± 0.14	33.92 ± 1.41	0.03 ± 0.01
	Red96-C	13.91 ± 6.07	75.90 ± 4.97	0.18 ± 0.07
	Red88-X	5.39 ± 0.85	11.50 ± 1.85	0.47 ± 0.05
	Red96-X	4.58 ± 1.57	29.60 ± 7.06	0.15 ± 0.02
	Red96-Fe	0.63 ± 0.30	0.91 ± 0.10	0.67 ± 0.28
	Red100-Fe	1.49 ± 0.43	0.80 ± 0.17	1.86 ± 0.29

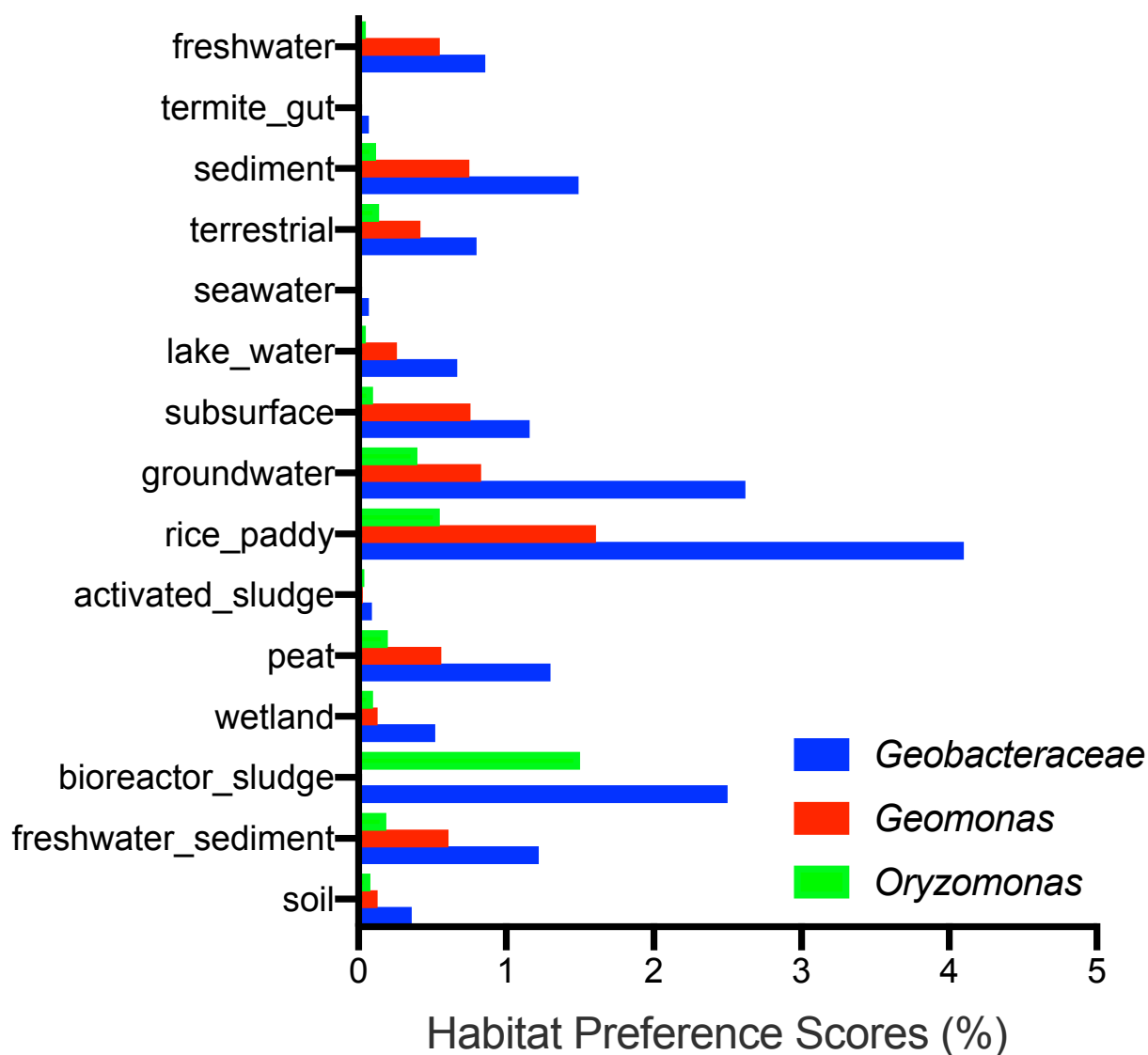


Fig. 3.1 Habitat preference scores of strains in the family *Geobacteraceae*, the genera *Geomonas* and *Oryzomonas* in the different environments based on EMP Prokaryotic Communities. The scores were calculated using the ProkAtlas database.



Fig. 3.3 Gene inventory implicated in nitrogen metabolism in genomes of the type strains of *Geobacteraceae* species. The copy numbers of each gene are denoted by the color bar.

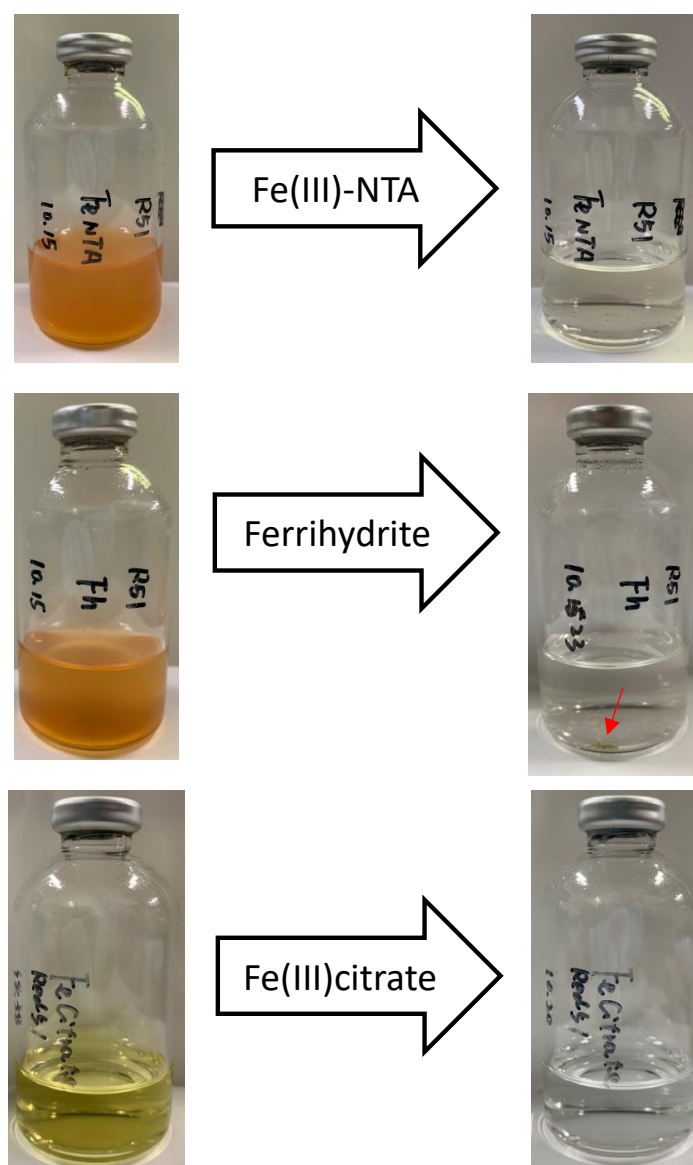


Fig. 3.4 Changed color of iron added medium (Left part) and the medium after bacteria incubated for 1 week (Right part). Red arrow indicates the mineral produced from ferrihydrite transformation.

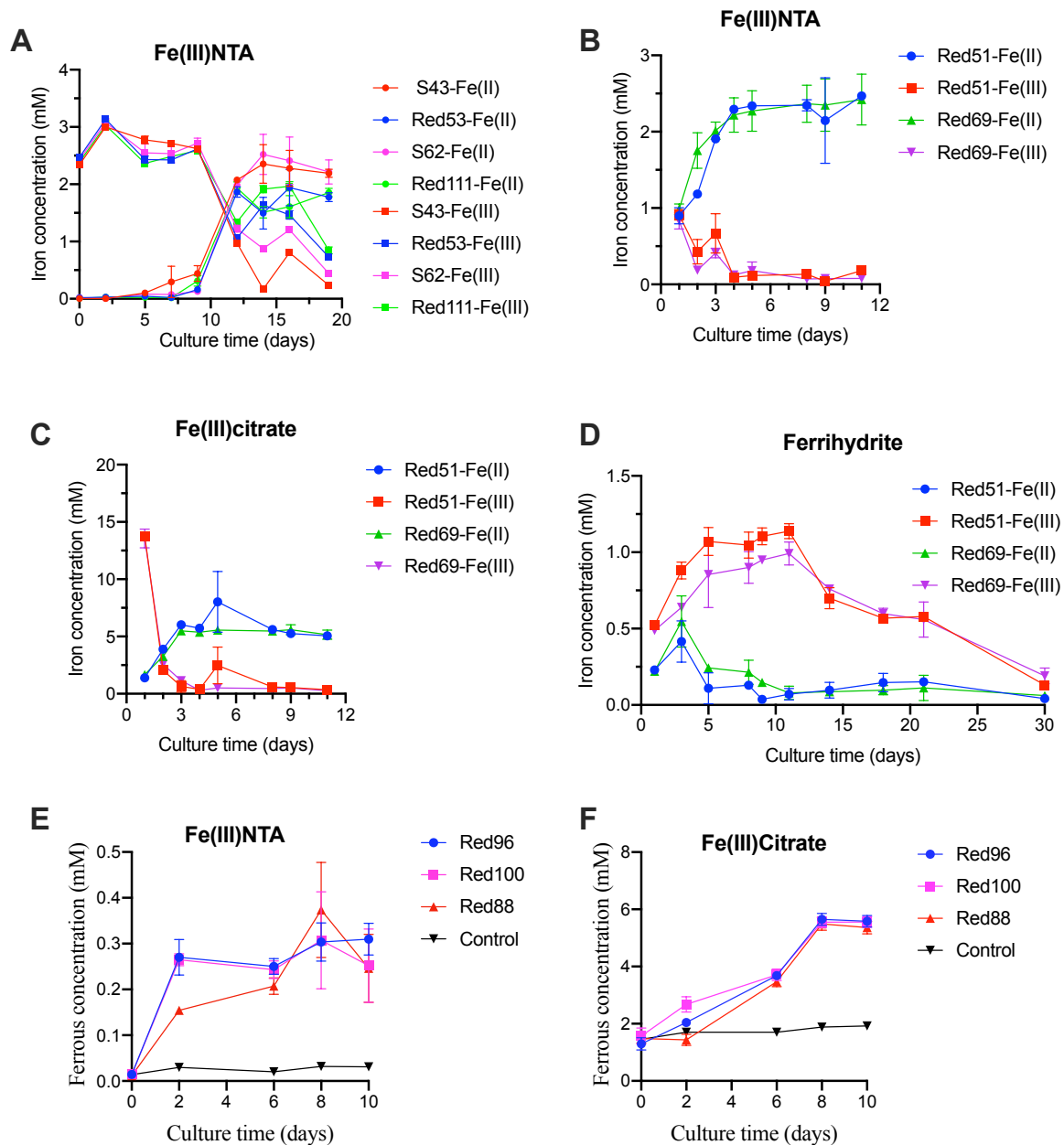


Fig. 3.5 Reduction of Fe(III) by the *Geomocans* (A, B, C, D) and *Oryzomonas* (E, F) strains at different culture time. Control means no-bacteria medium. Data were all presented as means \pm standard deviations (SD) of triplicate. When not shown, error bars are smaller than the symbol size.

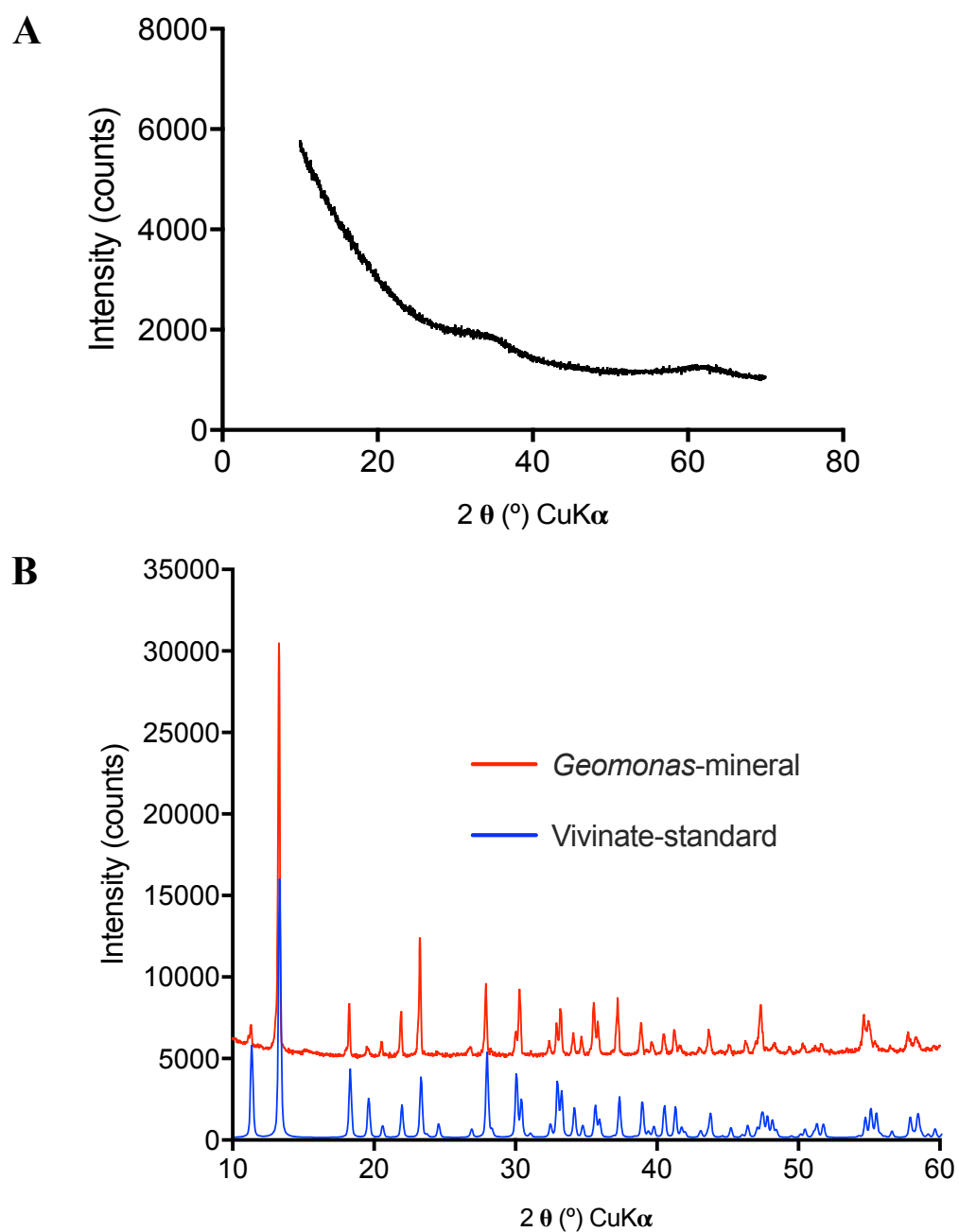


Fig. 3.6 XRD spectra of ferrihydrite (A) and biomineralization products during ferrihydrite reduction by the *Geomonas* strains (B).

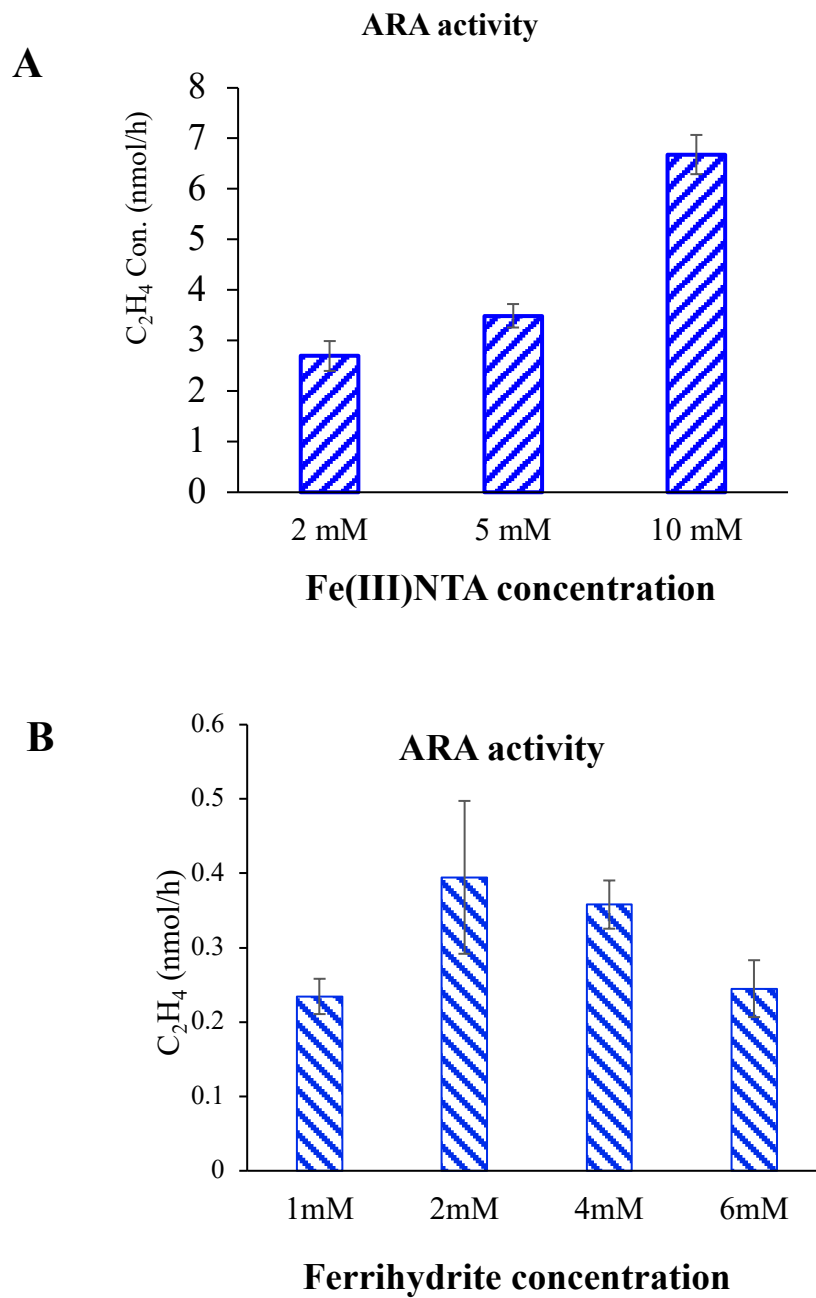


Fig. 3.7 Nitrogen fixing activities under different concentration of Fe(III)-NTA (A) and ferrihydrite (B). Data were all presented as means \pm standard deviations (SD) of triplicate.

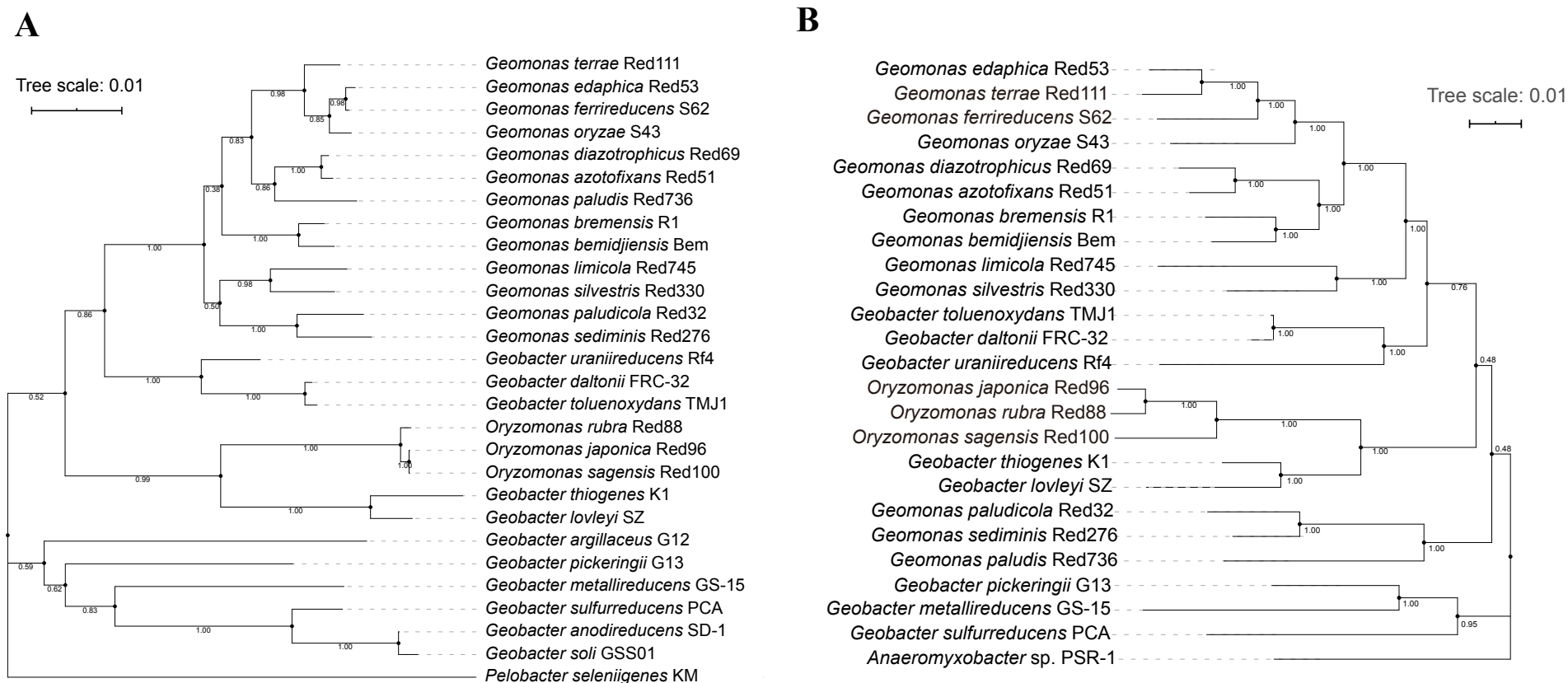


Fig. 3.8 Phylogenetic trees of species in the family *Geobacteraceae* based on 16S rRNA gene sequences (**A**) and concatenated *nifHDK* gene sequences (**B**). The both trees were inferred by the neighbor-joining (NJ) algorithm using MEGA X with Kimura 2-parameter model. Bar, 0.01 substitutions per nucleotide position

Chapter 4: Conclusion and prospect

Paddy soils, as the largest anthropogenic wetlands on the Earth, represent a unique ecosystem that cycles between waterlogged and drained states during long-term paddy cultivation, containing complicated microorganism communities related to multiple biogeochemical cycles. In a previous metatranscriptomic study of paddy soil in Japan performed in our laboratory, it was found that most of the gene transcripts involved in reductive nitrogen transformation were derived from the genera *Geobacter* and *Anaeromyxobacter*, known as iron-reducing bacteria. However, to date, there has been no *Geobacter* and *Anaeromyxobacter* species with a validly published name isolated from paddy soil, and their ability of nitrogen transformations also has not been reported. For this, I performed this study aiming to isolate paddy soil-derived strains and explore their special roles in biogeochemical cycles, especially the functions related to nitrogen transformation.

In this study, 63 different *Geobacter*-like strains and 3 different *Anaeromyxobacter* strains were successfully isolated from paddy soils and nearby places collected all over Japan with an enrichment isolation process. Polyphasic taxonomic analysis revealed that 14 out of these 63 *Geobacter*-like isolates are novel species that belong to 2 novel genera in the family *Geobacteraceae*, for which the names *Geomonas* gen. nov. (11 novel species) and *Oryzomonas* gen. nov. (3 novel species) were proposed, while 3 *Anaeromyxobacter* strains were all characterized as novel species. Further genomic analysis showed that the phylogenetic relationships among the species in the family *Geobacteraceae* are paraphyletic and require taxonomic reclassification. Thus, a reclassification study aimed at dividing the family *Geobacteraceae* into 11 novel genera has also been performed.

A meta-analysis based on the public metagenomic data indicated that the paddy soils are the preferred habitats for *Geobacteraceae* strains. Further studies focusing on paddy soils in Japan showed that the novel genus *Geomonas*, rather than the traditional *Geobacter*, is the predominant driver in the nitrogen reduction process. Thus, I explored the particular role of the novel genus *Geomonas*, and then confirmed that all the tested *Geomonas* strains deeply participate in biogeochemical processes in the soils, by totally reducing Fe(III) to Fe(II), including transforming ferrihydrite to vivianite, a common mineral in the environment. These studied strains also exhibited a high nitrogen-fixing ability, with values ranging from 0.08 to 4.1 nmol/h/10⁹ cells. Moreover, the isolated *Geomonas* strains were found to utilize not only acetate, but also high-molecular cellulose and xylan, the major components of rice straw, as the carbon source to fix nitrogen, indicating that these strains can obtain carbon source from rice straw directly and further couple carbon and nitrogen cycles in paddy soils. Thus, it was supposed that these iron-reducers, isolated and studied in this study, deeply participate and play crucial roles in biogeochemical cycles in natural paddy soils.

In addition, all of the tested *Geomonas* strains showed DNRA activities, reducing NO₃⁻ to NH₄⁺ with the intermediate NO₂⁻, as well as a small amount of N₂O produced (about 1% of added NO₃⁻). N₂O is a damaging greenhouse gas that is mainly produced from the nitrogen cycles in agricultural soils. To date, few reports have clearly answered how the N₂O is produced through DNRA process. In this study, I clarified the mechanism of N₂O emission from DNRA process that N₂O emission is a biotic process and mainly produced from the intermediate NO₂⁻ (ca. 90%) and less from the other intermediate NO (ca. 10%). Furthermore, the site preference (SP) of N₂O from DNRA process was first determined with a value of 46-47‰, the highest value reported so far for biologically produced N₂O. Using the transcriptomic analysis along with RT-qPCR, *nar* gene cluster were abnormally high expressed under the nitrite treatment, which is consistent with the phenotypic results of N₂O generation. Thus, it was supposed that *nar* gene

cluster is mostly the genetic driver reducing nitrite to N₂O in the *Geomonas* strains. Besides, the pH and C/N ratio were found to clearly affect the N₂O emission during the DNRA process via the accumulation of NO₂⁻, which might be a useful reference for N₂O emission mitigation in agricultural management.

Although dozens of *Geobacteraceae* strains have been successfully isolated from paddy soils, the diversities are not consistent with my expectation, because most strains are phylogenetic neighbors, rather than distributed in every phylogenetic branch of the family *Geobacteraceae*. Hence, isolation work for more strains is still strongly needed in the future. Besides, the *Geomonas* strains studied here were confirmed with the special ability using cellulose and xylan as the carbon sources and electron donors for growth, but physiological tests did not find common intermediates during the bacterial utilization processes, which imply more deep researches relying on genetic operations and physiological analysis are required to illustrate this pathway of high-molecular polysaccharide utilization. Furthermore, it was concluded that N₂O was generated from nitrite during the DNRA process and *nar* gene cluster was supposed as the genetic driver, but more detailed information, such as the amount of nitrate for bacteria growth, the genetic mechanism of regulating N₂O emission, and so on, is still unclear. Also, it still lacks physiological evidence to answer whether the *nar* genes or which genes in *nar* cluster are in the leading role for N₂O emission. Thus, further studies are still in need to understand well for this study. Finally, my studies focusing on function clarification of *Geomonas* strains mainly performed using batch experiments with less consideration of natural conditions they were inhabited, so that may cause some biased results for bacterial description. Therefore, bacterial cultivation *in situ* may be a complementary choice for the following studies.

References

- Akiyama, H., Yan, X., and Yagi, K. (2006). Estimations of emission factors for fertilizer-induced direct N₂O emissions from agricultural soils in Japan: Summary of available data. *Soil Sci. Plant Nutr.* 52, 774–787.
- Ali, M. A., Inubushi, K., Kim, P. J., and Amin, S. (2019). “Management of Paddy Soil towards Low Greenhouse Gas Emissions and Sustainable Rice Production in the Changing Climatic Conditions,” in *Soil Contamination and Alternatives for Sustainable Development*, ed. K. Inubushi (Rijeka: IntechOpen), Ch. 6.
- Aliyu, H., Lebre, P., Blom, J., Cowan, D., and De Maayer, P. (2016). Phylogenomic re-assessment of the thermophilic genus *Geobacillus*. *Syst. Appl. Microbiol.* 39, 527–533.
- Aziz, R. K., Bartels, D., Best, A. A., DeJongh, M., Disz, T., Edwards, R. A., et al. (2008). The RAST Server: rapid annotations using subsystems technology. *BMC Genomics* 9, 75.
- Baggs, E. M. (2011). Soil microbial sources of nitrous oxide: Recent advances in knowledge, emerging challenges and future direction. *Curr. Opin. Environ. Sustain.* 3, 321–327.
- Banning, N. C., Maccarone, L. D., Fisk, L. M., and Murphy, D. V (2015). Ammonia-oxidising bacteria not archaea dominate nitrification activity in semi-arid agricultural soil. *Sci. Rep.* 5, 11146.
- Boetzer, M., Henkel, C. V, Jansen, H. J., Butler, D., and Pirovano, W. (2010). Scaffolding pre-assembled contigs using SSPACE. *Bioinformatics* 27, 578–579.
- Boetzer, M., and Pirovano, W. (2012). Toward almost closed genomes with GapFiller. *Genome Biol.* 13, R56.
- Breidenbach, B., Pump, J., and Dumont, M. G. (2016). Microbial community structure in the rhizosphere of rice plants. *Front. Microbiol.* 6, 1537.

- Caccavo, F., Lonergan, D. J., Lovley, D. R., and Davis, M. (1994). *Geobacter sulfurreducens* sp. nov., a hydrogen-and acetate-oxidizing dissimilatory metal-reducing microorganism. *Microbiology* 60, 3752–3759.
- Cai, X., Huang, L., Yang, G., Yu, Z., Wen, J., and Zhou, S. (2018). Transcriptomic, proteomic, and bioelectrochemical characterization of an exoelectrogen *Geobacter soli* grown with different electron acceptors. *Front. Microbiol.* 9, 1075.
- Cairo, G., Bernuzzi, F., and Recalcati, S. (2006). A precious metal: Iron, an essential nutrient for all cells. *Genes Nutr.* 1, 25–39.
- Chun, J., Oren, A., Ventosa, A., Christensen, H., Arahal, D. R., da Costa, M. S., et al. (2018). Proposed minimal standards for the use of genome data for the taxonomy of prokaryotes. *Int. J. Syst. Evol. Microbiol.* 68, 461–466.
- Coby, A. J., and Picardal, F. W. (2005). Inhibition of NO_3^- and NO_2^- reduction by microbial Fe(III) reduction: Evidence of a reaction between NO_2^- and cell surface-bound Fe^{2+} . *Appl. Environ. Microbiol.* 71, 5267–5274.
- Cole, J. A., and Brown, C. M. (1980). Nitrite reduction to ammonia by fermentative bacteria: A short circuit in the biological nitrogen cycle. *FEMS Microbiol. Lett.* 7, 65–72.
- Cornell, R. M., and Schwertmann, U. (2003). *The iron oxides: structure, properties, reactions, occurrences and uses*. John Wiley & Sons.
- Cummings, D. E., Snoeyenbos-West, O. L., Newby, D. T., Niggemyer, A. M., Lovley, D. R., Achenbach, L. A., et al. (2003). Diversity of *Geobacteraceae* species inhabiting metal-polluted freshwater lake sediments ascertained by 16S rDNA analyses. *Microb. Ecol.* 46, 257–269.
- Daims, H., Lebedeva, E. V., Pjevac, P., Han, P., Herbold, C., Albertsen, M., et al. (2015). Complete nitrification by *Nitrospira* bacteria. *Nature* 528, 504–509.
- Dean, J. F., Middelburg, J. J., Röckmann, T., Aerts, R., Blauw, L. G., Egger, M., et al. (2018). Methane feedbacks to the global climate system in a warmer world. *Rev. Geophys.* 56, 207–250.

- Decock, C., and Six, J. (2013). How reliable is the intramolecular distribution of ^{15}N in N_2O to source partition N_2O emitted from soil? *Soil Biol. Biochem.* 65, 114–127.
- Devêvre, O. C., and Horváth, W. R. (2000). Decomposition of rice straw and microbial carbon use efficiency under different soil temperatures and moistures. *Soil Biol. Biochem.* 32, 1773–1785.
- Dixon, R., and Kahn, D. (2004). Genetic regulation of biological nitrogen fixation. *Nat. Rev. Microbiol.* 2, 621–631.
- Emerson, D., Fleming, E. J., and McBeth, J. M. (2010). Iron-oxidizing bacteria: An environmental and genomic perspective. *Annu. Rev. Microbiol.* 64, 561–583.
- FAO. (2001). FAOSTAT, FAO statistical databases.
- Folin, O., and Denis, W. (1916). Nitrogen determination by direct nesslerization. *J. Biol. Chem.* 26, 473–489.
- Francis, C. A., Beman, J. M., and Kuypers, M. M. M. (2007). New processes and players in the nitrogen cycle: the microbial ecology of anaerobic and archaeal ammonia oxidation. *ISME J.* 1, 19–27.
- Frenzel, P., Bosse, U., and Janssen, P. H. (1999). Rice roots and methanogenesis in a paddy soil: ferric iron as an alternative electron acceptor in the rooted soil. *Soil Biol. Biochem.* 31, 421–430.
- Gamble, T. N., Betlach, M. R., and Tiedje, J. M. (1977). Numerically dominant denitrifying bacteria from world soils. *Appl. Environ. Microbiol.* 33, 926–939.
- Giblin, A. E., Tobias, C. R., Song, B., Weston, N., Banta, G. T., and Rivera-Monroy, V. H. (2013). The importance of dissimilatory nitrate reduction to ammonium (DNRA) in the nitrogen cycle of coastal ecosystems. *Oceanography* 26, 124–131.
- Giles, M., Morley, N., Baggs, E. M., and Daniell, T. J. (2012). Soil nitrate reducing processes - Drivers, mechanisms for spatial variation, and

- significance for nitrous oxide production. *Front. Microbiol.* 3, 1–16.
- Hallin, S., Philippot, L., Löffler, F. E., Sanford, R. A., and Jones, C. M. (2018). Genomics and ecology of novel N₂O-reducing microorganisms. *Trends Microbiol.* 26, 43–55.
- Han, G. Z., and Zhang, G. L. (2013). Changes in magnetic properties and their pedogenetic implications for paddy soil chronosequences from different parent materials in south China. *Eur. J. Soil Sci.* 64, 435–444.
- Hattori, S., Savarino, J., Kamezaki, K., Ishino, S., Dyckmans, J., Fujinawa, T., et al. (2016). Automated system measuring triple oxygen and nitrogen isotope ratios in nitrate using the bacterial method and N₂O decomposition by microwave discharge. *Rapid Commun. Mass Spectrom.* 30, 2635–2644.
- Hayatsu, M., Tago, K., and Saito, M. (2008). Various players in the nitrogen cycle: Diversity and functions of the microorganisms involved in nitrification and denitrification. *Soil Sci. Plant Nutr.* 54, 33–45.
- Healy, M., Huong, J., Bittner, T., Lising, M., Frye, S., Raza, S., et al. (1994). Microbial DNA typing by automated repetitive-sequence-based PCR. *J. Clin. Microbiol.* 43, 199–207.
- Hegler, F., Posth, N. R., Jiang, J., and Kappler, A. (2008). Physiology of phototrophic iron(II)-oxidizing bacteria: implications for modern and ancient environments. *FEMS Microbiol. Ecol.* 66, 250–260.
- Heo, H., Kwon, M., Song, B., and Yoon, S. (2020). Involvement of NO₃⁻ in ecophysiological regulation of dissimilatory nitrate/nitrite reduction to ammonium (DNRA) is implied by physiological characterization of soil DNRA bacteria isolated via a colorimetric screening method. *Appl. Environ. Microbiol.* 86.
- Hirano, K., Sugiyama, T., Kosugi, A., Nioh, I., Asai, T., and Nakai, H. (2001). Relationship between number of nitrogen-fixing rhizobacteria and growth pattern of rice varieties in the nature farming. *Breed. Res.* 3, 3–12.
- Holmes, D. E., Dang, Y., Walker, D. J. F., and Lovley, D. R. (2016). The

- electrically conductive pili of *Geobacter* species are a recently evolved feature for extracellular electron transfer. *Microb. genomics* 2, e000072–e000072.
- Holmes, D. E., Giloteaux, L., Chaurasia, A. K., Williams, K. H., Luef, B., Wilkins, M. J., et al. (2015). Evidence of *Geobacter*-associated phage in a uranium-contaminated aquifer. *ISME J.* 9, 333–346.
- Holmes, D. E., Nevin, K. P., and Lovley, D. R. (2004). Comparison of 16S rRNA, *nifD*, *recA*, *gyrB*, *rpoB* and *fusA* genes within the family *Geobacteraceae* fam. nov. *Int. J. Syst. Evol. Microbiol.* 54, 1591–1599.
- Hori, T., Müller, A., Igarashi, Y., Conrad, R., and Friedrich, M. W. (2010). Identification of iron-reducing microorganisms in anoxic rice paddy soil by ¹³C-acetate probing. *ISME J.* 4, 267–278.
- Huang, L., Jia, X., Shao, M., Chen, L., Han, G., and Zhang, G. (2018). Phases and rates of iron and magnetism changes during paddy soil development on calcareous marine sediment and acid Quaternary red-clay. *Sci. Rep.* 8, 444.
- Hussain, Q., Liu, Y., Jin, Z., Zhang, A., Pan, G., Li, L., et al. (2011). Temporal dynamics of ammonia oxidizer (*amoA*) and denitrifier (*nirK*) communities in the rhizosphere of a rice ecosystem from Tai Lake region, China. *Appl. Soil Ecol.* 48, 210–218.
- Ishii, S., Ikeda, S., Minamisawa, K., and Senoo, K. (2011a). Nitrogen cycling in rice paddy environments: past achievements and future challenges. *Microbes Environ.* 26, 282–292.
- Ishii, S., Ohno, H., Tsuboi, M., Otsuka, S., and Senoo, K. (2011b). Identification and isolation of active N₂O reducers in rice paddy soil. *ISME J.* 5, 1936–1945.
- Ishii, S., Yamamoto, M., Kikuchi, M., Oshima, K., Hattori, M., Otsuka, S., et al. (2009). Microbial populations responsive to denitrification-inducing conditions in rice paddy soil, as revealed by comparative 16S rRNA gene analysis. *Appl. Environ. Microbiol.* 75, 7070 – 7078.

- Itoh, H., Ishii, S., Shiratori, Y., Oshima, K., Otsuka, S., Hattori, M., et al. (2013). Seasonal transition of active bacterial and archaeal communities in relation to water management in paddy soils. *Microbes Environ.* ME13030.
- Ji, M., Zhou, L., Zhang, S., Luo, G., and Sang, W. (2020). Effects of biochar on methane emission from paddy soil: Focusing on DOM and microbial communities. *Sci. Total Environ.* 743, 140725.
- Jin, S., and Chen, H. (2007). Near-infrared analysis of the chemical composition of rice straw. *Ind. Crops Prod.* 26, 207–211.
- Kanehisa, M., and Goto, S. (2000). KEGG: kyoto encyclopedia of genes and genomes. *Nucleic Acids Res.* 28, 27–30.
- Kanehisa, M., Sato, Y., and Morishima, K. (2016). BlastKOALA and GhostKOALA: KEGG tools for functional characterization of genome and metagenome sequences. *J. Mol. Biol.* 428, 726–731.
- Karhu, K., Mattila, T., Bergström, I., and Regina, K. (2011). Biochar addition to agricultural soil increased CH₄ uptake and water holding capacity – Results from a short-term pilot field study. *Agric. Ecosyst. Environ.* 140, 309–313.
- Kim, M., Oh, H. S., Park, S. C., and Chun, J. (2014). Towards a taxonomic coherence between average nucleotide identity and 16S rRNA gene sequence similarity for species demarcation of prokaryotes. *Int. J. Syst. Evol. Microbiol.* 64, 346–351.
- Kim, Y., and Liesack, W. (2015). Differential assemblage of functional units in paddy soil microbiomes. *PLoS One* 10, e0122221.
- Kimura, M. (2000). Anaerobic microbiology in waterlogged rice fields. *Soil Biochem.* 10, 35–138.
- Kimura, M., Murase, J., and Lu, Y. (2004). Carbon cycling in rice field ecosystems in the context of input, decomposition and translocation of organic materials and the fates of their end products (CO₂ and CH₄). *Soil Biol. Biochem.* 36, 1399–1416.
- Kits, K. D., Jung, M.-Y., Vierheilig, J., Pjevac, P., Sedlacek, C. J., Liu, S., et al.

- (2019). Low yield and abiotic origin of N₂O formed by the complete nitrifier *Nitrospira inopinata*. *Nat. Commun.* 10, 1836.
- Knoblauch, C., Maarifat, A. A., Pfeiffer, E. M., and Haefele, S. M. (2011). Degradability of black carbon and its impact on trace gas fluxes and carbon turnover in paddy soils. *Soil Biol. Biochem.* 43, 1768–1778.
- Kohanski, M. A., Dwyer, D. J., Hayete, B., Lawrence, C. A., and Collins, J. J. (2007). A common mechanism of cellular death induced by bactericidal antibiotics. *Cell* 130, 797–810.
- Köhsler, M., Leitsch, D., Müller, N., and Walochnik, J. (2020). Validation of reference genes for the normalization of RT-qPCR gene expression in *Acanthamoeba* spp. *Sci. Rep.* 10, 10362.
- Könneke, M., Bernhard, A. E., de la Torre, J. R., Walker, C. B., Waterbury, J. B., and Stahl, D. A. (2005). Isolation of an autotrophic ammonia-oxidizing marine archaeon. *Nature* 437, 543–546.
- Kondo, M. 1993. Acetylene reduction activity of paddy field soils. *Tohoku Agric. Res.* 46, 97–98 (in Japanese).
- Konstantinidis, K. T., and Tiedje, J. M. (2005). Towards a genome-based taxonomy for prokaryotes. *J. Bacteriol.* 187, 6258–6264.
- Kudo, K., Yamaguchi, N., Makino, T., Ohtsuka, T., Kimura, K., Dong, D. T., et al. (2013). Release of arsenic from soil by a novel dissimilatory arsenate-reducing bacterium, *Anaeromyxobacter* sp. strain PSR-1. *Appl. Environ. Microbiol.* 79, 4635–4642.
- Kumar, S., Stecher, G., Li, M., Knyaz, C., and Tamura, K. (2018). MEGA X: Molecular evolutionary genetics analysis across computing platforms. *Mol. Biol. Evol.* 35, 1547–1549.
- Kunapuli, U., Jahn, M. K., Lueders, T., Geyer, R., Heipieper, H. J., and Meckenstock, R. U. (2010). *Desulfitobacterium aromaticivorans* sp. nov. and *Geobacter toluenoxydans* sp. nov., iron-reducing bacteria capable of anaerobic degradation of monoaromatic hydrocarbons. *Int. J. Syst. Evol.*

- Microbiol.* 60, 686–695.
- Kuypers, M. M. M., Marchant, H. K., and Kartal, B. (2018). The microbial nitrogen-cycling network. *Nat. Rev. Microbiol.* 16, 263.
- Lagier, J.-C., Dubourg, G., Million, M., Cadoret, F., Bilen, M., Fenollar, F., et al. (2018). Culturing the human microbiota and culturomics. *Nat. Rev. Microbiol.* 16, 540–550.
- Li, L., Jia, R., Qu, Z., Li, T., Shen, W., and Qu, D. (2020a). Coupling between nitrogen-fixing and iron(III)-reducing bacteria as revealed by the metabolically active bacterial community in flooded paddy soils amended with glucose. *Sci. Total Environ.* 716, 137056.
- Li, X., McInerney, M. J., Stahl, D. A., and Krumholz, L. R. (2011). Metabolism of H₂ by *Desulfovibrio alaskensis* G20 during syntrophic growth on lactate. *Microbiology* 157, 2912–2921.
- Li, Y. L., Zhang, Y. L., Hu, J., and Shen, Q. R. (2007). Contribution of nitrification happened in rhizospheric soil growing with different rice cultivars to N nutrition. *Biol. Fertil. Soils* 43, 417–425.
- Li, Y., Shahbaz, M., Zhu, Z., Chen, A., Nannipieri, P., Li, B., et al. (2020b). Contrasting response of organic carbon mineralisation to iron oxide addition under conditions of low and high microbial biomass in anoxic paddy soil. *Biol. Fertil. Soils*. 1–13.
- Li, Y., Xue, H., Sang, S., Lin, C., and Wang, X. (2017). Phylogenetic analysis of family *Neisseriaceae* based on genome sequences and description of *Populibacter corticis* gen. nov., sp. nov., a member of the family *Neisseriaceae*, isolated from symptomatic bark of *Populus × euramericana* canker. *PLoS One* 12, e0174506.
- Liesack, W., Schnell, S., and Revsbech, N. P. (2000). Microbiology of flooded rice paddies. *FEMS Microbiol. Rev.* 24, 625–645.
- Liu, Y., Yang, M., Wu, Y., Wang, H., Chen, Y., and Wu, W. (2011). Reducing CH₄ and CO₂ emissions from waterlogged paddy soil with biochar. *J. Soils*

Sediments 11, 930–939.

- Lopes-Santos, L., Castro, D. B. A., Ferreira-Tonin, M., Corrêa, D. B. A., Weir, B. S., Park, D., et al. (2017). Reassessment of the taxonomic position of *Burkholderia andropogonis* and description of *Robbsia andropogonis* gen. nov., comb. nov. *Antonie van Leeuwenhoek* 110, 727–736.
- Love, M. I., Huber, W., and Anders, S. (2014). Moderated estimation of fold change and dispersion for RNA-seq data with DESeq2. *Genome Biol.* 15, 550.
- Lovley, D. R., Giovannoni, S. J., White, D. C., Champine, J. E., Phillips, E. J. P., Gorby, Y. A., et al. (1993). *Geobacter metallireducens* gen. nov. sp. nov., a microorganism capable of coupling the complete oxidation of organic compounds to the reduction of iron and other metals. *Arch. Microbiol.* 159.
- Lovley, D. R., and Phillips, E. J. P. (1986). Organic matter mineralization with reduction of ferric iron in anaerobic sediments. *Appl. Environ. Microbiol.* 51, 683–689.
- Lovley, D. R., Ueki, T., Zhang, T., Malvankar, N. S., Shrestha, P. M., Flanagan, K. A., et al. (2011). *Geobacter. The Microbe Electric's Physiology, Ecology, and Practical Applications*. 1st ed. Elsevier Ltd.
- Lovley, D. R., and Walker, D. J. F. (2019). *Geobacter* protein nanowires. *Front. Microbiol.* 10, 2078.
- Luo, C., Rodriguez-R, L. M., and Konstantinidis, K. T. (2014). MyTaxa: an advanced taxonomic classifier for genomic and metagenomic sequences. *Nucleic Acids Res.* 42, e73–e73.
- Malvankar, N. S., and Lovley, D. R. (2014). Microbial nanowires for bioenergy applications. *Curr. Opin. Biotechnol.* 27, 88–95.
- Mancinelli, R. L. (1996). The nature of nitrogen: an overview. *Life Support Biosph. Sci.* 3, 17–24.
- Mark Moore, C., Mills, M. M., Achterberg, E. P., Geider, R. J., LaRoche, J., Lucas, M. I., et al. (2009). Large-scale distribution of Atlantic nitrogen fixation controlled by iron availability. *Nat. Geosci.* 2, 867–871.

- Masuda, Y., Itoh, H., Shiratori, Y., Isobe, K., Otsuka, S., and Senoo, K. (2017). Predominant but previously-overlooked prokaryotic drivers of reductive nitrogen transformation in paddy soils, revealed by metatranscriptomics. *Microbes Environ.* 32, 180–183.
- Masuda, Y., Yamanaka, H., Xu, Z. X., Shiratori, Y., Aono, T., Amachi, S., et al. (2020). Diazotrophic *Anaeromyxobacter* isolates from soils. *Appl. Environ. Microbiol.* 86, 1–12.
- Medinets, S., Skiba, U., Rennenberg, H., and Butterbach-Bahl, K. (2015). A review of soil NO transformation: Associated processes and possible physiological significance on organisms. *Soil Biol. Biochem.* 80, 92–117.
- Meier-Kolthoff, J. P., Klenk, H. P., and Göker, M. (2014). Taxonomic use of DNA G+C content and DNA-DNA hybridization in the genomic age. *Int. J. Syst. Evol. Microbiol.* 64, 352–356.
- Mendler, K., Chen, H., Parks, D. H., Lobb, B., Hug, L. A., and Doxey, A. C. (2019). AnnoTree: visualization and exploration of a functionally annotated microbial tree of life. *Nucleic Acids Res.* 47, 4442–4448.
- Meyer, F., Paarmann, D., D’Souza, M., Olson, R., Glass, E. M., Kubal, M., et al. (2008). The metagenomics RAST server – a public resource for the automatic phylogenetic and functional analysis of metagenomes. *BMC Bioinformatics* 9, 386.
- Mills, M. M., Ridame, C., Davey, M., La Roche, J., and Geider, R. J. (2004). Iron and phosphorus co-limit nitrogen fixation in the eastern tropical North Atlantic. *Nature* 429, 292–294.
- Mise, K., and Iwasaki, W. (2020). Environmental atlas of prokaryotes enables powerful and intuitive habitat-based analysis of community structures. *iScience* 23, 101624.
- Montzka, S. A., Dlugokencky, E. J., and Butler, J. H. (2011). Non-CO₂ greenhouse gases and climate change. *Nature* 476, 43–50.
- Moreira, A. P. B., Pereira, N., and Thompson, F. L. (2011). Usefulness of a real-

- time PCR platform for G+C content and DNA-DNA hybridization estimations in vibrios. *Int. J. Syst. Evol. Microbiol.* 61, 2379–2383.
- Mouser, P. J., Holmes, D. E., Perpetua, L. A., DiDonato, R., Postier, B., Liu, A., et al. (2009). Quantifying expression of *Geobacter* spp. oxidative stress genes in pure culture and during in situ uranium bioremediation. *ISME J.* 3, 454–465.
- Na, S. I., Kim, Y. O., Yoon, S. H., Ha, S., Baek, I., and Chun, J. (2018). UBCG: Up-to-date bacterial core gene set and pipeline for phylogenomic tree reconstruction. *J. Microbiol.* 56, 280–285.
- Nakajima, A., Aono, T., Tsukada, S., Siarot, L., Ogawa, T., and Oyaizu, H. (2012). Lon protease of *Azorhizobium caulinodans* ORS571 is required for suppression of *reb* gene expression. *Appl. Environ. Microbiol.* 78, 6251–6261.
- Nakamura, A., Tun, C. C., Asakawa, S., and Kimura, M. (2003). Microbial community responsible for the decomposition of rice straw in a paddy field: estimation by phospholipid fatty acid analysis. *Biol. Fertil. Soils* 38, 288–295.
- Nevin, K. P., Holmes, D. E., Woodard, T. L., Hinlein, E. S., Ostendorf, D. W., and Lovley, D. R. (2005). *Geobacter bemidjensis* sp. nov. and *Geobacter psychrophilus* sp. nov., two novel Fe(III)-reducing subsurface isolates. *Int. J. Syst. Evol. Microbiol.* 55, 1667–1674.
- Nojiri, Y., Shiratori, Y., Ohte, N., Senoo, K., Kaneko, Y., Azegami, Y., et al. (2020). Dissimilatory nitrate reduction to ammonium and responsible microbes in Japanese rice paddy soil. *Microbes Environ.* 35, 1–7.
- Onley, J. R., Ahsan, S., and Sanford, R. A. (2018). Denitrification by *Anaeromyxobacter dehalogenans*, a common soil bacterium lacking the nitrite reductase genes *nirS* and *nirK*. *Appl. Environ. Microbiol.* 84, 1–14.
- Orata, F. D., Meier-Kolthoff, J. P., Sauvageau, D., and Stein, L. Y. (2018). Phylogenomic analysis of the gammaproteobacterial methanotrophs (order

- methylococcales*) calls for the reclassification of members at the genus and species levels. *Front. Microbiol.* 9, 1–17.
- Philippot, L., Hallin, S., and Schloter, M. (2007). Ecology of denitrifying prokaryotes in agricultural soil. *Advances in agronomy*, 96, 249–305.
- Ponnamperuma, F. N. (1972). The chemistry of submerged soils. In *Advances in agronomy* (Vol. 24, pp. 29-96). Academic Press.
- Ponnamperuma, F. N. (1981). Some aspects of the physical chemistry of paddy soils. In *Proceedings of Symposium on Paddy Soils* (pp. 59-94). Springer, Berlin, Heidelberg.
- Postgate, J. R. (1972). Chapter XIII The acetylene reduction test for nitrogen fixation. In *Methods in microbiology* (Vol. 6, pp. 343-356). Academic Press.
- Poth, M., and Focht, D. D. (1985). N kinetic analysis of N₂O production by *Nitrosomonas europaea*: an examination of nitrifier denitrification. *Appl. Environ. Microbiol.* 49, 1134–1141.
- Prakash, O., Gihring, T. M., Dalton, D. D., Chin, K. J., Green, S. J., Akob, D. M., et al. (2010). *Geobacter daltonii* sp. nov., an Fe(III)- and uranium(VI)-reducing bacterium isolated from a shallow subsurface exposed to mixed heavy metal and hydrocarbon contamination. *Int. J. Syst. Evol. Microbiol.* 60, 546–553.
- Pruitt, K. D., Tatusova, T., and Maglott, D. R. (2005). NCBI Reference Sequence (RefSeq): a curated non-redundant sequence database of genomes, transcripts and proteins. *Nucleic Acids Res.* 33, D501–D504.
- Qin, Q. L., Xie, B. B., Zhang, X. Y., Chen, X. L., Zhou, B. C., Zhou, J., et al. (2014). A proposed genus boundary for the prokaryotes based on genomic insights. *J. Bacteriol.* 196, 2210–2215.
- Ranatunga, T., Hiramatsu, K., Onishi, T., and Ishiguro, Y. (2018). Process of denitrification in flooded rice soils. *Rev. Agric. Sci.* 6, 21–33.
- Ratering, S., and Schnell, S. (2001). Nitrate-dependent iron(II) oxidation in paddy soil. *Environ. Microbiol.* 3, 100–109.

- Raymond, J., Siefert, J. L., Staples, C. R., and Blankenship, R. E. (2004). The natural history of nitrogen fixation. *Mol. Biol. Evol.* 21, 541–554.
- Reguera, G., and Kashefi, K. (2019). The electrifying physiology of *Geobacter* bacteria, 30 years on. *Adv. Microb. Physiol.* 74, 1–96.
- Revsbech, N. P., Pedersen, O., Reichardt, W., and Briones, A. (1999). Microsensor analysis of oxygen and pH in the rice rhizosphere under field and laboratory conditions. *Biol. Fertil. Soils* 29, 379–385.
- Richardson, D. J., Rowley, G., Felgate, H., Stremińska, M. A., and Baggs, E. M. (2011). Nitrous oxide production in soil isolates of nitrate-ammonifying bacteria. *Environ. Microbiol. Rep.* 4, 66–71.
- Richter, M., and Rosselló-Móra, R. (2009). Shifting the genomic gold standard for the prokaryotic species definition. *Proc. Natl. Acad. Sci. U. S. A.* 106, 19126–19131.
- Richter, M., Rosselló-Móra, R., Oliver Glöckner, F., and Peplies, J. (2016). JSpeciesWS: a web server for prokaryotic species circumscription based on pairwise genome comparison. *Bioinformatics* 32, 929–931.
- Rickard, D. (2012). Sedimentary iron biogeochemistry. In *Developments in sedimentology* (Vol. 65, pp. 85–119). Elsevier.
- Rocha, D. J. P., Santos, C. S., and Pacheco, L. G. C. (2015). Bacterial reference genes for gene expression studies by RT-qPCR: survey and analysis. *Antonie van Leeuwenhoek* 108, 685–693.
- Roger, P. A., Zimmerman, W. J., and Lumpkin, T. A. (1993). Microbiological management of wetland rice fields. *Soil Microb. Ecol. Appl. Agric. Environ. Manag.*, 417–455.
- Röling, W. F. M. (2014). “The Family *Geobacteraceae* BT - The Prokaryotes: *Deltaproteobacteria* and *Epsilonproteobacteria*,” in, eds. E. Rosenberg, E. F. DeLong, S. Lory, E. Stackebrandt, and F. Thompson (Berlin, Heidelberg: Springer Berlin Heidelberg), 157–172.
- Rosselló-Móra, R., and Amann, R. (2015). Past and future species definitions for

- Bacteria and Archaea. *Syst. Appl. Microbiol.* 38, 209–216.
- Rothe, M., Kleeberg, A., and Hupfer, M. (2016). The occurrence, identification and environmental relevance of vivianite in waterlogged soils and aquatic sediments. *Earth-Science Rev.* 158, 51–64.
- Rütting, T., Boeckx, P., Müller, C., and Klemmedtsson, L. (2011). Assessment of the importance of dissimilatory nitrate reduction to ammonium for the terrestrial nitrogen cycle. *Biogeosciences* 8, 1779–1791.
- Sander, B. O., Samson, M., and Buresh, R. J. (2014). Methane and nitrous oxide emissions from flooded rice fields as affected by water and straw management between rice crops. *Geoderma* 235, 355–362.
- Sanford, R. A., Cole, J. R., and Tiedje, J. M. (2002). Characterization and description of *Anaeromyxobacter dehalogenans* gen. nov., sp. nov., an aryl-halorespiring facultative anaerobic *Myxobacterium*. *Appl. Environ. Microbiol.* 68, 893–900.
- Sasakawa, H., and Yamamoto, Y. (1978). Comparison of the uptake of nitrate and ammonium by rice seedlings: influences of light, temperature, oxygen concentration, exogenous sucrose, and metabolic inhibitors. *Plant Physiol.* 62, 665–669.
- Sass, R. L., Fisher, F. M., Turner, F. T., and Jund, M. F. (1991). Methane emission from rice fields as influenced by solar radiation, temperature, and straw incorporation. *Global Biogeochem. Cycles* 5, 335–350.
- Satoh, T., Hom, S. S. M., and Shanmugam, K. T. (1983). Production of nitrous oxide from nitrite in *Klebsiella pneumoniae*: Mutants altered in nitrogen metabolism. *J. Bacteriol.* 155, 454–458.
- Scheid, D., Stubner, S., and Conrad, R. (2004). Identification of rice root associated nitrate, sulfate and ferric iron reducing bacteria during root decomposition. *FEMS Microbiol. Ecol.* 50, 101–110.
- Schink, B. (1984). Fermentation of 2,3-butanediol by *Pelobacter carbinolicus* sp. nov. and *Pelobacter propionicus* sp. nov., and evidence for propionate

- formation from C₂ compounds. *Arch. Microbiol.* 137, 33–41.
- Schmittgen, T. D., and Livak, K. J. (2008). Analyzing real-time PCR data by the comparative CT method. *Nat. Protoc.* 3, 1101–1108.
- Serrano-silva, N., Sarria-guzman, Y., Dendooven, L., and Luna-guido, M. (2014). Methanogenesis and methanotrophy in soil: A review. *Pedosphere* 24, 291–307.
- Shi, L., Dong, H., Reguera, G., Beyenal, H., Lu, A., Liu, J., et al. (2016). Extracellular electron transfer mechanisms between microorganisms and minerals. *Nat. Rev. Microbiol.* 14, 651–662.
- Shi, X., and Wang, J. (2015). Engineering and characterization of a symbiotic selection-marker-free vector-host system for therapeutic plasmid production. *Mol Med Rep* 12, 4669–4677.
- Shoun, H., Kim, D. H., Uchiyama, H., and Sugiyama, J. (1992). Denitrification by fungi. *FEMS Microbiol. Lett.* 94, 277–281.
- Shrestha, P. M., Rotaru, A. E., Summers, Z. M., Shrestha, M., Liu, F., and Lovley, D. R. (2013). Transcriptomic and genetic analysis of direct interspecies electron transfer. *Appl. Environ. Microbiol.* 79, 2397–2404.
- Sirohi, S. K., Pandey, N., Singh, B., and Puniya, A. K. (2010). Rumen methanogens: a review. *Indian J. Microbiol.* 50, 253–262.
- Skenneron, C. T., Ward, L. M., Michel, A., Metcalfe, K., Valiente, C., Mullin, S., et al. (2015). Genomic reconstruction of an uncultured hydrothermal vent gammaproteobacterial methanotroph (Family *Methylothermaceae*) indicates multiple adaptations to oxygen limitation. *Front. Microbiol.* 6, 1–12.
- Smith, M. S. (1983). Nitrous oxide production by *Escherichia coli* is correlated with nitrate reductase activity. *Appl. Environ. Microbiol.* 45, 1545–1547.
- Spokas, K. A., and Reicosky, D. C. (2009). Impacts of sixteen different biochars on soil greenhouse gas production. *Ann. Environ. Sci.* 179.
- Straub, K. L., Benz, M., Schink, B., and Widdel, F. (1996). Anaerobic, nitrate-dependent microbial oxidation of ferrous iron. *Appl. Environ. Microbiol.* 62,

1458–1460.

- Straub, K. L., and Buchholz-cleven, B. E. E. (2001). *Geobacter bremensis* sp. nov. and *Geobacter pelophilus* sp. nov., two dissimilatory ferric-iron-reducing bacteria. *Int. J. Syst. Evol. Microbiol.*, 1805–1808.
- Strohm, T. O., Griffin, B., Zumft, W. G., and Schink, B. (2007). Growth yields in bacterial denitrification and nitrate ammonification. *Appl. Environ. Microbiol.* 73, 1420–1424.
- Sun, D., Wang, A., Cheng, S., Yates, M., and Logan, B. E. (2014). *Geobacter anodireducens* sp. nov., an exoelectrogenic microbe in bioelectrochemical systems. *Int. J. Syst. Evol. Microbiol.* 64, 3485–3491.
- Syaftika, N., and Matsumura, Y. (2018). Comparative study of hydrothermal pretreatment for rice straw and its corresponding mixture of cellulose, xylan, and lignin. *Bioresour. Technol.* 255, 1–6.
- Takayuki Saito, Ishii, S., Otsuka, S., Nishiyama, M., and Senoo, K. (2008). Identification of novel *Betaproteobacteria* in a succinate-assimilating population in denitrifying rice paddy soil by using stable isotope probing. *Microbes Environ.* 23, 192–200.
- Terasawa, S. (1975). Physical properties of paddy soil in Japan. *Jpn Agric Res Q* 9, 18–23.
- Thauer, R. K., Kaster, A. K., Seedorf, H., Buckel, W., and Hedderich, R. (2008). Methanogenic archaea: ecologically relevant differences in energy conservation. *Nat. Rev. Microbiol.* 6, 579–591.
- Thompson, L. R., Sanders, J. G., McDonald, D., Amir, A., Ladau, J., Locey, K. J., et al. (2017). A communal catalogue reveals Earth’s multiscale microbial diversity. *Nature* 551, 457–463.
- Thomson, A. J., Giannopoulos, G., Pretty, J., Baggs, E. M., and Richardson, D. J. (2012). Biological sources and sinks of nitrous oxide and strategies to mitigate emissions. *Philos. Trans. R. Soc. Lond. B. Biol. Sci.* 367, 1157–1168.
- Tiedje, J. M., Sexstone, A. J., Myrold, D. D., and Robinson, J. A. (1983).

- Denitrification: ecological niches, competition and survival. *Antonie Van Leeuwenhoek* 48, 569–583.
- Tiedje, J.M. 1992. Denitrifiers, p. 245-265. In R.W. Weaver, J.S. Angle, and P.J. Bottomley (ed.), *Methods of Soil Analysis*, Part 2-Microbiological and Biochemical Properties. Soil Science Society of America, Inc., Madison, Wis.
- Tilman, D., and Clark, M. (2014). Global diets link environmental sustainability and human health. *Nature* 515, 518–522.
- Tipayno, S. C., Truu, J., Samaddar, S., Truu, M., Preem, J. K., Oopkaup, K., et al. (2018). The bacterial community structure and functional profile in the heavy metal contaminated paddy soils, surrounding a nonferrous smelter in South Korea. *Ecol. Evol.* 8, 6157–6168.
- Torres, M. J., Simon, J., Rowley, G., Delgado, M. J., Richardson, D. J., Gates, A. J., et al. (2016). Nitrous oxide metabolism in nitrate-reducing bacteria. In *Advances in microbial physiology* (Vol. 68, pp. 353-432). Academic Press.
- Toyoda, S., and Yoshida, N. (1999). Determination of nitrogen isotopomers of nitrous oxide on a modified isotope ratio mass spectrometer. *Anal. Chem.* 71, 4711–4718.
- Toyoda, S., Yoshida, N., and Koba, K. (2017). Isotopocule analysis of biologically produced nitrous oxide in various environments. *Mass Spectrom. Rev.*, 135–160.
- Treacy, M. M. J., Newsam, J. M., and Deem, M. W. (1991). A general recursion method for calculating diffracted intensities from crystals containing planar faults. *Proc. R. Soc. London. Ser. A Math. Phys. Sci.* 433, 499–520.
- Treude, N., Rosencrantz, D., Liesack, W., and Schnell, S. (2003). Strain FAc12, a dissimilatory iron-reducing member of the *Anaeromyxobacter* subgroup of *Myxococcales*. *FEMS Microbiol. Ecol.* 44, 261–269.
- van den Berg, E. M., van Dongen, U., Abbas, B., and van Loosdrecht, M. C. M. (2015). Enrichment of DNRA bacteria in a continuous culture. *ISME J.* 9,

2153–2161.

- van Kessel, M. A. H. J., Speth, D. R., Albertsen, M., Nielsen, P. H., Op den Camp, H. J. M., Kartal, B., et al. (2015). Complete nitrification by a single microorganism. *Nature* 528, 555–559.
- Viulu, S., Nakamura, K., Okada, Y., Saitou, S., and Takamizawa, K. (2013). *Geobacter luticola* sp. nov., an Fe (III)-reducing bacterium isolated from lotus field mud. *Int. J. Syst. Evol. Microbiol.* 2, 442–448.
- Waite, D. W., Chuvochina, M., Pelikan, C., Parks, D. H., Yilmaz, P., Wagner, M., et al. (2020). Proposal to reclassify the proteobacterial classes *Deltaproteobacteria* and *Oligoflexia*, and the phylum *Thermodesulfobacteria* into four phyla reflecting major functional capabilities. *Int. J. Syst. Evol. Microbiol.* 70, 5972–6016.
- Walker, D. J. F., Adhikari, R. Y., Holmes, D. E., Ward, J. E., Woodard, T. L., Nevin, K. P., et al. (2018). Electrically conductive pili from pilin genes of phylogenetically diverse microorganisms. *ISME J.* 12, 48–58.
- Wang, M., Hu, R., Ruser, R., Schmidt, C., and Kappler, A. (2020a). Role of chemodenitrification for N₂O emissions from nitrate reduction in rice paddy soils. *ACS Earth Sp. Chem.* 4, 122–132.
- Wang, X., Bei, Q., Yang, W., Zhang, H., Hao, J., Qian, L., et al. (2020b). Unveiling of active diazotrophs in a flooded rice soil by combination of NanoSIMS and ¹⁵N₂-DNA-stable isotope probing. *Biol. Fertil. Soils*, 1189–1199.
- Weber, K. A., Achenbach, L. A., and Coates, J. D. (2006). Microorganisms pumping iron: Anaerobic microbial iron oxidation and reduction. *Nat. Rev. Microbiol.* 4, 752–764.
- Wegner, C. E., and Liesack, W. (2016). Microbial community dynamics during the early stages of plant polymer breakdown in paddy soil. *Environ. Microbiol.* 18, 2825–2842.
- Wirth, J. S., and Whitman, W. B. (2018). Phylogenomic analyses of a clade

- within the roseobacter group suggest taxonomic reassignments of species of the genera *Aestuariivita*, *Citreicella*, *Loktanella*, *Nautella*, *Pelagibaca*, *Ruegeria*, *Thalassobius*, *Thiobacimonas* and *Tropicibacter*, and the proposal of six novel genera. *Int. J. Syst. Evol. Microbiol.* 68, 2393–2411.
- Xie, F., Xiao, P., Chen, D., Xu, L., and Zhang, B. (2012). miRDeepFinder: a miRNA analysis tool for deep sequencing of plant small RNAs. *Plant Mol. Biol.* 80, 75–84.
- Xu, Z., Masuda, Y., Hayakawa, C., Ushijima, N., Kawano, K., Shiratori, Y., et al. (2020a). Description of three novel members in the family *Geobacteraceae*, *Oryzomonas japonicum* gen. nov., sp. nov., *Oryzomonas sagensis* sp. nov., and *Oryzomonas ruber* sp. nov. *Microorganisms* 8, 634.
- Xu, Z., Masuda, Y., Itoh, H., Ushijima, N., and Shiratori, Y. (2019). *Geomonas edaphica* sp. nov., *Geomonas ferrireducens* sp. nov., *Geomonas terrae* sp. nov., four ferric-reducing bacteria isolated from paddy soil, and reclassification of three species of the genus *Geobacter* as members of the genus *Geomonas* gen. nov. *Front. Microbiol.* 10, 1–17.
- Xu, Z., Yu, P., Liang, Q., Mu, D., and Du, Z. (2020b). Inducible expression of agar-degrading genes in a marine bacterium *Catenovulum maritimus* Q1^T and characterization of a β -agarase. *Appl. Microbiol. Biotechnol.* 104, 10541–10553.
- Yamamoto, E., Muramatsu, H., and Nagai, K. (2014). *Vulgatibacter incomptus* gen. nov., sp. nov. and *Labilithrix luteola* gen. nov., sp. nov., two myxobacteria isolated from soil in Yakushima island, and the description of *Vulgatibacteraceae* fam. nov., *Labilitrichaceae* fam. nov. and *Anaeromyxobacteraceae* fam. *Int. J. Syst. Evol. Microbiol.* 64, 3360–3368.
- Yao, H., Conrad, R., Wassmann, R., and Neue, H. U. (1999). Effect of soil characteristics on sequential reduction and methane production in sixteen rice paddy soils from China, the Philippines, and Italy. *Biogeochemistry* 47, 269–295.

- Yarza, P., Yilmaz, P., Pruesse, E., Glöckner, F. O., Ludwig, W., Schleifer, K. H., et al. (2014). Uniting the classification of cultured and uncultured bacteria and archaea using 16S rRNA gene sequences. *Nat. Rev. Microbiol.* 12, 635.
- Yoon, S., Cruz-García, C., Sanford, R., Ritalahti, K. M., and Löffler, F. E. (2015). Denitrification versus respiratory ammonification: Environmental controls of two competing dissimilatory $\text{NO}_3^-/\text{NO}_2^-$ reduction pathways in *Shewanella loihica* strain PV-4. *ISME J.* 9, 1093–1104.
- Yoon, S. H., Ha, S. M., Kwon, S., Lim, J., Kim, Y., Seo, H., et al. (2017). Introducing EzBioCloud: A taxonomically united database of 16S rRNA gene sequences and whole-genome assemblies. *Int. J. Syst. Evol. Microbiol.* 67, 1613–1617.
- Yu, K., and Pauls, K. P. (1992). Optimization of the PCR program for RAPD analysis. *Nucleic Acids Res.* 20, 2606.
- Zerbino, D. R., and Birney, E. (2008). Velvet: Algorithms for de novo short read assembly using de Bruijn graphs. *Genome Res.* 18, 821–829.
- Zhang, L., Jiang, M., Ding, K., and Zhou, S. (2019). Iron oxides affect denitrifying bacterial communities with the *nirS* and *nirK* genes and potential N_2O emission rates from paddy soil. *Eur. J. Soil Biol.* 93, 103093.
- Zhou, S., Yang, G., Lu, Q., and Wu, M. (2014). *Geobacter soli* sp. nov., A dissimilatory Fe(III)-reducing bacterium isolated from forest soil. *Int. J. Syst. Evol. Microbiol.* 64, 3786–3791.

Supplementary materials

Table 4.1 Primers used in this study

	Gene name	Primer sequence
Candidate reference genes	rpoB-F	ARGGYAAGGTGACCGACGAGG
	rpoB-R	ACCGACCAGCACGAAYTCGC
	recA-F	GTCVAAGTGTGCGTCATCT
	recA-R	GTTCTTSACCACTTSACGC
	rpoD-F	CGTGCTCTCCACCCTGAC
	rpoD-R	CCTGRCCCACCTCTTCCA
	proC-F	TGCATSSCSGCGATGGTGGT
	proC-R	ACGTGCTSACCTTCATCGAG
	recC-F	KYVAGGCTTCGGTCSGCGATG
	recC-R	TGGTRATGACVCCSGACATCG
	gyrA-F	CCTCCTTCGGCATCATCATG
	gyrA-R	GCGATCTTSARGCCTTCCA
	16S rRNA-F	TCAGCTCGTGTCTGAGAT
	16S rRNA-R	YCTTTGTACCGGCCATTGT
RT-qPCR for strain Red111	norB-F	CTTCCACCCGAGTGTTCC
	norB-R	CTTGCCTTGCGTCCATCC
	nifH-F	GGCAAATCCACCACCACA
	nifH-R	CGCCATAGCCGACCTTCAT
	nifK-F	GCGATACCCACGGCAAGT
	nifK-R	CACAGGTCTCGTCACGGATG
	nrfD-F	CAGCCATCTCGCTCTACCTC
	nrfD-R	GCAAGGACCAGGAGCAACG
	napA-F	AGTCGCTCCCGAACCTGAAC
	napA-R	TCCGTGTTGCCGAAGACCC
	narG-F	TCGGGCACCTCGGTTTACA
	narG-R	TCCGCCACCACCTTCTCGTC
	narH-F	CCACACCTGTTCCATTTCTT
	narH-R	GCCTTGAGCTTCAGTTTCTT
	narJ-F	GACAACCAGAAAAAAGGGGG
	narJ-R	TGTGCGAGGAAGGAGAGAAG
	narI-F	CGAAAGGTCCTCTACTGGG
	narI-R	GCGAAAAGGGTCTGCTGGT
	nifD-F	ATCCACTGCTACCGCTCCAT
	nifD-R	ACCGCCTCCACCCTCTCCTT
	napD-F	CCTCGAAACTGTGGTAGGCA

RT-qPCR for strain Red32	napD-R	GATCGTAGCGGTGATCGAGG
	narI-F	GGAGACTGGCTGGTCCTCTA
	narI-R	CGGAAGATCGGTCACGTAGG
	narJ-F	CCTCGATTATCCCCGTGAGC
	narJ-R	GTCGAAGCGGGTGACGTAAT
	napA-F	ATGGTCGGGCTTGTTCTTGT
	napA-R	GGCTCCCTACGAGGAGTACA
	nifK-F	GCATCCTACTACCGCTCCAC
	nifK-R	GCAGGAGGTGAAGACCGAAA
	nifH-F	GCGAAAACAAGGCGGAAGAG
	nifH-R	GGTGTTACGGGAGTTGCAGA
	norB-F:	GGAATGCGAACGGGATCTCT
	norB-R:	ATCTCACCTTGGCGGTGAAG
	norC-F:	CAACTGCAACGATTGCCACA
	norC-F	ATCTCGCCCACCCATTTTCAG
	narH-F	AGGGTGCCGAATACATGTGG
	narH-R	GCGGAGCTTTAACTGGTTGC
	nrfA-F	GAGCAAGGTGGGGAACATCA
	nrfA-R	GGTGACACCGTTCATCCAGT
	norB-F	TGGCTCTCCATCAACTACGC
	norB-F	AGCTGGAGATAGGCGATCCT
	nifD-F	TCTCGGTTCTTTCCGAGTGC
	nifD-R	TGGTGTCGTTGGAGATGTGG
	narG-F	GCAGTACGACAAGGTGGTCA
	narG-R	CGTCGAACTGGGGATAGTCG
	rpoB-F	CGTCGAACTGGGGATAGTCG
	ropB-R	GTGAAGGACGGCAGGGTTAC

Abstract

論文の内容の要旨

応用生命化学専攻

平成 30 年度博士課程入学

氏 名 許 振興

指導教員名 妹尾 啓史

論文題目

Isolation and characterization of iron-reducing bacteria, potential drivers of reductive nitrogen transformation in paddy soils

(水田土壌の還元的窒素変換を担う鉄還元細菌の分離と性状解析)

Chapter 1: Introduction

Paddy soil is the largest anthropogenic wetlands on the Earth and represents a unique ecosystem that cycles between waterlogged and drained states during long-term paddy cultivation. These seasonal cycles between waterlogged and drained conditions of paddy soils further revolve the aerobic and anaerobic conditions, which greatly affects the soil properties and sets in motion a series of unique physical, chemical, and biological processes not found in dryland soils. Reductive nitrogen transformation (RNT) in paddy soils, including denitrification ($\text{NO}_3^- \rightarrow \text{NO}_2^- \rightarrow \text{NO} \rightarrow \text{N}_2\text{O} \rightarrow \text{N}_2$), dissimilatory nitrate reduction to ammonium (DNRA; $\text{NO}_3^- \rightarrow \text{NO}_2^- \rightarrow \text{NH}_4^+$), and nitrogen fixation ($\text{N}_2 \rightarrow \text{NH}_4^+$), is a microorganism-driven process that is crucial for sustainable rice production and environmental conservation, due to the contributions to reduce leaching of nitrogen pollutants (NO_3^- , NO_2^- , and N_2O) into the environment and increase retention of nitrogen-based nutrients (NH_4^+) for rice plants under waterlogged conditions. Thus, the identification of microbial drivers of RNT in paddy soils is pivotal for successful rice production with minimal environmental nitrogen burden.

To investigate RNT microbes in paddy soils, a metatranscriptomic study, with soil RNA extracted from paddy soils in Japan under waterlogged and drained conditions, was previously performed in our laboratory. The results showed that most of the gene transcripts involved in RNT are derived from the order *Deltaproteobacteria*, specifically the genera *Geobacter* and *Anaeromyxobacter*, both known as iron-reducing bacteria. Moreover, other reports also revealed that the *Geobacter* and *Anaeromyxobacter* strains were possible drivers coupling metal reduction with nitrogen cycles based on the culture-independent analysis in paddy soils. However, to date, no such bacteria with a validly published name have been isolated from paddy soils, and their ability to transform nitrogen also has yet to be confirmed. Thus, I performed this study aiming to isolate paddy soil-derived *Geobacter*-like and *Anaeromyxobacter*-like strains and explore their special roles in biogeochemical cycles, especially the functions related to nitrogen transformation.

Chapter 2: Isolation and identification of *Geobacter*-like and *Anaeromyxobacter*-like strains and reclassification of the family *Geobacteraceae*

To obtain isolated iron-reducing bacteria from the paddy soil for the following studies, hundreds of paddy soil or related sediment samples were collected from all over Japan. After multiple enrichment processes under anaerobic conditions, a total of 63 different *Geobacter*-like strains and 3 different *Anaeromyxobacter*-like strains were successfully isolated. Through a polyphasic taxonomy analysis, the 14 of the 63 *Geobacter*-like isolates were identified as novel species and belong to 2 novel genera in the family *Geobacteraceae*, for which we proposed the names as *Geomonas* gen. nov., including 11 novel species and two reclassified species, *Geobacter bremensis* and *Geobacter bemidjiensis*, and *Oryzomonas* gen. nov., including 3 novel species, while the 3 *Anaeromyxobacter*-like strains were characterized as novel species. With further genomic analysis, it was found that the phylogenetic relationships among the species in the family *Geobacteraceae* are paraphyletic and need a taxonomic reclassification. Based on the phylogenetic analysis and genomic identities, the family *Geobacteraceae* was divided into 11 clades, thus, 11 genera containing all of the species in the family *Geobacteraceae* were proposed.

Chapter 3: Habitat preferences and biogeochemical roles of *Geomonas* and *Oryzomonas* strains

Although the members of the family *Geobacteraceae* reported previously were mostly isolated from sediments, especially contaminated terrestrial environments, the two novel

genera *Geomonas* and *Oryzomonas* were proved to prefer paddy soils as habitats with high preference scores. Moreover, a meta-analysis based on the public metagenomic data derived from the paddy soils in Japan revealed the genus *Geomonas* rather than the traditional genus, *Geobacter*, is the predominant group related to the nitrogen cycle in the paddy soil, suggesting the great potential of *Geomonas* strains in biogeochemical cycles. Using culture experiments with *Geomonas* and *Oryzomonas* strains isolated in this study, it was confirmed that all tested strains can reduce ferric irons (10 mM) to ferrous irons within 10 days. X-Ray diffraction (XRD) results also showed that these strains transformed ferrihydrite to vivianite, a common mineral in many geological environments. Nitrogen-fixing capacity was tested for these isolated strains using acetylene reduction assay (ARA). ARA values of all tested *Geomonas* and *Oryzomonas* strains were detectable with a range from 0.08 to 4.1 nmol/h/10⁹ cells. The relative high concentration of Fe(III)-NTA was found to strengthen bacterial nitrogen fixing ability, while nitrate and nitrite inhibit the activity completely. Moreover, the isolated *Geomonas* and *Oryzomonas* strains were also found to utilize not only acetate, but also high-molecular cellulose and xylan, the major components of rice straw, as the carbon source to fix nitrogen, indicating that these strains can obtain carbon source from rice straw directly and further couple carbon and nitrogen cycles in paddy soils.

Chapter 4: Confirmation of DNRA pathway and clarification of DNRA-derived N₂O production in *Geomonas* strains

Besides the special functions related to biogeochemical cycles of all studied strains, all of them were also confirmed to contain the complete DNRA pathway, reducing NO₃⁻ to NH₄⁺ with the intermediate NO₂⁻, as well as a small amount of N₂O produced. N₂O is a damaging greenhouse gas that is mainly produced from the nitrogen cycles in agricultural soils. To date, few reports have clearly answered how the N₂O is produced through the DNRA process. Based on several physiological tests on two *Geomonas* strains, Red111 and Red32, it was proved that N₂O emission is a biotic process and mainly produced from DNRA process via the intermediate, nitrite (ca. 90%), while less from the other intermediate, NO (ca. 10%). These facts suggested that the DNRA process is also an N₂O source in soil environments. However, quantitative analysis revealed that ammonium was the major product, accounting for more than 50% of added nitrate, while N₂O was the byproduct, only accounting for less than 2% of added nitrate, which implied that DNRA is indeed a process to produce ammoniacal nitrogen and maintain the soil fertility. Furthermore, the site preference (SP) of N₂O from the DNRA process was first determined with a value of 46 – 47‰, the highest value reported so far for biologically

produced N_2O , indicating the SP value would be a useful tool to identify the N_2O of the DNRA process. Using the transcriptomic analysis along with RT-qPCR, nitrate reductase (Nar) gene cluster was highly expressed under the nitrite treatment, which is consistent with the phenotypic results of N_2O generation. Along with previous reports that *narG* mutant strains produced less N_2O than wild strains, it was supposed that *nar* gene cluster is mostly the genetic driver reducing nitrite to N_2O in *Geomonas* strains (Fig. 1). Besides, the pH and C/N ratio were found to obviously affect the N_2O emission during the DNRA process via the accumulation of NO_2^- , which might be a useful reference for N_2O emission mitigation in agricultural management.

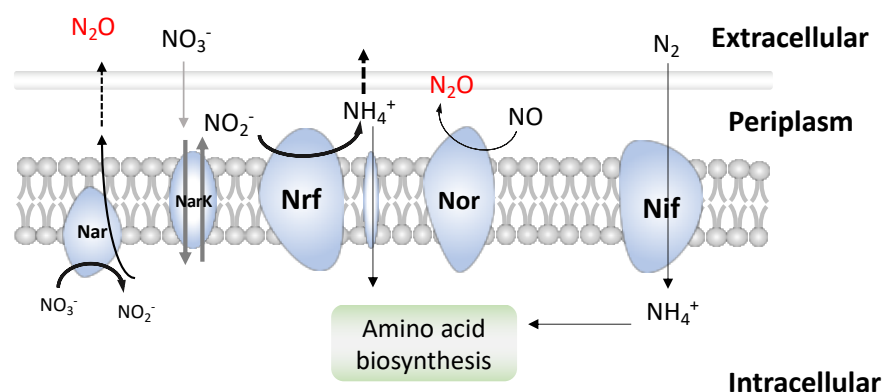
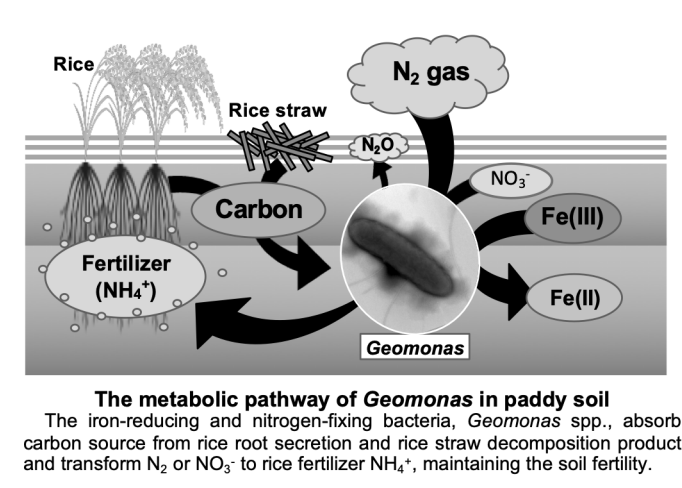


Fig. 1 Schematic description of the N_2O generation from DNRA process

Chapter 5: Conclusion and Prospect

In this study, a total of 63 *Geobacteraceae* and 3 *Anaeromyxobacter* strains from Japanese paddy fields and nearby places were successfully isolated, including 17 novel species and 2 novel genera (*Geomonas* and *Oryzomonas*). At the same time, the phylogenetic positions of all species in the family *Geobacteraceae* were reclassified and all strains were reclustered into 11 genera. Next, the abilities of ferric reduction, nitrogen fixation, cellulose- and xylan-degradation, and nitrate reduction (DNRA) were confirmed with biochemical methods, indicating that these *Geomonas* and *Oryzomonas* strains could be important drivers of the biogeochemical cycle in paddy soil, especially the ammonium production. Finally, based on biochemical and transcriptomic studies, I concluded that N_2O , as a byproduct, is mainly produced from nitrite in the DNRA process, and *nar* gene cluster should be the key role driving N_2O emission, which might be a useful reference for mitigation of N_2O emission in agricultural management. This study confirmed that iron-reducing microbes are indeed key drivers in nitrogen cycles, especially the ammonium production, implying the great potential of iron fertilization in paddy soils, which would be a reference for sustainable agricultural style of

paddy soils with less nitrogenous fertilizer, but higher rice production. However, my studies focusing on function clarification of *Geomonas* strains mainly performed using culture experiments with less consideration of natural conditions they were inhabited, mostly causing some biased results for bacterial description. Therefore, bacterial ecological study *in situ* may be a complementary choice for the following studies.



Publication:

- [1] **Z. Xu**, Y. Masuda, H. Itoh, N. Ushijima, Y. Shiratori, K. Senoo. *Geomonas oryzae* gen. nov., sp. nov., *Geomonas edaphica* sp. nov., *Geomonas ferrireducens* sp. nov., *Geomonas terrae* sp. nov., four ferric-reducing bacteria isolated from paddy soil, and reclassification of three species of the genus *Geobacter* as members of the genus *Geomonas* gen. nov. *Front. Microbiol.* 2019;10: 2201.
- [2] **Z. Xu**, Y. Masuda, C. Hayakawa, N. Ushijima, K. Kawano, Y. Shiratori, K. Senoo, H. Itoh. Description of *Oryzomonas japonicum* gen. nov., sp. nov., *Oryzomonas niigatensis* sp. nov., and *Oryzomonas ruber* sp. nov., three novel members of the family *Geobacteraceae* isolated from paddy soil and pond sediment. *Microorganisms*, 2020; 8, 634.
- [3] H. Itoh[#], **Z. Xu**[#], Y. Masuda, N. Ushijima, C. Hayakawa, Y. Shiratori, K. Senoo. *Geomonas silvestris* sp. nov., *Geomonas paludis* sp. nov. and *Geomonas limicola* sp. nov., isolated from terrestrial environments, and emended description of the genus *Geomonas*. *Int. J. Syst. Evol. Microbiol.* 2020. Doi: 10.1099/ijsem.0.004607 ([#]Co-first author)
- [4] Y. Masuda, H. Yamanaka, **Z. Xu**, Y. Shiratori, T. Aono, S. Amachi, K. Senoo, H. Itoh. Diazotrophic ability of *Anaeromyxobacter* isolated from soils. *Appl. Environ. Microbiol.*, 86, e00956-20.

Acknowledgements

Upon the coming of my graduate time, I would like to dedicate my thesis to all those who have offered me tremendous assistance and support during the three years of my doctoral course in the department of Applied Biological and Chemistry, the University of Tokyo.

First of all, I would like to express my heartfelt gratitude to my supervisor, Professor Senoo Keishi, for his helpful guidance, valuable suggestions and constant encouragement during my study. He provided a comfortable and relax research environment where I can feel play for myself. I feel deeply grateful and fortunate to be his student.

Also, I want to show my sincere appreciation to the Associate Prof. Shigeto Otsuka and Assistant Prof. Kazuo Isobe, for their valuable suggestions both in my study and in my life. Besides, I would like to express my sincere gratitude to Dr. Masuda Yoko, who directly guided this work and taught me much more experimental skills and experiences that greatly broadened my horizon and enriched my knowledge in my study. I also want to thank Dr. Hideomi Itoh of the AIST for not only his enormous help in my research, but also his influence of academic attitude. It is indeed a nice experience cooperating with them.

Then, I would like to extend my heart-felt thanks to all members of the Soil Science Laboratory. Without their help, I was unable to finish my research task smoothly. Their selfless help and ongoing support were my cherished memory.

Finally, I would like to give my deep gratefulness and love to my family and my friends, especially to my wife and my son, whose accompany and support have made my accomplishments possible. They are my forever harbor in my life.

XU Zhenxing

2020. 12. 14